University of Nebraska - Lincoln
DigitalCommons@University of Nebraska - Lincoln

Department of Agronomy and Horticulture: Dissertations, Theses, and Student Research

Agronomy and Horticulture Department

12-2023

High Throughput Phenotyping: Field Based Triticale Breeding and Educational Resource Impact

Catherine Kay Mick

Follow this and additional works at: https://digitalcommons.unl.edu/agronhortdiss

 Part of the Agricultural Science Commons, Agriculture Commons, Agronomy and Crop Sciences Commons, Other Plant Sciences Commons, and the Plant Biology Commons

Mick, Catherine Kay, "High Throughput Phenotyping: Field Based Triticale Breeding and Educational Resource Impact" (2023). *Department of Agronomy and Horticulture: Dissertations, Theses, and Student Research*. 252.
https://digitalcommons.unl.edu/agronhortdiss/252

This Article is brought to you for free and open access by the Agronomy and Horticulture Department at DigitalCommons@University of Nebraska - Lincoln. It has been accepted for inclusion in Department of Agronomy and Horticulture: Dissertations, Theses, and Student Research by an authorized administrator of DigitalCommons@University of Nebraska - Lincoln.

HIGH THROUGHPUT PHENOTYPING: FIELD BASED TRITICALE BREEDING AND EDUCATIONAL RESOURCE IMPACT

by

Catherine Kay Mick

A THESIS

Presented to the Faculty of

The Graduate College at the University of Nebraska

In Partial Fulfillment of Requirements

For the Degree of Master of Science

Major: Agronomy

Under the Supervision of Professor Donald Lee and Leah Sandall

Lincoln, Nebraska

December, 2023

HIGH THROUGHPUT PHENOTYPING: FIELD BASED TRITICALE BREEDING AND EDUCATIONAL RESOURCE IMPACT

Catherine Kay Mick, M.S.

University of Nebraska, 2023

Advisors: Donald Lee, Leah Sandall

Triticale (Triticosecale) is a multifunctional hybrid cereal crop that adopted the hardiness of rye and wheat's high-yielding and nutritional qualities. Plant breeding programs work to improve the quality and number of varieties available to producers through multiple rounds of evaluation and selection. However, traditional phenotyping methods are labor-intensive, time-consuming, and destructive, creating a phenotyping bottleneck. Remote sensing using unmanned aerial systems has the potential to alleviate this issue and change the evaluation of phenotypes in a breeding. Demand for educational resources to advance public awareness and prepare the workforce has increased with the utilization of more technology in agriculture. Limited research focuses on using UAV-derived vegetation indices to measure biomass in triticale. In addition, agriculture professionals need more education and understanding about the potential benefits and practical implementation of remote sensing technologies in plant breeding contexts. This research aims to (1) Evaluate the potential of UAV-derived vegetation indices to estimate above-ground biomass in triticale and (2) Assess the impact of open educational resources on the change in self-reported and objectively assessed knowledge of phenotype evaluation using high throughput phenotyping. The results of study one show high correlations between biomass and several vegetation indices, indicating that UAV-derived vegetation

indices have the potential to be used as an alternative to destructive biomass sampling for phenotyping biomass in triticale. The results of study two show the open educational resource *High Throughput Phenotyping in Plant Breeding* increases learner overall self-reported knowledge, UAV self-reported knowledge and cross-listed self-reported knowledge. In addition, the lesson increases overall objectively assessed knowledge and cross-listed objectively assessed knowledge.

ACKNOWLEDGMENTS

I want to express my most sincere gratitude to my advisors, Dr. Don Lee and Leah Sandall, for mentoring me over the last 2 ½ years but, more importantly, for helping me realize my potential. Thank you, Dr. Yeyin Shi and Dr. Katherine Frels, for opening your labs and providing me with resources and expertise to complete my research projects. Thank you to the members of both labs. Pascal Izere for taking me under his wing and teaching me everything about using UAV and Jiating Li for helping with the post-flight processing; in addition, all the individuals from the small grains program for giving your time and energy to help collect data. Thank you to Dr. Christine Booth for the weekly writing sessions and all the tea and cookies that helped me finish writing. Thank you to Amelia Miramonti at the UNL NEAR center for the time and dedication she put into my statistical analysis. And finally, to my family and friends for supporting me through this journey and believing in my future. I don't know where I'm going, but I know where I belong♥ Thank you for filling up my cup. I wouldn't be me without you.

GRANT INFORMATION

This project was primarily funded by a USDA-NIFA grant, High Intensity Phenotyping Sites: Transitioning to a Nationwide Plant Phenotyping Network (Award # 2020-68013-32371). Additional support was provided by the Nebraska Wheat Board.

TABLE OF CONTENTS

LIST OF MULTIMEDIA OBJECTS

Tables

Figures

CHAPTER 1 | LITERATURE REVIEW

The world population is projected to reach 9.7 billion by 2050 (United Nations, 2022). To feed the growing population, food production needs to increase by approximately 49 percent (Food and Agriculture Organization of the United Nations, 2017). Crop production increases when science discovery transitions to technology that can be applied to farming practices. The improvement of farming practices and the creation of new crop genotypes through plant breeding have advanced through science and technology to increase on-farm yields.

Plant breeding is the process used to improve crops to meet the growing demand for food, fiber, and plant-based products. All plant breeding programs use selection and breeding methods to develop plant varieties with desirable traits (NAPB, n.d.). The primary objective of plant breeding programs is to develop varieties with increased production and adaptability to biotic and abiotic stresses. The specific objectives vary depending on the crop produced, end-use purpose, and target environment.

Plant breeding is done by implementing several practices based on research and theory. Conventional breeding methods rely heavily on selection and hybridization. Selection is the process of choosing varieties that possess desirable traits. This is done by evaluating plants' observable characteristics and ability to perform under adverse conditions. This process of assessing a plant's genotype under environmental influence is known as phenotyping. Hybridization is the process of crossing two different varieties to produce offspring with desirable combinations of traits. Plant breeding programs will combine these methods and perform multiple rounds of selection and hybridization to

develop a suitable variety. To meet the demand for global food production, we need to invest in various crops. One up-and-coming small grains crop is triticale.

Triticale (*Triticosecale)* is a hybrid grain cereal crop developed in the late 19th century by crossing wheat (*Triticum aestivum)* and rye *(Secale cereale)* (Franke & Meinel, 1990; Wilson, 1873). Triticale adopted the hardiness of rye and the high-yielding and nutritional qualities of wheat. It is a multifunctional cereal crop that can be used as a feed grain, food grain, forage, and cover crop (Mergoum et al., 2009). Triticale has an increased resistance to biotic factors and a higher tolerance to environmental conditions. Research has shown the potential of triticale to produce higher grain yields and increased biomass under adverse conditions compared to other cereal crops (Estrada-Campuzano et al., 2022; Ford et al., 1984; Mergoum & Gómez Macpherson, 2004). In addition, the high biomass quality of triticale lends itself to higher weed suppression when used as a cover crop (Petrosino et al., 2015). Despite triticale's documented success in comparison to other small cereal crops, there is still room to improve the quality and number of varieties available to producers. Breeding programs are in a position to continue making progress, developing additional varieties.

Modern breeding techniques have capitalized on advanced technologies to enhance the speed and accuracy of plant breeding. Marker-assisted selection (MAS) was first introduced in 1923 by Karl Sax. MAS takes advantage of linkage disequilibrium to make indirect selections of desirable traits. This allows the characterization of parental genotypes, improving the effectiveness of parental selection for specific traits. The issue with MAS is that recombination can interrupt linkage disequilibrium, eliminating the

effectiveness of identified markers. Furthermore, quantitative traits are controlled by multiple genes limiting the usefulness of MAS.

Genomic selection (GS) was first introduced by Lande and Thompson (1990) before being popularized by Meuwissen and others (2001). GS model creation combines genetic information and phenotypic performance to identify desirable alleles at specific loci for selection and genetic gain. GS builds on MAS by utilizing genetic markers covering the whole genome to calculate genomic estimated breeding values. This method has the potential to improve selection for complex quantitative traits.

Triticale breeding can benefit from genomic selection methods. However, marker development in triticale lags behind other cereal crops. In addition, most markers developed for use in triticale came from wheat or rye, and the transferability of these markers is low (Badea et al., 2011; Kuleung et al., 2003).

The ability to rapidly sequence crop whole-genomes has the potential to move triticale plant breeding in the direction of a high-throughput era. Genomic data sets can measure genetic differences along the crops' chromosomes at thousands of locations. Automating these procedures allows plant breeders to gather genetic data from hundreds or thousands of plants. Coupling the analysis of genomic data with phenotypic data has the potential to reveal the connection between genotype and phenotype, providing valuable information for how a genotype will perform when exposed to different environments. This will elevate the plant breeders' ability to evaluate more genotypes and make selections to accelerate plant breeding progress. However, the acquisition of large-scale phenotype data to support marker development has lagged, creating a phenomenon known as the "phenotyping bottleneck" (W. Yang et al., 2020).

Traditional phenotyping methods are labor-intensive, time-consuming, and destructive. This motivates plant breeders to explore methods that can be scaled to evaluate more significant numbers of plant genotypes and capture meaningful phenotype data. Technology is advancing the ability to collect phenotype data. Sensor-based phenotype data is collected digitally, creating massive data sets for evaluation and ranking. This area of work is called high throughput phenotyping (HTP).

High throughput phenotyping is a rapid, non-destructive, and non-invasive method of phenotyping traits. High throughput phenotyping capitalizes on concepts of remote sensing to extract information about plant structures and increase the amount of phenotypic data captured in one growing season. The influx of phenotypic information improves genomic selection. The potential of this technology to improve plant breeding lies in its ability to increase the repeatability of evaluations and accelerate the pace of selections, thereby facilitating faster genetic gain.

High throughput phenotyping utilizes sensors deployed on various platforms to assess plant characteristics. The variation in morphological, physiological, and biochemical attributes creates unique spectral properties detectable with non-invasive sensors. The goal is to relate sensor measurements accurately to plant health and growth.

High throughput phenotyping sensors are deployed on several phenotyping platforms. Ground-based platforms have been effective at gathering proximal phenotypic data in agriculture using mobile (Bai et al., 2016; Deery et al., 2014; Jimenez-Berni et al., 2018; Mueller-Sim et al., 2017), gantry-based (Virlet et al., 2017), and cable-suspended systems (Bai et al., 2019a; Kirchgessner et al., 2017). However, these systems are limited by their inability to conduct large-scale phenotyping and inflexible maneuverability.

Aerial platforms such as satellites and unmanned aircraft systems (UAS) are more suitable for capturing large-scale data in less time. Unmanned aerial systems are becoming a more enticing option for phenotypic data collection due to their high spatial and temporal resolution and flexibility in spectral resolution and maneuverability.

An unmanned aircraft system is the combination of an unmanned aircraft vehicle (UAV) and all additional components used to safely operate the aircraft, where an unmanned aircraft is "…an aircraft that is operated without the possibility of human intervention from within or on the aircraft," (FAA Modernization and Reform Act of 2012, 2012).

Unmanned aerial vehicles are classified as fixed-wing or rotary-wing systems. While fixed-wing systems have longer flight times and faster flight speeds, the slower flight speeds of rotary-wing UAV provide increased spatial resolution and data precision (Boon et al., 2017). Rotary-wing UAV also have an increased payload capacity allowing different sensors to be combined for data collection. Due to their advantages over fixed-wing systems, research and development of rotary-wing systems has increased.

Unmanned aerial system-derived red-greed-blue (RGB) imagery has been shown to measure various morphological characteristics in cereal crops accurately. Studies have demonstrated the efficacy of using UAV-derived crop surface models (CSM) to estimate plant height and biomass in maize (Li et al., 2016), wheat (Herzig et al., 2021; Holman et al., 2016; Lu et al., 2019; Madec et al., 2017), triticale (Peña et al., 2019), barley (Bendig et al., 2015), oats (Acorsi et al., 2019), and sorghum (Pugh et al., 2018).

Physiological and biochemical characteristics imperceptible to the human eye can be detected using reflectance in the near-infrared (NIR) region. These characteristics can be

detected using vegetation indices (VI) calculated from UAV-derived multispectral imagery. UAV-derived VI have been effective in monitoring nitrogen status in wheat (Kefauver et al., 2017; Liu et al., 2022; Walsh et al., 2018; M. Yang et al., 2020), and barley (Kefauver et al., 2017). Several UAV-derived vegetation indices have positive correlations with grain yield in wheat (Kyratzis et al., 2017) and have been used to predict yield using regression models in wheat (Fu et al., 2020a; Han et al., 2021; Herzig et al., 2021; Liu et al., 2022) and barley (Herzig et al., 2021; Kefauver et al., 2017). Other phenotypic traits measured using VI were vegetation cover in barley (Herzig et al., 2021), leaf area index (LAI) and leaf dry matter in wheat (Fu et al., 2020), and LAI and SPAD in wheat (Han et al., 2021).

Various methods have also been researched to estimate the above-ground biomass (AGB) in wheat (Atkinson Amorim et al., 2022; Cristian et al., 2018a; Geipel et al., 2016; Hunt et al., 2011; Ostos-Garrido et al., 2019), rye (Roth et al., 2023; Yuan et al., 2019), barley (Cristian et al., 2018), and rice (Devia et al., 2019).

Although there is extensive UAV research on other cereal crops, relatively few studies have been conducted on triticale, and even fewer on using UAV-derived multispectral imagery to measure above-ground biomass in triticale. One study used a UAV-derived digital surface model to measure plant height (Peña et al., 2019). Two studies utilized VI derived from ground-based platforms (Busemeyer et al., 2013; Prabhakara et al., 2015). Mihaylov et al. (2021) measured UAV-derived VI but did not relate the measured vegetation indices to any crop characteristics. One study found positive but low correlations between UAV-derived normalized difference vegetation index (NDVI) and triticale biomass (Noack, 2016). Another found high correlations

between vetch and pea-based triticale associations and the NDVI, normalized difference red edge (NDRE), green-red vegetation index (GRVI), and greenness (Gr) (Plaza et al., 2021). Cristian et al., (2018) found triticale biomass to have an average correlation to the dark green chlorophyll index (DGCI). Similarly, another study also found NIR-based VI were more appropriate to measure biomass, specifically NDVI and GNDVI (Ostos-Garrido et al., 2019). Only one study used UAV-derived VI to build prediction models for estimating biomass (Yuan et al., 2019). Research to test the effectiveness and support the implementation of UAV technology would advance triticale breeding programs toward providing farmers with improved annual forage options.

Remote sensing using UAV has become increasingly popular for plant phenotyping due to its ability to provide high-resolution, non-destructive data in a cost-effective and timely manner. Plant breeding programs recognize the advantages of UAV technologies, and those with the resources adapt the technology to assist with evaluation and selection. However, the adoption of UAV technology relies on an engaged workforce that understands both plant breeding and UAV technology to use the technology effectively. This has created a need to develop learning resources for academic coursework and workforce training. The potential benefits and effective utilization of UAV imagery requires expertise in drone operation and data analysis and interpretation. Drone mapping mission planning takes precise planning and setting selection, affecting the quality of data generated. Unmanned aerial systems capture a large amount of data that needs to be processed and analyzed correctly to extract meaningful information. It requires the use of specialized software and image processing skills. A limited

understanding of these components creates resistance to change. Resistance to change and lack of awareness can limit the adoption of UAV in agriculture.

The high cost of traditional textbooks (Bliss et al., 2013; Buczynski, 2007; Hanson, 2022) can be a financial burden for students, limiting their educational opportunities. In addition, textbook updating is slow, which adds to this expense. Advancements in UAV technology are rapidly emerging creating a gap between information discovery and dissemination. We need to rapidly publish relevant work that is effective and efficient and out there in a way that everyone can access it.

One way to accomplish this is to integrate components of an open scholarship framework into research methods. There is little consensus on one definition of open scholarship, but a universal agreement is that open scholarship is the movement toward democratizing education and knowledge through various techniques (Kim & Lee, 2022; Martin, 2022). The impact of research findings is valuable when new knowledge is discovered but is maximized when that knowledge is shared with others.

One component of open scholarship that increases the accessibility of information is Open Educational Resources (OER) (Geith & Vignare, 2007). The United Nations Education, Scientific, and Cultural Organization (UNESCO, 2023) defined OER as "...learning, teaching, and research materials in any format and medium that reside in the public domain or are under copyright that have been released under an open license, that permit no-cost access, re-use, re-purpose, adaptation and redistribution by others." Similarly, in a report conducted to understand the future of pedagogical development better, the Organization for Economic Co-operation and Development (OECD, 2007) states, "the definition of OER currently most often used is digitized materials offered

freely and openly for educators, students and self-learners to use and reuse for teaching, learning and research." Open educational resources can reduce economic and geographic barriers to education while maintaining rigorous education standards.

The technological nature of OER gives them an adaptability and accessibility edge compared to traditional learning materials. OER take on many formats: learning modules, online texts, videos, audio. These elements can be organized into a learning environment that creates an enhanced learning experience for users.

Open educational resources also have a customizable nature, allowing them to be changed and updated as new research findings emerge. In STEM fields, technology is advancing at a rapid pace. Writing, printing, and distributing a physical book can take years. By this time, the technology and research in the publications need to be updated. Online materials can be consistently updated with new information for users as soon as new research and findings surface, keeping them up-to-date and relevant. This makes learning collaborative, engaging, and adaptable to meet learner needs.

In addition, the accessibility of OER can mitigate geographic barriers to education. Open educational resources are an internet-based method for the global distribution of learning resources. Online availability allows anyone with an internet connection to access them anywhere. This makes educational resources available to individuals who may need access to traditional educational materials or individuals outside of the university setting.

The effective use of OER has been demonstrated. When compared to textbook use in a traditional learning environment, using OER provides improved or similar student performance across a variety of disciplines, such as agriculture (Pounds &

Bostock, 2019), chemistry (Allen et al., 2015; Fischer et al., 2015), physics (Hendricks et al., 2017), math (Fischer et al., 2015; J. L. Hilton III et al., 2013), psychology (Hardin et al., 2019; J. Hilton III & Laman, 2012; Jhangiani et al., 2018), and many more (Colvard et al., 2018; Fischer et al., 2015; Winitzky-Stephens & Pickavance, 2017). OERS have also been adequate resources for the professional development of educators (Kim & Lee, 2022), in food safety training (Geith et al., 2010), as well as corporate training (Merkel & Cohen, 2015). These studies demonstrate that OER are practical materials for increasing learner knowledge.

Many broad content OER repositories exist, like YouTube (https://www.youtube.com/), Wikipedia (https://www.wikipedia.org/), and TEDEd (https://ed.ted.com/). More niche OER repositories have been created for themes like workforce training materials (SkillsCommons, https://www.skillscommons.org/), STEM education (PhET, https://phet.colorado.edu/), and vocational training (TESDA, https://e-tesda.gov.ph/). Knowledge acquisition of agricultural advancements in an informal setting occurs through extension efforts (USDA, n.d.). Multiple niche repositories exist to house agriculture related OER that can help facilitate extension efforts (Geith & Vignare, 2013; Jain & Veeranjaneyulu, 2013). We need to understand what the impact is they have on learners.

Only one study was found assessing the size of impact OER have on new agriculture advancements. Muniafu et al. (2013) sought to create a collaborative environment between universities and farmers. They reported that farmers gained knowledge when interacting with OER but needed clarification on how the knowledge was assessed.

Unmanned aerial systems are increasingly used in agricultural contexts. Remote sensing using UAV is expected to advance as a technology with reliable and cost-effective applications in plant breeding and the seed industry. Effectively using these systems to make meaningful contributions relies on remote sensing and agriculture industry knowledge and skill. Agriculture is moving in the direction of interdisciplinarity. Individuals require the depth and understanding needed for effective communication and implementation of new technologies in agricultural contexts. This creates a need for resources that provide accurate information on multidisciplinary applications that anyone can access. Unfortunately, relatively few quality materials exist that focus on UAV in agriculture. The literature shows that OER can provide quality education at little or no cost, making them a good option. Open educational resources can be used, adapted, and shared by anyone, which makes them a powerful tool for democratizing education and promoting access to learning opportunities.

Despite the breadth of research surrounding the use of UAV-derived imagery to phenotype traits in various crop species, the efficacy of UAV-derived imagery cannot be assumed to be accurate for all crops and characteristics. There is limited research focusing on using UAV-derived vegetation indices to measure biomass in triticale, so this research was conducted to test the effectiveness of this method. In addition, agriculture professionals need more education and understanding about the potential benefits and practical implementation of remote sensing technologies in plant breeding contexts. The purpose of this research is to:

1. Evaluate the potential of UAV-derived vegetation indices to estimate above-ground biomass in triticale.

2. Assess the impact of an open educational resource on the change in self-reported and objectively assessed knowledge of phenotype evaluation using high throughput phenotyping.

CHAPTER 2 | ABOVE GROUND BIOMASS ESTIMATION IN TRITICALE THROUGH FIELD BASED UAV MULTISPECTRAL IMAGERY

ABSTRACT

Triticale (Triticosecale) plant breeding programs work to improve the quality and number of varieties available to producers through multiple rounds of evaluation and selection. However, traditional phenotyping methods are labor-intensive, time-consuming, and destructive, creating a phenotyping bottleneck. Remote sensing using unmanned aerial systems has the potential to alleviate this issue and revolutionize the amount of breeding we can do. To understand this potential of UAV technology this research aims to (1) Understand the association between destructive biomass sampling and eight vegetation indices and (2) Assess the ability of vegetation indices to classify genotypes as high, medium, or low-yielding lines. The results show high correlations between triticale biomass and several vegetation indices indicating the potential of UAV-derived vegetation indices the be used as an alternative to destructive biomass sampling. The results do not show conclusive evidence supporting the use of vegetation indices to classify triticale genotypes as high, medium, or low yielding lines. Further research is needed to understand the ability of vegetation indices to classify genotypes.

INTRODUCTION

Triticale (Triticosecale) is a hybrid grain cereal crop developed in the late 19th century by crossing wheat (Triticum aestivum) and rye (Secale cereale) (Franke & Meinel, 1990; Wilson, 1873). The hybrid nature of triticale gives it the hardiness of rye and wheat's high-yield and nutritional traits. Research has shown the potential of triticale to produce higher grain yields and increased biomass under adverse conditions compared to other cereal crops (Estrada-Campuzano et al., 2022; Ford et al., 1984; Mergoum & Gómez Macpherson, 2004). An interest in triticale has developed because of its use as a feed grain, food grain, and forage crop (Mergoum et al., 2009).

Advancements in triticale characteristics can be made through plant breeding efforts that rely heavily on hybridization to create families or populations with genetic variation, followed by evaluation and selection. Triticale breeding programs focus on improving traits of economic and agronomic importance to improve triticale's nutritional value, productivity, and adaptability. One trait of high economic importance for producers that grow triticale as an annual forage or cover crop is above-ground biomass (AGB) yield. Triticale breeding programs that focus on this end use work towards increasing AGB yields.

Modern breeding techniques have capitalized on technologies to advance the rate of progress and evaluation accuracy in the plant breeding program through marker-assisted selection (MAS) and genomic selection (GS) (Lande & Thompson, 1990; Sax, 1923). However, these methods are underdeveloped for triticale breeding (Badea et al., 2011; Kuleung et al., 2003). The ability to rapidly sequence crop whole-genomes can move triticale plant breeding toward a high-throughput era. However, the acquisition of

large-scale phenotype data to support marker development lags, creating a phenomenon known as the “phenotyping bottleneck” (W. Yang et al., 2020). The development of improved phenotypic evaluation methods will mitigate this issue.

Traditionally, AGB has been characterized using destructive and proximal sampling methods. Destructive sampling, or direct sampling, is a method in which plant material is collected by destroying or removing a portion of the plant or plot. Destructive sampling compromises the plant's normal growth and productivity and can impact seed production which could prevent the advance of genetic diversity within a program. Furthermore, this removes the possibility of repeat measurements of the same portion of the crop.

Research has led to the development of proximal phenotyping technologies to measure above-ground biomass (AGB) without destructive sampling. Two widely accepted indirect sampling technologies are ceptometers and plant canopy analyzers (Casa et al., 2019).

A ceptometer is a handheld sensor that determines how much light the canopy intercepts by measuring the amount of photosynthetically active radiation (PAR) above and below the canopy. PAR is the portion of the electromagnetic spectrum (400-700 nm) plants use to conduct photosynthesis. This ratio is used to calculate the leaf area index (LAI) of a crop. LAI quantifies the one-sided leaf material in a given area, which is directly correlated with above-ground biomass (Levy & Jarvis, 1999; Watson, 1947).

Plant canopy analyzers are very similar devices. A plant canopy analyzer is a handheld sensor that calculates the interception of blue light (320-490 nm). This device

provides information about the amount of foliage in a canopy and the orientation of the vegetation (LI-COR, Lincoln, NE, USA).

Collecting phenotyping data by hand has been an effective method to assess and measure how a small population performs. However, the rapid acquisition of large-scale phenotypic data to supplement GS and MAS continues to lag. This motivates plant breeders to explore methods that can be scaled to evaluate larger numbers of plant genotypes and capture meaningful phenotype data. This area of work is called high throughput phenotyping (HTP).

High throughput phenotyping (HTP) is a rapid and non-destructive technique used to measure phenotypic data related to plant growth, structure, and function. The implementation of HTP methods in the field can be done using ground-based platforms (Bai et al., 2016, 2019b; Deery et al., 2014; Jimenez-Berni et al., 2018; Kirchgessner et al., 2017; Mueller-Sim et al., 2017; Virlet et al., 2017) but these systems are limited by their inflexible maneuverability and inability to phenotype enough genotypes.

A solution that mitigates these issues is utilizing unmanned aircraft systems (UAV) equipped with sensors. UAV platforms provide data with higher spatial and temporal resolution than ground-based platforms. This allows the collection of higher-quality data at more frequent intervals. UAV platforms are adaptable and can be equipped with one or more sensors (RGB, multispectral, hyperspectral, LiDAR) depending on the trait and crop of interest. Aerial imagery provides the data necessary to calculate vegetation indices (VI). Vegetation indices are derived from the measure of spectral reflectance of wavelengths of light striking the plant canopy (see Image 2.1).

Image 2.1

Spectral Reflectance

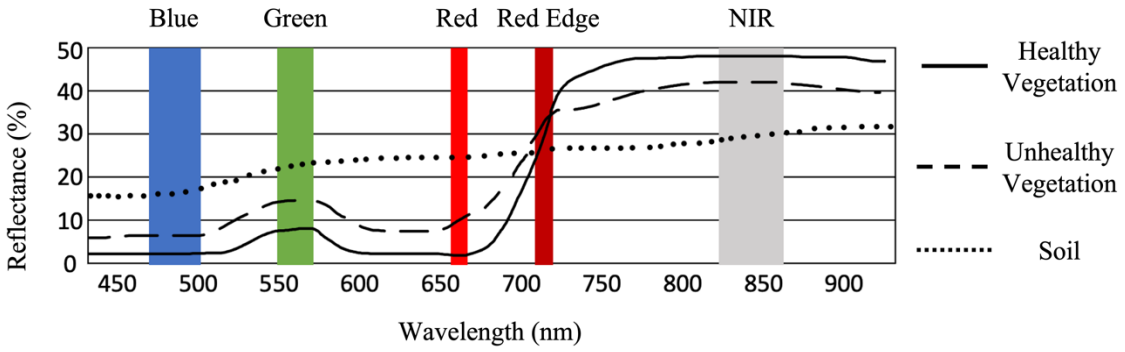

Note. In the visible spectrum, healthy vegetation reflects higher amounts of green light than red or blue. Healthy vegetation also reflects more near-infrared and red edge light than visible light. In the visible spectrum, unhealthy vegetation reflects more red and blue light than healthy vegetation. Unhealthy vegetation also reflects less near-infrared and red-edge light than healthy vegetation.

Measuring the reflectance of specific wavelengths can create an index that correlates with the quantity of biomass and plant vigor of crops. One of the most used indices is the normalized difference vegetation index (NDVI), which quantifies vegetation biomass by measuring reflectance in the near-infrared (NIR) and red regions (Rouse et al., 1974). The use of red wavelengths of light causes NDVI to saturate at relatively low amounts of biomass. Saturation occurs when spectral reflectance values are no longer sensitive to changes in biomass. Saturation in wheat occurs when leaf area index equals 2.5 and above ground biomass measures 1 kg/m^2 (Wang et al., 2016). Reflectance in the green and red edge regions is more sensitive to increased chlorophyll concentrations when compared to reflectance in the red band (Gitelson et al., 2003). This results in the improvement of this VI sensitivity to plant chlorophyll at higher

concentrations, avoiding saturation. These indices are the normalized difference red edge (NDRE) and green normalized difference vegetation index (GNDVI).

The NDRE quantifies the chlorophyll content in leaves by measuring reflectance in the red edge band (Gitelson & Merzlyak, 1994). The GNDVI quantifies vegetation photosynthetic activity by measuring the difference in reflectance between the NIR and green band (Gitelson et al., 1996). The higher sensitivity to increased chlorophyll concentrations means NDRE and GNDVI can measure plant characteristics late in the growing season when crops reach maturity, and NDVI saturates. These are three indices commonly used in agriculture; however, many different VI can be used to investigate various biotic and abiotic factors.

The ability of UAV-derived VI to effectively measure several crop parameters has been demonstrated in small cereal crops such as wheat (Fu et al., 2020b; Kyratzis et al., 2017; Liu et al., 2022; Walsh et al., 2018), barley (Herzig et al., 2021; Kefauver et al., 2017), rye (Corti et al., 2022; Roth et al., 2023), oats (Corti et al., 2022), and forage associations (Plaza et al., 2021). Due to the high forage production of triticale, the effectiveness of UAV-derived VI in other small grains cannot be assumed to be accurate for triticale.

Limited research has been done on high throughput phenotyping in triticale and on UAV biomass estimation. One study used a UAV-derived digital surface model (DSM) to measure plant height in triticale, wheat, and barley (Peña et al., 2019). Two studies utilized ground based derived VI to measure biomass in triticale (Busemeyer et al., 2013) and triticale, wheat, barley, rye, and ryegrass (Prabhakara et al., 2015). Mihaylov and colleagues (2021) charted the change in UAV-derived VI for wheat and

triticale over the growing season but did not investigate their relationship with any crop traits. Noack (2016) used UAV-derived NDVI to estimate dry matter yield in triticale and found significant but loose correlations. One study found significant high correlations between biomass and VI in vetch and pea-based triticale associations (Plaza et al., 2021). Two papers studied VI use in wheat, barley, and triticale to measure biomass. One study found significant but average correlations between triticale biomass and the dark green color index (DGCI) (Cristian et al., 2018). The other found NDVI and GNDVI to have the highest significant correlations with triticale biomass (Ostos-Garrido et al., 2019). The final study used UAV imagery to build prediction models to estimate biomass in rye and triticale (Yuan et al., 2019). Of these, the studies conducted by Ostos-Garrido et al. (2019) and Peña et al. (2019) used the UAV-derived VI to rank accessions for plant breeding purposes.

The relatively few studies that use UAV-derived VI to estimate triticale biomass in a plant breeding context leave a gap for further research. This study aims to assess the effectiveness of UAV-derived vegetation indices to estimate triticale biomass. The specific objectives of this study are to:

1. Determine the association between VI measures and destructive biomass sampling at different crop development stages.
2. Assess the ability of VI to classify genotypes as high, medium, or low-yielding lines.

MATERIALS AND METHODS

Field Layout and Genotype Selection

Thirty advanced breeding triticale lines (F_3:F_{7+}) were grown in University of Nebraska-Lincoln (UNL) research fields located in Lincoln, NE (40.85828° N, 96.61182° W) and Mead, NE (41.16250° N, 96.41253° W) in 2022 and 2023. The experimental design utilized in both fields was a randomized complete block design. The study was replicated three times for a total of 90 plots. Each plot contained five rows and measured 1.524 m in width and 3.048 m in length for a total area of 0.405 m^2. In year one, the Mead location was planted on September 28, 2021, and the Lincoln location was planted on October 1, 2021. In year two, the Mead location was planted on September 29, 2022, and the Lincoln location was planted on October 11, 2022. Agronomic practices were typical for small grains production in the region.

Ten of the thirty genotypes planted in the research plots were selected for data collection based on biomass type. To ensure sample variability, selected biomass types ranged from high to low (Table 2.1) determined by analyzing destructive biomass data from previous years. In year two, selected genotypes varied from year one due to accessions being removed from the breeding program. Seven genotypes were the same for year one and year two. One genotype was a reselection of a line used in year one. Two genotypes were new selections unrelated to year one. A sampling error resulted in different genotypes sampled in 2022 at the Mead location on date one (see Table A1).

Table 2.1

Genotypes Sampled Each Year

2022		2023	
Name	**Biomass Type**	**Name**	**Biomass Type**
NE03T416-1	Low	NE03T416-1	Low
NE03T416-3	Low	NE03T416-3	Low
NT12404-1	Low	NT12404-1	Low
NT14407	Medium/Low	NT14407	Medium/Low
NT441	Medium/Low	NT441	Medium/Low
NT14433	High/Medium	NT14433	High/Medium
NT19443	High	NT19443	High
NT20417	High	NT20427	High
NT20432	High	NT21436	High
NT17441	High	NT19441	High

Ground Measurement Data Collection

***Year 1* -** Ground measurement data collection occurred on May 18, 2022 (booting), June 2, 2022 (flowering), and June 27, 2022 (senescence). Three replicates for each genotype were collected.

***Year 2* –** Ground measurement data collection occurred on May 10, 2023 (jointing), May 22, 2023 (booting), and June 5, 2023 (flowering/grain fill). Three replicates for each genotype were collected.

Destructive Biomass Samples

One foot of the row was harvested using a rice knife to cut the plants at the soil level. Samples were harvested from a center row of each plot in an area representative of the whole plot to avoid edge effects. The fresh weight of each sample was collected in the lab on the same day as harvesting. Samples were stored in a drying chamber until a

constant weight was reached. At this point, the dry weight was recorded. Each plot's fresh weight and dry weight measurements were converted into biomass per plot using a conversion equation (see Tables A2-A13).

Leaf Area Index

The leaf area index was recorded using an AccuPar LP-80 Ceptometer (Pullman, WA, USA). LAI is calculated as the ratio of incoming radiation to intercepted light. Three readings were taken per plot and distributed between the North and South edges of the plot to get a representative measure. Readings were taken between the second and third, and third and fourth rows to avoid edge effects. The average plot LAI was calculated from these three measurements (see Tables A2-A13).

Plant Height Measurements

Measurements were taken using a measuring stick with markings every ½ centimeter. The height was measured to the nearest centimeter at three random locations distributed between the three center rows. Plant height was calculated as the average of three measurements per plot (see Tables A2-A13).

UAV Data Collection

Year 1 - UAV flights occurred on May 18, 2022, June 2, 2022, and June 27, 2022. The UAV was a DJI Matrice 300 RTK (DJI, Shenzen, China) equipped with a MicaSense Altum Multispectral sensor (MicaSense, Seattle, WA, USA). The multispectral sensor has five bands: red, green, blue, red edge, and near-infrared (see Table A14). An automated flight path was created using DJI Pilot software (DJI, Shenzen, China) with 90% front and side overlap and a flight altitude of 25 meters with a ground sampling distance of less than 1.2 centimeters. Images of a MicaSense calibrated reflectance panel

were captured prior to flying to be used for radiometric calibration during image processing. Seven ground control points (GCP) were placed around the edge and middle of each field prior to flying for geolocation calibration during image processing. The coordinates of each GCP were measured using a Topcon Hiper V RTK positioning system (Topcon, Tokyo, Japan). The GCP coordinates had an accuracy within 1.6 cm (except at Mead on 06/02/22 due to shadow effects during post-processing, which resulted in an accuracy of 5.8 cm).

Year 2 – UAV flights occurred on May 10, 2023, May 22, 2023, and June 5, 2023. The UAV was a DJI Mavic 3M (DJI, Shenzen, China) with built-in multispectral and RGB sensors. The multispectral sensor has four bands: green, red, red edge, and near-infrared (see Table A15). An automated flight path was created using DJI Pilot software (DJI, Shenzen, China) with 85% front and side overlap and a flight altitude of 25 meters with a ground sampling distance of less than 1.23 cm. Images of a Sentera calibrated reflectance panel (Sentera, Saint Paul, MI, USA) were captured prior to flying for radiometric calibration. Six ground control points were placed around the edge of each field prior to flying for geolocation calibration during image processing. The coordinates of each ground control point were measured using a Topcon Hiper V RTK positioning system (Topcon, Tokyo, Japan). The GCP coordinates had an accuracy of 1.8 cm.

Data Processing and Extraction

Multispectral imagery was processed using Pix4D software (Pix4D, Prilly, Switzerland, version 4.8.4). The three steps of image processing are: 1. Initial processing 2. Point cloud and mesh, and 3. DSM, orthomosaic, and index. Radiometric and

geolocation calibrations were done as part of image processing. The results of processing year one data yielded five single-layer reflectance maps. The results of processing year two data yielded four single-layer reflectance maps and one three-layer reflectance map.

Plot boundaries were defined using shapefiles created in ArcMap software (see Image 2.2) (ESRI, Redlands, CA, USA, version 10.8.2). Shapefiles and reflectance maps were read into Python (Wilmington, DE, USA, version 3.9.7) to extract plot-level vegetation indices. The vegetation index for each plot was calculated as an average of all the pixel values within the plot boundary. A list of vegetation indices and their respective formulas used for this research is outlined in Table 2.2.

Image 2.2

Example Plot Boundary Shapefiles

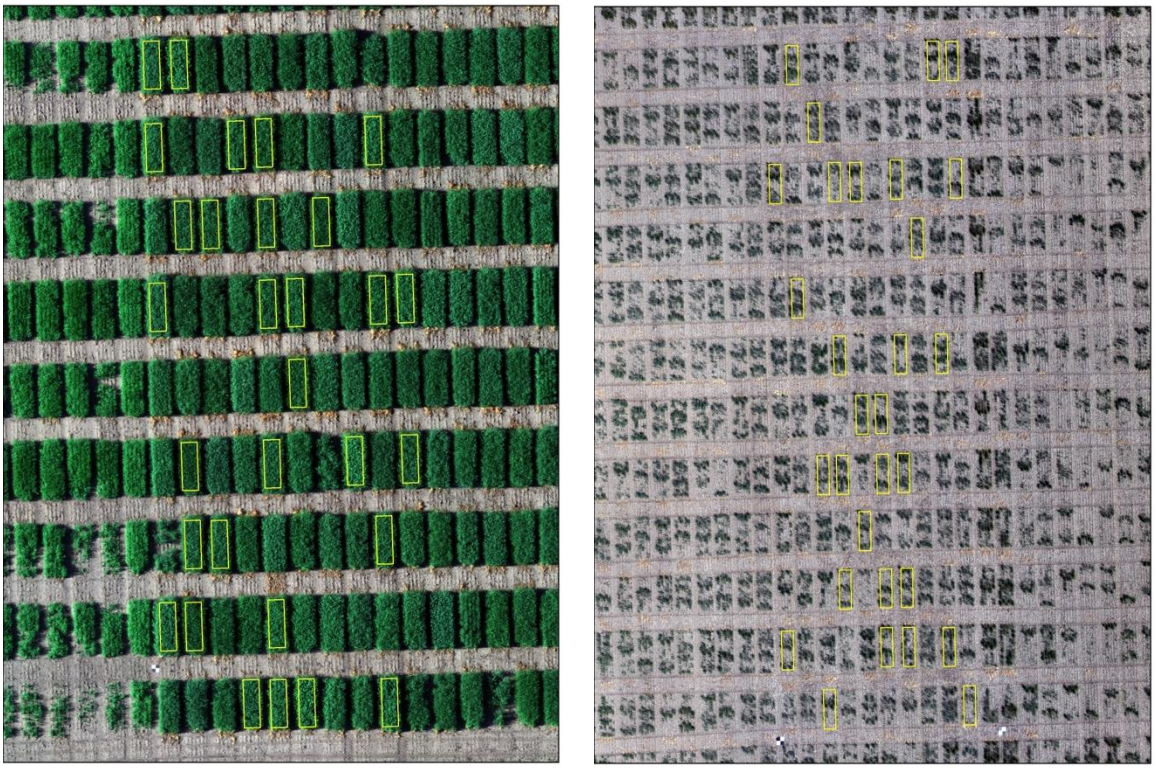

Note. Yellow polygons delineate plot boundaries. Lincoln 05/18/22 (left) average biomass is 6292.351kg/hec compared to Lincoln 05/22/23 (right) average biomass is 2299.328 kg/hec.

Table 2.2

Vegetation Index Formulas

Vegetation Index	Formula	Reference
Normalized Difference Vegetation Index (NDVI)	$\frac{(NIR - Red)}{(NIR + Red)}$	(Rouse et al., 1974)
Green Normalized Vegetation Index (GNDVI)	$\frac{(NIR - Green)}{(NIR + Green)}$	(Gitelson et al., 1996)
Normalized Difference Red Edge (NDRE)	$\frac{(NIR - RedEdge)}{(NIR + RedEdge)}$	(Gitelson & Merzlyak, 1994)
Green-Red Vegetation Index (GRVI)	$\frac{(Green - Red)}{(Green + Red)}$	(Tucker, 1979)
Green-Red Vegetation Index RedEdge (GRVIRE)	$\frac{(Green - RedEdge)}{(Green + RedEdge)}$	(Plaza et al., 2021)
Chlorophyll Index Green (GCI)	$\frac{(NIR)}{(Green)} - 1$	(Gitelson et al., 2003)
Chlorophyll Index Red Edge (RCI)	$\frac{(NIR)}{(RedEdge)} - 1$	(Gitelson et al., 2003)
Excess Green Index (ExG)	$(2 * Green - Red - Blue)$	(Woebbecke et al., 1995)

The Excess Green Index was used for segmentation. A threshold was determined for each date to classify pixels as vegetation or soil (see Table A16 for threshold values). The threshold was determined by plotting a histogram of ExG pixel values and using the pixel identification tool in ArcMap to determine values of vegetation coverage versus soil areas. ExG was used to calculate percent of vegetative pixels per plot. All plot-level extracted VI are in Appendix A (see Tables A17-A28).

Statistical Analysis

A Pearson correlation coefficient was calculated to determine the relationship between UAV-derived VI and ground sampling measurements using R Studio statistical software (Boston, MA, USA, version 2023.06.0). Correlations were evaluated based on the scale presented in Mukaka (2012) (Table 2.3).

Classifications based on destructive sampling methods were calculated using dry weight data because dry weight is a more direct biomass measurement than fresh weight. These were taken to be the 'true' or correct classification. A least significant difference test did not identify significant differences between genotype means and therefore could not be used for classification. Instead, the dry weight mean and standard deviation were calculated for each genotype, location, date, and year to be used for classification. The upper and lower bounds were delineated by multiplying the upper and lower standard deviations by .43 to create three equal categories for classification.

Table 2.3

Correlation Strength Scale

Size of Correlation	Interpretation
.90 to 1.00 (−.90 to −1.00)	Very high positive (negative) correlation
.70 to .90 (−.70 to −.90)	High positive (negative) correlation
.50 to .70 (−.50 to −.70)	Moderate positive (negative) correlation
.30 to .50 (−.30 to −.50)	Low positive (negative) correlation
.00 to .30 (.00 to −.30)	Negligible correlation

Note. The shaded box colors are used in Table 2.6 and 2.7 to indicate the strength of correlations found in this study.

The same process was repeated for each of the eight vegetation indices. These were taken to be the predicted classification. Genotypes were classified as low, medium, or high yielding lines using these upper and lower bounds.

The typical approach in plant breeding is to remove the worst genotypes from a program rather than selecting the best genotypes to advance. Therefore, this study looked at the balanced accuracy (average between the sensitivity and specificity) to understand how well VI classifications are at correctly including genotypes belonging to a class and correctly excluding genotypes not belonging to said class. The balanced accuracy is evaluated using a scale aligned with the general rule of thumb (see Table 2.4).

This was supplemented with the weighted Cohen's kappa. The weighted Cohen's kappa measures the level of agreement between the true classifications and the predicted classifications overall. The weighted Cohen's kappa values are evaluated using the scale suggested by Cohen (see Table 2.5). A high balanced accuracy and weighted Cohen's kappa would mean plant breeders can trust VI can accurately classify genotypes, avoiding the unfavorable removal of high-yielding biomass lines. Due to the sampling error, data collected in Mead on date 2 was filtered to remove genotypes with only one sample contributing to the mean.

Table 2.4

Balanced Accuracy Interpretation Categories

Balanced Accuracy Range	Interpretation
0.9-1.00	Very good
0.7-0.9	Good
0.6-0.7	OK
0-0.6	Poor

Table 2.5

Weighted Cohen's Kappa Value Interpretation Categories

Weighted Cohen's Kappa Value	Interpretation
0.81-1.00	Almost perfect agreement
0.61-0.80	Substantial
0.41-0.60	Moderate
0.21-0.40	Fair
0.01-0.20	None to slight
<= 0	No agreement

Note. Weighted Cohen's kappa value interpretations as suggested by Cohen. The shaded box colors are used in Table 2.8-2.11 to indicate the amount of agreement between VI classifications and dry weight classifications.

RESULTS

Correlations

A Pearson correlation coefficient was calculated to determine the relationship between fresh and dry biomass and the seven vegetation indices. Significant correlations were found in the Lincoln and Mead locations for 2022 and 2023.

Table 2.6

Numeric Correlations for 2022

	2022					
	Date 1 - booting		Date 2 - flowering		Date 3 - senescence	
Biomass/Vegetation Index	**Mead**	**Lincoln**	**Mead**	**Lincoln**	**Mead**	**Lincoln**
Fresh Weight						
NDVI	*0.69	0.29	0.26	0.05	*0.51	0.16
GNDVI	*0.7	0.16	0.28	0.01	*0.43	0.11
NDRE	*0.71	0.16	0.29	0.01	*0.44	0.22
GRVI	*0.7	*0.37	0.26	0.07	*0.52	0.22
GRVIRE	*-0.7	-0.11	-0.26	-0.02	-0.29	0.09
GCI	*0.7	0.17	0.29	0.01	*0.41	0.14
RCI	*0.71	0.17	0.3	0.01	*0.43	0.23
Pixel Percent	*0.58	-0.18	0.08	0.19	*0.41	0.12
Dry Weight						
NDVI	*0.67	0.27	0.15	-0.09	0.23	-0.15
GNDVI	*0.68	0.12	0.16	-0.08	0.24	-0.19
NDRE	*0.69	0.11	0.17	-0.09	0.16	-0.15
GRVI	*0.67	*0.39	0.16	-0.08	0.18	-0.06
GRVIRE	*-0.67	-0.13	-0.16	0.05	-0.29	0.23
GCI	*0.67	0.14	0.19	-0.08	0.22	-0.17
RCI	*0.68	0.12	0.19	-0.09	0.16	-0.14
Pixel Percent	*0.56	-0.17	0.04	0.11	0.08	-0.08

Note. The shaded boxes indicate size of correlation. A 5-color scale from black to white is used (see Table 2.3) where a black shaded box indicates the strongest correlations. As the box shading gets lighter this indicates a weaker correlation.

*$p<0.05$

Table 2.7

Numeric Correlations for 2023

	2023					
	Date 1 - jointing		Date 2 - booting		Date 3 - flowering/grain fill	
Biomass/Vegetation Index	**Mead**	**Lincoln**	**Mead**	**Lincoln**	**Mead**	**Lincoln**
Fresh Weight						
NDVI	*0.75	*0.64	*0.67	*0.52	*0.62	*0.36
GNDVI	*0.77	*0.6	*0.69	*0.49	*0.61	0.3
NDRE	*0.76	*0.39	*0.71	*0.48	*0.57	0.17
GRVI	*0.72	*0.68	*0.59	*0.52	*0.54	*0.4
GRVIRE	*-0.74	*-0.67	*-0.53	*-0.45	*-0.62	*-0.35
GCI	*0.83	*0.62	*0.68	*0.55	*0.62	0.3
RCI	*0.79	*0.39	*0.72	*0.51	*0.58	0.17
Pixel Percent	*0.61	*0.66	*0.47	*0.4	*0.61	*0.42
Dry Weight						
NDVI	*0.75	*0.64	*0.68	*0.52	*0.56	0.21
GNDVI	*0.76	*0.6	*0.7	*0.49	*0.56	0.18
NDRE	*0.77	*0.4	*0.76	*0.49	*0.55	0.04
GRVI	*0.72	*0.68	*0.6	*0.51	*0.48	0.24
GRVIRE	*-0.74	*-0.66	*-0.54	*-0.44	*-0.55	-0.25
GCI	*0.84	*0.62	*0.72	*0.54	*0.56	0.17
RCI	*0.8	*0.4	*0.77	*0.51	*0.55	0.04
Pixel Percent	*0.59	*0.66	*0.45	*0.39	*0.54	0.26

Note. The shaded boxes indicate size of correlation. A 5-color scale from black to white is used (see Table 2.3) where a black shaded box indicates the strongest correlations. As the box shading gets lighter this indicates a weaker correlation.

*$p<0.05$

Across all dates, locations, and years, more significant correlations were found at the Mead location than at the Lincoln location. In addition, data collected earlier in the season produced more substantial correlations.

In 2022, during booting (date 1), moderate to high correlations were found between fresh weight and all the VI tested at the Mead location (see Table 2.6). NDRE and RCI were the best-performing indices on this date, having high correlations with fresh weight. Similar but lower correlations were found between dry weight and all VI. Conversely, during booting (date 1) at the Lincoln location, there were only two significant, low correlations.

During senescence (date 3), low to moderate correlations were found with fresh weight at the Mead location. Though the correlations were not as strong as those found during booting, these results indicate these VI perform as well as, if not better than, VI in similar studies.

No significant correlations exist between fresh or dry weight and any VI during flowering (date 2). Additionally, there were no significant correlations with dry weight at the Mead location or fresh or dry weight at the Lincoln location during senescence (date 3).

2023 was very dry compared to 2022, resulting in significantly less biomass overall (see Image 2.2). Therefore, indices did not saturate as quickly, resulting in more significant correlations in 2023. At the Mead location, indices significantly correlate to fresh and dry weight across all dates and at or above correlations found in previously published literature (Cristian et al., 2018). Correlations were highest during jointing (date 1) and decreased through flowering/grain fill (date 3) (see Table 2.7). Moderate to high

correlations exist for all indices during jointing. Similarly, during booting (date 2), all indices except pixel percent had moderate to high correlations. NDRE, RCI, and GCI have the highest correlations with dry weight, with NDRE and RCI showing similar correlations with fresh weight. Correlations at the Lincoln location were moderate to low during jointing (date 1) and booting (date 2). These correlations are lower than those found at Mead. Low to negligible correlations were found during flowering/grain fill (date 3).

The best performing VI in this study differs for each growth stage sampled. However, some VI perform more consistently across time and environments. In 2022, the most consistently performing VI were GRVI and NDVI, which had moderate correlations during booting and senescence but only in the Mead environment (see Table 2.6). In 2023, NDVI, GRVI, and GCI had consistent correlations during jointing, booting, and flowering/grain fill in both environments (see Table 2.7). Furthermore, a trend was revealed for correlations with NDRE and RCI during booting across both years. In 2022 and 2023, NDRE and RCI had the strongest correlations with fresh and dry weight, indicating their potential to measure biomass in high and low-yielding environments during booting adequately.

Confusion Matrices

Confusion matrices were constructed to define the yield classification performance based on the VI (see Tables A29-A34). Classifications based on destructive sampling methods were calculated using dry weight data because dry weight is a more direct biomass measurement than fresh weight. The weighted Cohen's Kappa and balanced accuracy were calculated to assess the level of agreement between predicted

vegetation class (based on VI) and actual vegetation class (based on destructive samples). The balanced accuracy indicates if the genotypes are classified in the correct class, factoring in the sensitivity and specificity. The weighted Cohen's kappa indicates the degree of wrongness across all classes. Of the 30 plots sampled at the Mead location during booting (date 1) in 2022, ten data points were removed from the data set to remove genotypes that calculated genotype mean based on one sample (see Table A35). Tables 2.8 – 2.11 display the results of these analyses.

Table 2.8

Balanced Accuracy and Weighted Kappa Results for Lincoln 2022

	Balanced Accuracy			
	Class			
Date/Vegetation Index	**Low**	**Mid**	**High**	**Weighted Kappa**
LN 05/18/22				
GCI	0.89***	0.29	0.36	0.26
GNDVI	0.39	0.17	0.36	0.00
GRVI	0.94***	0.50	0.52	0.42
NDRE	0.39	0.38	0.60	0.25
NDVI	0.94***	0.38	0.36	0.25
RCI	0.39	0.38	0.60	0.25
GRVIRE	0.39	0.50	0.52	-0.05
Pixel Percent	0.39	0.50	0.52	-0.05
LN 06/02/22				
GCI	0.52	0.38	0.29	-0.17
GNDVI	0.52	0.50	0.36	-0.18
GRVI	0.52	0.38	0.52	0.17
GRVIRE	0.29	0.38	0.52	-0.17
NDRE	0.45	0.38	0.36	-0.17
NDVI	0.60	0.29	0.29	0.00
Pixel Percent	0.43	0.21	0.52	0.20
RCI	0.45	0.38	0.36	-0.17
LN 06/27/22				
GCI	0.25	0.38	0.63*	-0.17
GNDVI	0.25	0.38	0.63*	-0.17
GRVI	0.46	0.38	0.63*	0.17
GRVIRE	0.67*	0.71**	0.69*	0.34
NDRE	0.25	0.38	0.63*	-0.17
NDVI	0.25	0.38	0.63*	-0.17
Pixel Percent	0.38	0.54	0.56	-0.14
RCI	0.25	0.38	0.63*	-0.17

Note. A balanced accuracy with three asterisks (***), two asterisks (**), one asterisk (*), and no asterisk indicate very good, good, ok, and poor accuracy respectively. The shaded weighted Cohen's kappa values indicate the level of agreement. A 5-color scale is used where the box shade gets darker as weighted kappa values are stronger (see Table 2.5).

Table 2.9

Balanced Accuracy and Weighted Kappa Results for Mead 2022

Date/Vegetation Index	Balanced Accuracy Class Low	Mid	High	Weighted Kappa
MD 05/18/22				
GCI	0.68*	0.58	0.42	0.03
GNDVI	0.43	0.35	0.33	-0.29
GRVI	0.68*	0.45	0.33	0.00
GRVIRE	0.68*	0.45	0.33	0.00
NDRE	0.68*	0.45	0.33	0.00
NDVI	0.43	0.35	0.33	-0.29
RCI	0.75***	0.7*	0.42	0.00
Pixel Percent	0.43	0.23	0.50	0.18
MD 06/02/22				
GCI	0.38	0.88**	0.44	-0.86
GNDVI	0.38	0.88**	0.44	-0.86
GRVI	0.44	0.67*	0.38	-0.57
GRVIRE	0.75**	0.88**	1***	0.86
NDRE	0.38	0.88**	0.44	-0.86
NDVI	0.38	0.79**	0.38	-0.75
Pixel Percent	0.38	0.29	0.31	-0.22
RCI	0.38	0.88**	0.44	-0.86
MD 06/27/22				
GCI	0.88***	0.62*	0.44	0.46
GNDVI	0.81***	0.55	0.44	0.39
GRVI	0.88***	0.79***	0.94***	0.65
GRVIRE	0.44	0.52	0.39	-0.29
NDRE	0.81***	0.71***	0.94***	0.57
NDVI	0.88***	0.79***	0.94***	0.65
Pixel Percent	0.69*	0.55	0.83***	0.47
RCI	0.81***	0.71***	0.94***	0.57

Note. A balanced accuracy with three asterisks (***), two asterisks (**), one asterisk (*), and no asterisk indicate very good, good, ok, and poor accuracy respectively. The shaded weighted Cohen's kappa values indicate the level of agreement. A 5-color scale is used where the box shade gets darker as weighted kappa values are stronger (see Table 2.5).

Table 2.10

Balanced Accuracy and Weighted Kappa Results for Lincoln 2023

Date/Vegetation Index	Balanced Accuracy Class Low	Mid	High	Weighted Kappa
LN 05/10/23				
GCI	0.75**	0.75**	0.75**	0.67
GNDVI	1***	0.92***	0.94***	0.89
GRVI	1***	0.79	0.69*	0.75
GRVIRE	0.38	0.67*	0.44	-0.57
NDRE	1***	0.92***	0.94***	0.89
NDVI	1***	0.88**	0.75**	0.86
Pixel Percent	0.75**	0.67*	0.69*	0.57
RCI	1***	0.92***	0.94***	0.89
LN 05/22/23				
GCI	1***	0.58	0.38	0.50
GNDVI	0.75**	0.58	0.63*	0.50
GRVI	0.69*	0.58	0.38	0.00
GRVIRE	0.44	0.54	0.44	-0.33
NDRE	0.75**	0.67*	0.69*	0.57
NDVI	0.75**	0.58	0.63*	0.50
Pixel Percent	0.75**	0.38	0.31	0.25
RCI	0.75**	0.67*	0.69*	0.57
LN 06/05/23				
GCI	0.76**	0.45	0.46	0.31
GNDVI	0.83**	0.38	0.25	0.15
GRVI	0.67*	0.24	0.33	0.18
GRVIRE	0.36	0.38	0.46	-0.19
NDRE	0.60	0.21	0.38	0.13
NDVI	0.83**	0.31	0.33	0.36
Pixel Percent	0.76**	0.38	0.33	0.18
RCI	0.60	0.21	0.38	0.13

Note. A balanced accuracy with three asterisks (***), two asterisks (**), one asterisk (*), and no asterisk indicate very good, good, ok, and poor accuracy respectively. The shaded weighted Cohen's kappa values indicate the level of agreement. A 5-color scale is used where the box shade gets darker as weighted kappa values are stronger (see Table 2.5).

Table 2.11

Balanced Accuracy and Weighted Kappa Results for Mead 2023

Date/Vegetation Index	Balanced Accuracy Class Low	Mid	High	Weighted Kappa
MD 05/10/23				
GCI	0.69*	0.69*	0.94***	0.57
GNDVI	0.69*	0.69*	0.94***	0.57
GRVI	0.69*	0.69*	0.94***	0.57
GRVIRE	0.38	0.62*	0.33	-0.46
NDRE	0.69*	0.62*	0.89**	0.51
NDVI	0.69*	0.69*	0.94***	0.57
Pixel Percent	0.69*	0.69*	0.94***	0.57
RCI	0.69*	0.62*	0.89**	0.51
MD 05/22/23				
GCI	0.63*	0.50	0.69*	0.44
GNDVI	0.63*	0.50	0.69*	0.44
GRVI	0.56	0.42	0.69*	0.40
GRVIRE	0.38	0.58	0.38	-0.50
NDRE	0.63*	0.50	0.69*	0.44
NDVI	0.63*	0.50	0.69*	0.44
Pixel Percent	0.75**	0.67*	0.69*	0.57
RCI	0.63*	0.50	0.69*	0.44
MD 06/05/23				
GCI	0.56	0.63*	1***	0.60
GNDVI	0.63*	0.71**	1***	0.67
GRVI	0.69*	0.58	0.69*	0.50
GRVIRE	0.25	0.46	0.25	-0.50
NDRE	0.63*	0.63*	0.94***	0.60
NDVI	0.69*	0.71**	0.94***	0.67
Pixel Percent	0.88**	0.67*	0.88**	0.67
RCI	0.63*	0.63*	0.94***	0.60

Note. A balanced accuracy with three asterisks (***), two asterisks (**), one asterisk (*), and no asterisk indicate very good, good, ok, and poor accuracy respectively. The shaded weighted Cohen's kappa values indicate the level of agreement. A 5-color scale is used where the box shade gets darker as weighted kappa values are stronger (see Table 2.5).

Overall, the highest agreement between VI and dry weight for classifying genotypes as high, medium, or low-yielding lines was in 2023 during jointing (date 1) at the Lincoln location. On this date and location, all VI except GRVIRE had moderate to almost perfect agreement (see Table 2.10). Of the indices, GNDVI, NDRE, and RCI performed the best. Each VI had very good balanced accuracy at both locations for high, medium, and low classes.

Conversely, for the Mead location in 2023, the highest agreement between VI and dry weight for classifying genotypes as high, medium, or low-yielding lines was during flowering/grain fill (date 3) (see Table 2.11). All VI, excluding GRVIRE, had moderate to substantial agreement on this date. The indices with the highest agreement were GNDVI, NDVI, and pixel percent. None of the indices on this date had consistent balanced accuracy across high, medium, and low classes. However, GNDVI, NDVI, and pixel percent performed very good in at least two classes. Most other VI performed best at classifying high-yielding genotypes.

In 2023, the Mead location had more consistent agreement across all three dates (fair to substantial). In contrast, the Lincoln location performed best during jointing (moderate to almost perfect agreement) but tapered off to have none to slight agreement by flowering/grain fill (date 3) (see Table 2.10). The balanced accuracy for both locations showed similar trends. The balanced accuracy at the Mead location was OK to very good for many classes on all three dates. In contrast, the Lincoln location had very good balanced accuracy during jointing but revealed poor accuracy through booting and flowering/grain fill. An interesting trend to note is that the VI at the Lincoln location maintained very good balanced accuracy for the low classifications through all three

dates. Despite not always being the highest-performing VI, GCI and NDVI performed consistently well across all three dates and locations in 2023.

Compared to 2023, 2022 did not show as high agreement or performance at classifying genotypes as high, medium, or low-yielding lines. The balanced accuracy was not very good across all VI, dates, and locations in 2022 (see Tables 2.8 and 2.9). 69% of the balanced accuracy measurements calculated on 2022 data fell in the poor class. The highest agreement in 2022 was during senescence (date 3) at the Mead location, ranging from fair to moderate agreement (see Table 2.9). The best-performing indices on this date were GRVI, NDVI, NDRE, and RCI. These indices showed very good balanced accuracy across high, medium, and low classes on this date.

Much like in 2023, the highest agreement at the Lincoln location in 2022 was found at the earliest sampling date during booting. GRVI, GCI, NDVI, RCI, and NDRE showed fair to moderate agreement, with GRVI agreeing the best (see Table 2.8). However, when we look at the balanced accuracy on this date, all VI except GCI, GRVI, and NDVI showed poor balanced accuracy. These three showed poor balanced accuracy for the medium and high classes but had very good balanced accuracy for the low class.

GRVI consistently performed reasonably well classifying genotypes as high, medium, or low-yielding lines across multiple dates and locations in 2022. GCI and pixel percent were two other VI that performed consistently across dates and locations. This result is interesting because GCI also performed with reasonable consistency in 2023.

Some trends appear across 2022 and 2023. During booting in both years, VI had fair to moderate agreement with dry weight for classifying genotypes as high, medium, or low-yielding lines. GRVI and GCI were the two most consistently performing VI across

dates, locations, and years; however, GCI performed better in 2023, whereas GRVI in 2022.

One unexpected result found in 2022 is the performance of GRVIRE in Mead during flowering (date 2) and Lincoln during senescence (date 3). During flowering, GRVIRE classifications had an almost perfect agreement with dry weight classifications (see Table 2.9) and fair agreement during senescence (see Table 2.8). These are the only two instances where GRVIRE showed significant agreement. On all other dates across both years, GRVIRE showed no agreement.

DISCUSSION

Correlations

The high correlations between biomass and vegetation indices indicate that UAV-derived VI have the potential to be used as an alternative to destructive biomass sampling for phenotyping biomass in triticale. However, the results do not suggest one best index to be used for phenotyping triticale biomass, though we can suggest some better suited for specific phenotyping applications.

Due to the offset of sampling dates between the two years, the first sampling date in 2023 was the earliest growth stage sampled (jointing) and is not comparable to any sampling dates in 2022. GCI and RCI have the highest correlations with dry weight at this growth stage, but NDVI, GNDVI, NDRE, GRVI, and GRVIRE all also have high correlations with destructive biomass sampling in the Mead environment (see Table 2.7). These results suggest that any one of these VI could be used to phenotype biomass during jointing. However, neither of the highest-performing VI in Mead is the highest-performing VI in Lincoln. In Lincoln, NDVI, GNDVI, GRVI, GRVIRE, GCI, and pixel

percent have moderate correlations, and NDRE and RCI have low correlations. These results still indicate a high potential for many, if not all, of these VI to phenotype triticale biomass during jointing. However, additional research across multiple locations is needed to determine the most effective VI for biomass phenotyping during jointing.

The offset of sampling dates between the two years resulted in the first sampling date in 2022 being more comparable to the second sampling date in 2023, as both occurred during the booting growth stage. During booting in 2022, the best-performing indices were NDRE, RCI, and GNDVI (see Table 2.6). During the same growth stage in 2023, NDRE, GCI, and RCI were the best performing VI (see Table 2.7). The similar performance of NDRE and RCI in 2022 and 2023 indicates that these indices have a high potential for phenotyping biomass around booting under high and low biomass conditions.

Similarly, sampling on dates 2 in 2022 and 3 in 2023 are comparable as they were performed around flowering/grain fill. At this growth stage in 2023, the highest-performing VI were NDVI, GRVIRE, and GCI (see Table 2.7). The performance results of NDVI are consistent with those found by Ostos-Garrido et al. (2019), and the GRVIRE and GCI correlations perform as high as different VI investigated Ostos-Garrido et al. However, in this study, no significant correlations were found in 2022 during flowering/grain fill (see Table 2.6), and those that performed well in 2023 were not consistent across multiple environments. Further research is needed to confirm the potential of these indices to be used around flowering/grain fill.

The final sampling date in 2022 was not until senescence. The delay in sampling was due to environmental factors that delayed sampling. At this stage, GRVI and NDVI

had moderate correlations with fresh weight only in one location (see Table 2.6). These results are explained by the phenomenon known as saturation (Huete et al., 1997). It was suggested by C. Wang (2016) that to avoid saturation, VI should include red-edge wavelengths. Our results disagree with this suggestion as none of the VI that incorporate the red-edge wavelength tested in this study have significant correlations after the crop had reached saturation and the two that did have significant correlations do not use the red-edge wavelength. More information is needed to draw meaningful conclusions about using VI to phenotype biomass during senescence. A considerable amount of research needs to be done to investigate further.

Overall, the VI performed better in lower biomass conditions. This is demonstrated by the more significant amount of moderate to high-performing VI in 2023 compared to 2022 when the biomass was significantly lower due to the severe drought experienced during the growing season (see Image 2.1). In addition, the indices performed better at earlier sampling dates during jointing and booting when biomass was the lowest. 78% of the significant correlations found in this study were moderate to high in strength. Few studies have conducted similar research in triticale, but those that have found similar strength correlations (Ostos-Garrido et al., 2019; Plaza et al., 2021). The correlations in this study were higher than those found by Ostos-Garrido et al., but slightly underperformed compared to those found by Plaza et al.

Although the highest correlations in this study were found during jointing, they are similar in strength to those found during booting by Plaza et al. (2021). This disagreement in when the highest correlations are found can be explained by the crop in this study reaching saturation. Plaza et al. (2021) studied vetch and pea associations that

did not produce enough biomass to reach saturation, where this study had triticale biomass far above 1 kg m^{-2}, a saturation threshold for wheat found by C. Wang et al. (2016) (see Tables A2-A13). Sampling earlier in the season can reveal if there are any saturation effects during jointing and if there is an earlier growth stage that will produce stronger correlations.

The best-performing VI in this study are different for each growth stage sampled. However, some VI perform more consistently across time and environments. In 2022, the most consistently performing VI were GRVI and NDVI, which had moderate correlations during booting and senescence but only in the Mead environment (see Table 2.6). In 2023, NDVI, GRVI and GCI had consistent correlations during jointing, booting, and flowering/grain fill in both environments (see Table 2.7). Plaza et al. (2021) reported similar results where they found NDVI, GRVI, and GR to have the best correlations over time. It is important to note that NDVI and GRVI performed consistently well across 2022 and 2023. These results demonstrate their effective use in both high and low-yielding biomass environments.

Classifications

The variation seen in the confusion matrix and weighted Cohen's kappa results indicate that further research is needed to understand the ability to classify genotypes as high, medium, or low-yielding lines.

The VI in 2022 did not show as high agreement or performance as in 2023 when classifying genotypes as high, medium, or low-yielding lines (see Tables 2.8-2.11). The main difference between 2022 and 2023 is the severe drought experienced that resulted in significantly less biomass in 2023 (see Image 2.1). The average dry weight of genotypes

in 2022 is 4.4 times higher than in 2023. These results suggest that the VI classification performs better in low biomass conditions. This also provides evidence that saturation may affect VI classification.

We see some contrasting conclusions if we limit the scope to within single years. The results show that some VI have an almost perfect agreement with dry weight classifications in Mead in 2022 (see Table 2.9) and Lincoln in 2023 (see Table 2.10). However, these findings are inconsistent across dates and locations. In both years, the highest agreement in Lincoln was during booting, whereas the highest agreement in Mead was found during grain fill/senescence. These results are antithetical, suggesting there are factors other than biomass amount that affect performance. Additional research is needed to understand better the patterns seen.

Future Studies

The sampling population in this research project is relatively small, having only three samples per genotype for each sampling date. Additional biomass data was made available after this study concluded. Analyzing a more robust dataset will support the strength of the correlations found and help distinguish VI with high correlations to biomass from VI with moderate and low correlations. Additional data also provides the opportunity to create a training and testing set. A natural next step would be to investigate the accuracy of VI-based biomass prediction models. In addition, future research should look at making selections based on the forage stage at which producers are cutting. This makes the research directly applicable to real-world production.

The classification method used in this study is elementary. Classification groups were delineated, and genotypes were classified using simple descriptive statistics. In

addition to biomass, this study also collected morphological data on height and LAI that were unused in the analysis. These and other morphological traits could be included with VI in a stepwise regression model to understand their significance for estimating and classifying biomass. Future studies can test more advanced classification models using regression tactics based on stepwise regression results.

CONCLUSION

The high correlations between biomass and vegetation indices indicate that UAV-derived VI have the potential to be used as an alternative to destructive biomass sampling to phenotype biomass in triticale. Additional research is needed to understand the potential of utilizing VI for classification. These findings add to the knowledge surrounding HTP applications in plant breeding, specifically, the non-destructive alternatives for evaluation and selection. Progress in this area will revolutionize plant breeding, benefiting plant breeders, producers, and global food production.

CHAPTER 3 | OPEN EDUCATIONAL RESOURCE IMPACT ON KNOWLEDGE AND CONFIDENCE OF PLANT BREEDING AND HIGH THROUGHPUT PHENOTYPING

ABSTRACT

Recent innovations in sensor technologies (UAV) have developed a remote high throughput phenotyping (HTP) approach to acquire large-scale phenotype data. The effective use and practical implementation of remote sensing technology in agriculture relies on an engaged workforce that understands plant breeding and UAV technology. This creates a need to develop relevant learning resources that provide an accessible and cost-effective solution for sharing new advancements. To alleviate this issue, this research aims to (1) Assess the impact of the open educational resource *High Throughput Phenotyping in Plant Breeding* on self-reported knowledge and (2) Assess the impact of the open educational resource *High Throughput Phenotyping in Plant Breeding* on objectively assessed knowledge. The results of this study indicate the open education resource *High Throughput Phenotyping in Plant Breeding* increases learner overall self-reported knowledge, UAV self-reported knowledge and cross-listed self-reported knowledge. In addition, the lesson increases overall objectively assessed knowledge and cross-listed objectively assessed knowledge

INTRODUCTION

Crop yields have been rising since the 1940s (USDA, 2019). This is due to improved agronomic practices and plant breeding efforts. Plant breeders have contributed by evaluating different varieties and selecting those that exhibit the most desirable characteristics that address abiotic and biotic stresses in a changing climate.

Plant breeding is the science of improving crops for human benefit. According to the National Association of Plant Breeders (NAPB, n.d.), plant breeding:

> "Involves the creation of multi-generation genetically diverse populations on which human selection is practiced to create adapted plants with new combinations of specific desirable traits. The selection process is driven by biological assessment in relevant target environments and knowledge of genes and genomes. Progress is assessed based on gain under selection, a function of genetic variation, selection intensity, and time."

Plant breeding progresses when the plant breeder sets the goal, creates new genetic variation by crossing parents that can contribute to the goal, evaluates plants across generations and locations, and culminates with selection. This process of crossbreeding and selection is repeated until the desired lines are achieved.

Plant breeders' success is based on their ability to evaluate large numbers of genotypes with reliable methods. New advances in DNA analysis provide the opportunity to evaluate based on genotype (Lande & Thompson, 1990b; Sax, 1923). DNA methods are getting faster and cheaper. The ability to predict phenotype from genotype varies

depending on the population and the trait under selection. Coupling the analysis of genomic data with phenotypic data has the potential to reveal the connection between genotype and phenotype. This will elevate the plant breeders' ability to evaluate more significant numbers of genotypes and make selections to accelerate plant breeding progress. The ability to rapidly sequence crop whole-genomes has moved plant breeding toward a high-throughput era. However, acquiring large-scale phenotype data has lagged, creating a phenomenon known as the "phenotyping bottleneck" (W. Yang et al., 2020).

Recent innovations in sensor technologies and unmanned aerial systems (UAV) have developed a remote high throughput phenotyping (HTP) approach to alleviate the phenotyping bottleneck. High throughput phenotyping methods can potentially replace the human energy and cost investment in the field to make phenotyping more efficient and objective and reduce destructive plot loss, improving selection during plant breeding. These technological advances positively impact agriculture in many ways. However, these advances and research will only continue if individuals are equipped with the knowledge and skills necessary to use the technology to make meaningful contributions.

Traditionally, knowledge acquisition of agricultural advancements occurs in the classroom setting. Outside the formal education system, extension education efforts play a significant role (USDA, n.d.). The dissemination of agriculture information in formal and informal settings can be achieved by integrating components of an open scholarship framework into existing methods using open educational resources (OER). Open scholarship makes information accessible to everyone with an internet connection. Open educational resources increase the accessibility of information.

The United Nations Education, Scientific, and Cultural Organization (UNESCO) defines open educational resources as "...learning, teaching, and research materials in any format and medium that reside in the public domain or are under copyright that have been released under an open license, that permit no-cost access, re-use, re-purpose, adaptation and redistribution by others" (2023). Similarly, in a report conducted to understand the future of pedagogical development better, the Organization for Economic Co-operation and Development (OECD, 2007) states, "the definition of OER currently most often used is digitized materials offered freely and openly for educators, students, and self-learners to use and reuse for teaching, learning, and research." Open educational resources are adaptable and accessible, reducing economic and geographic barriers to education while maintaining rigorous education standards.

The technological nature of OER allows them to be organized into a learning environment that creates an enhanced learning experience for users. This makes learning collaborative, engaging, and adaptable to meet learner needs. In addition, online availability allows OER to provide immediate and continued access globally, mitigating geographic barriers to education.

The efficacy of OER has been demonstrated where they provide improved or similar student performance when compared to traditional textbooks across a variety of disciplines (Allen et al., 2015; Colvard et al., 2018; Fischer et al., 2015; Hendricks et al., 2017; J. L. Hilton III et al., 2013; J. Hilton III & Laman, 2012; Jhangiani et al., 2018; Muniafu, 2013; Pounds & Bostock, 2019; Winitzky-Stephens & Pickavance, 2017). Open educational resources have also been effective resources for professional development and corporate training (Geith et al., 2010; Kim & Lee, 2022; Merkel & Cohen, 2015).

Multiple agriculture-related repositories exist that contain OER, which can help facilitate extension efforts (Geith & Vignare, 2013; Jain & Veeranjaneyulu, 2013; PASSeL, https://passel2.unl.edu/). The infrastructure exists to house OER and there is documented success of these resources, however, there is relatively few OER focused on UAV use in agriculture.

Advancements in UAV technology are emerging at a rapid pace, creating a gap between discovery and information dissemination. Agriculture has transformed into a multidisciplinary field where professionals must understand how new technology and plant breeding work to make meaningful contributions. Access to relevant resources on applying UAV technology to agriculture, specifically plant breeding, will support the learning students and professionals require. Online searches yielded incomplete learning materials to address the application of UAV technology in plant breeding.

To mitigate the issue of limited learning materials, an open educational resource called *High Throughput Phenotyping in Plant Breeding* was created to communicate technological advancements to a broad audience. This open educational resource focuses on plant breeding and high throughput phenotyping in a broad context before narrowing it to a specific example of technologies used for measuring above-ground biomass. The lesson focuses on ways technology is implemented into plant breeding programs, how plant breeding programs work, why the technology can create valuable images, and how those images are processed and used to make decisions. This study aims to assess the effectiveness of an open educational resource to improve self-reported and objectively assessed knowledge of HTP in plant breeding. The specific objectives of this study are to:

1. Assess the impact of the lesson *High Throughput Phenotyping in Plant Breeding* on self-reported knowledge.
2. Assess the impact of the lesson *High Throughput Phenotyping in Plant Breeding* on objectively assessed knowledge.

MATERIALS AND METHODS

Lesson Development

An open education resource, *High Throughput Phenotyping in Plant Breeding*, was developed to test the impact of online resources on student self-reported and objectively assessed knowledge. The online lesson is intended for a broad audience to introduce the application of high throughput phenotyping to provide the data needed by plant breeders for the evaluation of potential new varieties. The lesson is accessible at the following web address: https://passel2.unl.edu/view/lesson/6241e9314ecf.

Lesson development occurred from May 2021 through June 2022. Information was gathered through research and reading peer-reviewed journal papers on topics surrounding high throughput phenotyping technologies and plant breeding. Information was supplemented by individuals at the University of Nebraska-Lincoln in the Department of Biological Systems Engineering with expertise in high throughput phenotyping technologies and individuals in the Department of Agronomy and Horticulture with expertise in small grains plant breeding. First-hand experience conducting in-field research for data collection and processing using unmanned aerial systems also contributed to the lesson development.

After the lesson was written, it was reviewed by four experts at the University of Nebraska-Lincoln and revised using their critiques. The final lesson was uploaded to the

University of Nebraska-Lincoln's Plant and Soil Sciences e-Library (PASSeL). PASSeL is an online library comprised of OER developed through the collaborative efforts of experts to provide free, reliable learning materials to improve science literacy (2023). Placing the lesson on the PASSeL website allows the lesson to be available to anyone at no cost.

The lesson contains eight sections and delivers information primarily through text, supplemented with images and videos to enhance the narrative (see Appendix B Tables B1 for outline and B2 for objectives). It was created as an introductory lesson for individuals with any level of background knowledge. The lesson first introduces plant breeding, by describing the goals, basic steps and progression toward creating new varieties for farmers. The lesson then covers high throughput phenotyping basics on sensors and how they work. It then brings the two ideas together and provides a step-by-step example of how high throughput phenotyping can enhance plant breeding.

Survey Creation

A pre-survey and post-survey were created in Qualtrics to test student's self-reported and objectively assessed knowledge before and after reading the lesson. Qualtrics is a web-based software that allows the creation and distribution of surveys (Qualtrics, Seattle, WA, USA). The pre-survey and post-survey were identical and consisted of four sections (Appendix B Table B3).

Section one contained the informed consent to inform individuals that their participation is voluntary and details on the research project.

Section two contained one multiple-choice fundamental demographic question. This question was used to categorize data for further analysis and comparison. The

options were undergraduate student, graduate student, agriculture industry professional, producer, and other.

Section three contained three questions using a 5-point Likert scale. These questions aimed to measure self-reported knowledge of high throughput phenotyping technology and plant breeding topics.

Section four contained eighteen questions: 17 multiple-choice and one drag-to-order. The purpose of this section was to objectively assess knowledge. This section contained content-heavy questions that measured plant breeding specific topics and cross-listed topics (high throughput phenotyping application in plant breeding).

Data Collection

Approval for conducting the survey was obtained from the University of Nebraska Lincoln Institutional Review Board (IRB; Approval #: 20221022192EX). The only identifiable information collected was IP addresses. This was done to try to connect pre and post data from the same learner to have a paired test for statistical analysis; however, in the end we did not use the IP addresses.

A pilot study took place in the Summer of 2022 with a group of students participating in a summer research experience for undergraduates at the University of Nebraska-Lincoln. This program included five students from varying backgrounds. The purpose of the pilot study was to get students' reactions and feedback to improve the lesson and survey before collecting actual data.

The treatment in this research study was the *High Throughput Phenotyping in Plant Breeding* lesson. Individuals were given a link to the pre-survey and expected to complete it. At the end of the pre-survey, a link was embedded, and instructions to direct

users to the lesson published on the PASSeL website. Individuals were expected to read the entire lesson and on the final page of the lesson, there was a link to complete the post-survey. This was done in an attempt to collect higher-quality data by encouraging individuals to read the lesson completely before accessing the post-survey to measure the effect of the treatment.

Sampling Population/Survey Deployment

The target populations included individuals from the following categories: undergraduate students, graduate students, agriculture industry professionals, producers, and other agriculture-related individuals.

The surveys and lesson were distributed in two ways: as an extra credit option in UNL courses and via email to colleagues of the High Intensity Phenotyping Sites: Transitioning to a Nationwide Plant Phenotyping Network project team. Courses were chosen based on the relevance of high throughput phenotyping and plant breeding to the course content. Students were given a link to complete the pre-survey and expected to complete the lesson reading, followed by the post-survey.

In the Fall semester of 2022, the lesson was used as an extra credit opportunity in a UNL Site-Specific Crop Management course offered at the undergraduate and graduate level. Students in this course were given three weeks to complete all parts of the research. In the Spring semester of 2023, the research opportunity was offered as an extra credit opportunity for three courses at the University of Nebraska Lincoln: Introduction to Plant Breeding, Breeding for Disease Resistance, and Genetics. The research opportunity was also emailed to selected agriculture professionals with connections to the University of Nebraska-Lincoln.

Statistical Analysis

All data collected was downloaded from Qualtrics and uploaded into R, a programming language used for statistical analysis (Boston, MA, USA). Recruitment efforts resulted in 132 pre-survey and 83 post-survey responses, with no unique identifying information collected to match pre-surveys to post-surveys. A subset of data was obtained by filtering data to ensure quality. It was decided that the question asking students to place the answers in the correct order was not a good indicator of knowledge and was removed from the final score (see Appendix B Table B3 for question). Survey responses were filtered based on a 95% completion threshold. The response was removed from the dataset if students completed less than 95% of the survey. Data was also filtered based on survey duration. Three test individuals (whose results were not used for analysis) were timed during survey completion. The average duration was calculated from these three responses, and a threshold of five minutes was determined. Any survey completed under five minutes was removed from the final data set. Data filtering removed 63 pre-surveys and 34 post-surveys, resulting in a final data set of 69 pre-surveys and 49 post-surveys.

The survey questions were divided into seven data subsets based on the subject matter to be further analyzed (see Appendix B Table B4). The 'UAV' and 'Plant Breeding' categories tested students' self-reported or objectively assessed knowledge on UAV or plant breeding, respectively. ‘Cross-Listed’ categories tested students' self-reported or objectively assessed knowledge in applying UAV in a plant breeding scenario. Categories labeled ‘Overall’ combine all self-reported or objectively assessed knowledge questions, respectively.

Table 3.1
Effect Size and Relative Magnitude of Difference

Effect Size	Magnitude of Difference
r < 0.05	Tiny
0.05 <= r < 0.1	Very small
0.1 <= r < 0.2	Small
0.2 <= r < 0.3	Medium
0.3 <= r < 0.4	Large
r >= 0.4	Very large

Note. The relative magnitude of difference as suggested by Funder and Ozer (2019). The shaded box colors are used in Table 3.2 to indicate the magnitude of difference between pre-survey and post-survey scores.

A Shapiro-Wilk normality test was used to check for normal distribution. It was determined that each subset residuals are non-parametric, necessitating the use of the Wilcoxon Rank-Sum test for statistical analysis. Categorizations are delineated as seen in Funder & Ozer (2019) (see Table 3.1).

RESULTS

The effect size for each subset was interpreted to determine the magnitude of the difference between pre-survey and post-survey results. The results of the Wilcoxon-Rank Sum Test and interpretations for each subcategory are summarized in Table 3.2. Graphical differences in the means of pre- and post-survey score subsets can be seen in Graphs B1-B7.

Table 3.2

Wilcoxon Rank-Sum Test Results

	Pre-Survey Score	Post-Survey Score	p-value	Effect Size
Self-Report Categories				
Plant Breeding Self-Report	3.403	4.020	0.052	0.176
UAV Self-Report	2.444	5.280	<0.001*	0.522
Cross-Listed Self-Report	2.639	4.660	<0.001*	0.443
Overall Self-Report	8.486	13.960	<0.001*	0.478
Objectively Assessed Knowledge Categories				
Plant Breeding Objectively Assessed	2.764	3.120	0.076	0.161
Cross-Listed Objectively Assessed	7.638	8.589	0.032*	0.194
Overall Objectively Assessed	10.402	11.709	0.019*	0.212

Note. This table shows the Wilcox Rank Sum statistics between the pre-survey (n = 72) and post-survey (n=50) scores. An asterisk (*) denotes a p-value of significance. The white, grey, and black highlighted boxes can be interpreted as small, medium, and very large magnitudes of difference respectively, as presented by Funder & Ozer (2019) (Table 3.1).

Self-Reported Knowledge

To assess the impact of *High Throughput Phenotyping in Plant Breeding* on self-reported knowledge, a Wilcoxon Rank-Sum Test was performed on the self-reported knowledge pre-survey and post-survey scores. Post-survey scores were significantly higher for overall UAV self-reported knowledge, cross-listed self-reported knowledge, and overall self-reported knowledge. However, self-reporting plant breeding knowledge did not significantly increase (see Table 3.2). The increase in self-reported knowledge for statistically significant groups had a very large difference between pre-survey and post-survey means. These findings indicate that the lesson *High Throughput Phenotyping in Plant Breeding* positively impacts learner self-reported knowledge in UAV applications in plant breeding, but not plant breeding itself.

Objectively Assessed Knowledge

To assess the impact of *High Throughput Phenotyping in Plant Breeding* on knowledge, a Wilcoxon Rank-Sum Test was performed on the objectively assessed knowledge pre-survey and post-survey scores. There was a significant increase in cross-listed and overall content knowledge with small and medium differences, respectively. However, there was no significant increase in plant breeding knowledge (see Table 3.2). These results indicate that the lesson *High Throughput Phenotyping in Plant Breeding* is effective at increasing knowledge about the application of UAV in plant breeding, but not plant breeding knowledge alone.

DISCUSSION

Traditional assessments to understand the efficacy of OER follow the 'COUP' framework measuring cost, outcomes, use, and perceptions (Bliss et al., 2013). Consequently, the majority of OER studies compare the use of OER in comparison to traditional texts. This study is unique because the OER was not designed to replace any textbook or other learning materials, so we cannot compare the results from using the OER to using traditional text. It does instead show the effectiveness of using an OER as a primary method to share information related to new advances in the agriculture industry.

This research aimed to assess the impact of the open educational resource *High Throughput Phenotyping in Plant Breeding* on self-reported and objectively assessed knowledge. The results from the Wilcoxon Rank-Sum Test indicate that reading the lesson increases overall self-reported knowledge and objectively assessed knowledge of phenotype evaluation using high throughput phenotyping (Table 3.2). These results are consistent with similar research findings (Allen et al., 2015; J. Hilton III & Laman, 2012; Muniafu, 2013). Reading the lesson impacted self-reported knowledge significantly more than objectively assessed knowledge.

Overall, UAV and cross-listed self-reported knowledge scores increased by a very large magnitude of difference between pre- and post-surveys (Table 3.2). Similarly, there was a significant increase in overall and cross-listed objectively assessed knowledge scores, though with a small to medium magnitude of difference. Conversely, neither plant breeding self-reported knowledge nor plant breeding objectively assessed knowledge had a significant increase in scores.

These results indicate that the lesson was more effective in increasing UAV self-reported and objectively assessed knowledge. Increased self-reported knowledge can indicate individuals with knowledge surrounding these topics. Confident individuals are more likely to trust their abilities, perform better, and make meaningful contributions to a team.

Though there was no significant increase in plant breeding self-reported or objectively assessed knowledge, this does not mean there were no benefits related to plant breeding that the lesson produced. The cross-listed self-reported and objectively assessed knowledge questions measured the ability of learners to apply UAV knowledge to plant breeding situations. The increase in both categories provides evidence that the lesson helped learners to apply basic knowledge they already have in novel situations.

Considering the sampling population provides reasons for the lack of a significant increase in basic plant breeding self-reported and objectively assessed knowledge. The population targeted in this study included individuals enrolled in agronomy courses and professionals in the agriculture industry. It is reasonable to believe the agriculture and plant breeding base knowledge these students and professionals possess is at or above the amount of knowledge the lesson would have imparted. This lesson was designed to introduce the application of UAV in plant breeding. Consequently, the survey questions were created to measure an introductory level of knowledge. Sufficient background knowledge increases pre-survey scores, which leaves less room for improvement in post-survey scores. We can see this in the inflated pre-survey scores for plant breeding categories compared to UAV and cross-listed categories (Table 3.2). This explains why

we did not see a significant increase in post-survey scores for categories about plant breeding topics.

Due to this, these findings may be less informative for different populations of learners. If, instead, the sample population included students enrolled in engineering courses, the results may have been the opposite, where there would have been a significant increase in plant breeding scores and not UAV scores. Furthermore, less than 1% of pre- and post-survey responses collected in this study were from agriculture professionals. Therefore, the survey results cannot provide any evidence for the increase in knowledge for individuals already in the workforce but rather for individuals preparing to enter the workforce.

Future Studies

Future studies should expand the sample population to include individuals with more diverse background knowledge and experience. This can be done by expanding the undergraduate pool to students enrolled in engineering courses with more formal UAV training. In addition, the lesson can be tested on individuals in the workforce who have a background in agriculture or engineering. Significant research studies the effects of replacing traditional textbooks with OER in the classroom setting. However, more research is needed to focus on OER impact on individuals continuing education outside of school. The agriculture industry is an interdisciplinary field, necessitating a workforce that understands agriculture's traditional and technological aspects. Balancing the sample population will produce more informative results for how practical the lesson is and provide insight for implementing the lesson in ways that will maximize the benefit.

It would also be interesting to see how different formats of OER impact the engagement with and efficacy of the lesson. The current format is majority text with few supplemental images and videos as additional support for the information found within the text. The lesson could be formatted in alternative ways that promote more interaction. One alternative is changing the lesson from text to video format for a more visual representation of the information. Another option is adding questions as knowledge checkpoints for readers to gauge current understanding before advancing further in the lesson.

CONCLUSION

As the utilization of technology in agriculture increases, there is a continued demand for educational resources to train individuals in the industry. Increasing the objective knowledge of individuals entering the agriculture workforce increases their confidence in their ability to work with new technologies. This results in individuals capable of producing meaningful contributions to the industry. The lesson in this study increased learners' self-reported and objectively assessed knowledge of UAV use and application in plant breeding, demonstrating the effectiveness of OER as a learning resource in agricultural contexts.

REFERENCES

Acorsi, M. G., das Dores Abati Miranda, F., Martello, M., Smaniotto, D. A., & Sartor, L. R. (2019). Estimating biomass of black oat using UAV-based RGB imaging. *Agronomy*, *9*(7), Article 7. https://doi.org/10.3390/agronomy9070344

Allen, G., Guzman-Alvarez, A., Smith, A., Gamage, A., Molinaro, M., & Larsen, D. S. (2015). Evaluating the effectiveness of the open-access ChemWiki resource as a replacement for traditional general chemistry textbooks. *Chemistry Education Research and Practice*, *16*(4), 939–948. https://doi.org/10.1039/C5RP00084J

Atkinson Amorim, J. G., Schreiber, L. V., de Souza, M. R. Q., Negreiros, M., Susin, A., Bredemeier, C., Trentin, C., Vian, A. L., de Oliveira Andrades-Filho, C., Doering, D., & Parraga, A. (2022). Biomass estimation of spring wheat with machine learning methods using UAV-based multispectral imaging. *International Journal of Remote Sensing*, *43*(13), 4758–4773. https://doi.org/10.1080/01431161.2022.2107882

Badea, A., Eudes, F., Salmon, D., Tuvesson, S., Vrolijk, A., Larsson, C.-T., Caig, V., Huttner, E., Kilian, A., & Laroche, A. (2011). Development and assessment of DArT markers in triticale. *Theoretical and Applied Genetics*, *122*, 1547–1560. https://doi.org/10.1007/s00122-011-1554-3

Bai, G., Ge, Y., Hussain, W., Baenziger, P. S., & Graef, G. (2016). A multi-sensor system for high throughput field phenotyping in soybean and wheat breeding. *Computers and Electronics in Agriculture*, *128*, 181–192. https://doi.org/10.1016/j.compag.2016.08.021

Bai, G., Ge, Y., Scoby, D., Leavitt, B., Stoerger, V., Kirchgessner, N., Irmak, S., Graef, G., Schnable, J., & Awada, T. (2019). NU-Spidercam: A large-scale, cable-driven, integrated sensing and robotic system for advanced phenotyping, remote sensing, and agronomic research. *Computers and Electronics in Agriculture*, *160*, 71–81. https://doi.org/10.1016/j.compag.2019.03.009

Bendig, J., Yu, K., Aasen, H., Bolten, A., Bennertz, S., Broscheit, J., Gnyp, M. L., & Bareth, G. (2015). Combining UAV-based plant height from crop surface models, visible, and near infrared vegetation indices for biomass monitoring in barley. *International Journal of Applied Earth Observation and Geoinformation*, *39*, 79–87. https://doi.org/10.1016/j.jag.2015.02.012

Bliss, T. J., Robinson, T. J., Hilton, J., & Wiley, D. A. (2013). An OER COUP: College teacher and student perceptions of open educational resources. *Journal of Interactive Media in Education*, *2013*(1), Article 1. https://doi.org/10.5334/2013-04

Boon, M. A., Drijfhout, A. P., & Tesfamichael, S. (2017). Comparison of a fixed-wing and multi-rotor UAV for environmental mapping applications: A case study. *The International Archives of the Photogrammetry, Remote Sensing and Spatial Information Sciences*, *XLII-2-W6*, 47–54. https://doi.org/10.5194/isprs-archives-XLII-2-W6-47-2017

Buczynski, J. A. (2007). Faculty Begin to Replace Textbooks with “Freely” Accessible Online Resources. *Internet Reference Services Quarterly*, *11*(4), 169–179. https://doi.org/10.1300/J136v11n04_11

Busemeyer, L., Mentrup, D., Möller, K., Wunder, E., Alheit, K., Hahn, V., Maurer, H. P., Reif, J. C., Würschum, T., Müller, J., Rahe, F., & Ruckelshausen, A. (2013). BreedVision—A multi-sensor platform for non-destructive field-based phenotyping in plant breeding. *Sensors*, *13*(3), Article 3. https://doi.org/10.3390/s130302830

Casa, R., Upreti, D., & Pelosi, F. (2019). Measurement and estimation of leaf area index (LAI) using commercial instruments and smartphone-based systems. *IOP Conference Series: Earth and Environmental Science*, *275*(1), 012006. https://doi.org/10.1088/1755-1315/275/1/012006

Colvard, N. B., Watson, C. E., & Park, H. (2018). The Impact of open educational resources on various student success metrics. *International Journal of Teaching and Learning in Higher Education*, *30*(2), 262–276.

Corti, M., Cavalli, D., Cabassi, G., Bechini, L., Pricca, N., Paolo, D., Marinoni, L., Vigoni, A., Degano, L., & Marino Gallina, P. (2022). Improved estimation of herbaceous crop aboveground biomass using UAV-derived crop height combined with vegetation indices. *Precision Agriculture*, *24*, 587–606. https://doi.org/10.1007/s11119-022-09960-w

Cristian, C., Mihai, H., Ciprian, R., & Florin, S. (2018). *Model prediction of chlorophyll and fresh biomass in cereal grasses based on aerial images*. 390003. https://doi.org/10.1063/1.5043987

Deery, D., Jimenez-Berni, J., Jones, H., Sirault, X., & Furbank, R. (2014). Proximal remote sensing buggies and potential applications for field-based phenotyping. *Agronomy*, *4*(3), Article 3. https://doi.org/10.3390/agronomy4030349

Devia, C. A., Rojas, J. P., Petro, E., Martinez, C., Mondragon, I. F., Patino, D., Rebolledo, M. C., & Colorado, J. (2019). High-throughput biomass estimation in rice crops using UAV multispectral imagery. *Journal of Intelligent & Robotic Systems*, *96*, 573–589. https://doi.org/10.1007/s10846-019-01001-5

Estrada-Campuzano, G., Slafer, G. A., & Miralles, D. J. (2022). Differences in yield, biomass and their components between triticale and wheat grown under contrasting water and nitrogen environments. *Field Crops Research*, *128*, 167–179. https://doi.org/10.1016/j.fcr.2012.01.003

FAA Modernization and Reform Act of 2012, Pub. L. No. 112-952012, 126 Stat. 72 (2012). https://www.govinfo.gov/app/details/PLAW-112publ95

Fischer, L., Hilton, J., Robinson, T. J., & Wiley, D. A. (2015). A multi-institutional study of the impact of open textbook adoption on the learning outcomes of post-secondary students. *Journal of Computing in Higher Education*, *27*, 159–172. https://doi.org/10.1007/s12528-015-9101-x

Food and Agriculture Organization of the United Nations (Ed.). (2017). *The future of food and agriculture: Trends and challenges*. Food and Agriculture Organization of the United Nations.

Ford, M. A., Austin, R. B., Morgan, C. L., & Gregory, R. S. (1984). A comparison of the grain and biomass yields of winter wheat rye and triticale. *Journal of Agricultural Science*, *103*(2), 395–404.

Franke, R., & Meinel, A. (1990). History of the first fertile amphidiploid wheat x rye hybrid W. Rimpau's triticale. *Cereal Research Communications*, *18*(1/2), 103–109.

Fu, Z., Jiang, J., Gao, Y., Krienke, B., Wang, M., Zhong, K., Cao, Q., Tian, Y., Zhu, Y., Cao, W., & Liu, X. (2020). Wheat Growth Monitoring and Yield Estimation based on Multi-Rotor Unmanned Aerial Vehicle. *Remote Sensing*, *12*(3), Article 3. https://doi.org/10.3390/rs12030508

Funder, D., & Ozer, D. (2019). Evaluating effect size in psychological research: Sense and nonsense. *Advances in Methods and Practices in Psychological Science*, *2*, 251524591984720. https://doi.org/10.1177/2515245919847202

Geipel, J., Link, J., Wirwahn, J. A., & Claupein, W. (2016). A programmable aerial multispectral camera system for in-season crop biomass and nitrogen content estimation. *Agriculture*, *6*(1), Article 1. https://doi.org/10.3390/agriculture6010004

Geith, C., & Vignare, K. (2007). Access to education with online learning and open educational resources: Can they close the gap? *Journal of Asynchronous Learning Networks*, *12*(1). https://doi.org/10.24059/olj.v12i1.39

Geith, C., & Vignare, K. (2013). Agshare open knowledge: Improving rural communities through university student action research. *Journal of Asynchronous Learning Networks*, *17*(2). https://doi.org/10.24059/olj.v17i2.368

Geith, C., Vignare, K., Bourquin, L. D., & Thiagarajan, D. (2010). Designing corporate training in developing economies using open educational resources. *Journal of Asynchronous Learning Networks*, *14*(3). https://doi.org/10.24059/olj.v14i3.142

Gitelson, A., Kaufman, Y. J., & Merzlyak, M. N. (1996). Use of a green channel in remote sensing of global vegetation from EOS-MODIS. *Remote Sensing of Environment*, *58*(3), 289–298. https://doi.org/10.1016/S0034-4257(96)00072-7

Gitelson, A., & Merzlyak, M. (1994). Quantitative estimation of chlorophyll-a using reflectance spectra: Experiments with autumn chestnut and maple leaves. *Journal of Photochemistry and Photobiology B: Biology*, *22*(3), 247–252. https://doi.org/10.1016/1011-1344(93)06963-4

Gitelson, A., Viña, A., Arkebauer, T. J., Rundquist, D. C., Keydan, G., & Leavitt, B. (2003). Remote estimation of leaf area index and green leaf biomass in maize canopies. *Geophysical Research Letters*, *30*(5). https://doi.org/10.1029/2002GL016450

Han, X., Wei, Z., Chen, H., Zhang, B., Li, Y., & Du, T. (2021). Inversion of winter wheat growth parameters and yield under different water treatments based on UAV multispectral remote sensing. *Frontiers in Plant Science*, *12*. https://doi.org/10.3389/fpls.2021.609876

Hanson, M. (2022, July 15). *Average cost of college textbooks*. Education Data Initiative. https://educationdata.org/average-cost-of-college-textbooks

Hardin, E. E., Eschman, B., Spengler, E. S., Grizzell, J. A., Moody, A. T., Ross-Sheehy, S., & Fry, K. M. (2019). What happens when trained graduate student instructors switch to an open textbook? A controlled study of the impact on student learning outcomes. *Psychology Learning & Teaching*, *18*(1), 48–64. https://doi.org/10.1177/1475725718810909

Hendricks, C., Reinsberg, S. A., & Rieger, G. W. (2017). The adoption of an open textbook in a large physics course: An analysis of cost, outcomes, use, and perceptions. *The International Review of Research in Open and Distributed Learning*, *18*(4). https://doi.org/10.19173/irrodl.v18i4.3006

Herzig, P., Borrmann, P., Knauer, U., Klück, H.-C., Kilias, D., Seiffert, U., Pillen, K., & Maurer, A. (2021). Evaluation of RGB and multispectral unmanned aerial vehicle (UAV) imagery for high-throughput phenotyping and yield prediction in barley breeding. *Remote Sensing*, *13*(14), Article 14. https://doi.org/10.3390/rs13142670

Hilton III, J. L., Gaudet, D., Clark, P., Robinson, J., & Wiley, D. (2013). The adoption of open educational resources by one community college math department. *The International Review of Research in Open and Distributed Learning*, *14*(4), 37–50. https://doi.org/10.19173/irrodl.v14i4.1523

Hilton III, J., & Laman, C. (2012). One college's use of an open psychology textbook. *Open Learning: The Journal of Open, Distance and e-Learning*, *27*(3), 265–272. https://doi.org/10.1080/02680513.2012.716657

Holman, F. H., Riche, A. B., Michalski, A., Castle, M., Wooster, M. J., & Hawkesford, M. J. (2016). High throughput field phenotyping of wheat plant height and growth rate in field plot trials using UAV based remote sensing. *Remote Sensing*, *8*(12), Article 12. https://doi.org/10.3390/rs8121031

Huete, A., Liu, H., & van Leeuwen, W. (1997). *The use of vegetation indices in forested regions: Issues of linearity and saturation*. *4*, 1966–1968. https://doi.org/10.1109/IGARSS.1997.609169

Hunt, E. R., Hively, W. D., McCarty, G. W., Daughtry, C. S. T., Forrestal, P. J., Kratochvil, R. J., Carr, J. L., Allen, N. F., Fox-Rabinovitz, J. R., & Miller, C. D. (2011). NIR-green-blue high-resolution digital images for assessment of winter cover crop biomass. *GIScience & Remote Sensing*, *48*(1), 86–98. https://doi.org/10.2747/1548-1603.48.1.86

Jain, A. K., & Veeranjaneyulu, K. (2013). *Repository Of indian national agricultural research & education system (NARES): Open access to institutional knowledge*. http://hdl.handle.net/11599/1830

Jhangiani, R. S., Dastur, F. N., Le Grand, R., & Penner, K. (2018). As good or better than commercial textbooks: Students' perceptions and outcomes from using open digital and open print textbooks. *The Canadian Journal for the Scholarship of Teaching and Learning*, *9*(1). https://doi.org/10.5206/cjsotl-rcacea.2018.1.5

Jimenez-Berni, J. A., Deery, D. M., Rozas-Larraondo, P., Condon, A. (Tony) G., Rebetzke, G. J., James, R. A., Bovill, W. D., Furbank, R. T., & Sirault, X. R. R. (2018). High throughput determination of plant height, ground cover, and above-ground biomass in wheat with LiDAR. *Frontiers in Plant Science*, *9*. https://doi.org/10.3389/fpls.2018.00237

Kefauver, S. C., Vicente, R., Vergara-Díaz, O., Fernandez-Gallego, J. A., Kerfal, S., Lopez, A., Melichar, J. P. E., Serret Molins, M. D., & Araus, J. L. (2017). Comparative UAV and field phenotyping to assess yield and nitrogen use efficiency in hybrid and conventional barley. *Frontiers in Plant Science*, *8*. https://www.frontiersin.org/articles/10.3389/fpls.2017.01733

Kim, H., & Lee, J. H. (2022). SMART teacher lab: A learning platform for the professional development of EFL teachers. *Language Learning & Technology*, *26*(2), 25–37. https://doi.org/10125/73475

Kirchgessner, N., Liebisch, F., Yu, K., Pfeifer, J., Friedli, M., Hund, A., & Walter, A. (2017). The ETH field phenotyping platform FIP: A cable-suspended multi-sensor system. *Functional Plant Biology*, *44*(1), 154. https://doi.org/10.1071/FP16165

Kuleung, C., Baenziger, P. S., & Dweikat, I. (2003). Transferability of SSR markers among wheat, rye, and triticale. *Theoretical and Applied Genetics*, *108*(6), 1147–1150. https://doi.org/10.1007/s00122-003-1532-5

Kyratzis, A. C., Skarlatos, D. P., Menexes, G. C., Vamvakousis, V. F., & Katsiotis, A. (2017). Assessment of vegetation indices derived by UAV imagery for durum wheat phenotyping under a water limited and heat stressed mediterranean environment. *Frontiers in Plant Science*, *8*. https://doi.org/10.3389/fpls.2017.01114

Lande, R., & Thompson, R. (1990). Efficiency of marker-assisted selection in the improvement of quantitative traits. *Genetics*, *124*(3), 743–756. https://doi.org/10.1093/genetics/124.3.743

Levy, P. E., & Jarvis, P. G. (1999). Direct and indirect measurements of LAI in millet and fallow vegetation in HAPEX-Sahel. *Agricultural and Forest Meteorology*, *97*(3), 199–212. https://doi.org/10.1016/S0168-1923(98)00092-6

Li, W., Niu, Z., Chen, H., Li, D., Wu, M., & Zhao, W. (2016). Remote estimation of canopy height and aboveground biomass of maize using high-resolution stereo images from a low-cost unmanned aerial vehicle system. *Ecological Indicators*, *67*, 637–648. https://doi.org/10.1016/j.ecolind.2016.03.036

Liu, J., Zhu, Y., Tao, X., Chen, X., & Li, X. (2022). Rapid prediction of winter wheat yield and nitrogen use efficiency using consumer-grade unmanned aerial vehicles multispectral imagery. *Frontiers in Plant Science*, *13*. https://doi.org/10.3389/fpls.2022.1032170

Lu, N., Zhou, J., Han, Z., Li, D., Cao, Q., Yao, X., Tian, Y., Zhu, Y., Cao, W., & Cheng, T. (2019). Improved estimation of aboveground biomass in wheat from RGB imagery and point cloud data acquired with a low-cost unmanned aerial vehicle system. *Plant Methods*, *15*(1), Article 17. https://doi.org/10.1186/s13007-019-0402-3

Madec, S., Baret, F., de Solan, B., Thomas, S., Dutartre, D., Jezequel, S., Hemmerlé, M., Colombeau, G., & Comar, A. (2017). High-throughput phenotyping of plant height: Comparing unmanned aerial vehicles and ground LiDAR estimates. *Frontiers in Plant Science*, *8*. https://doi.org/10.3389/fpls.2017.02002

Martin, V. (2022). *The complete guide to open scholarship*. Libraries Unlimited an imprint of ABC-CLIO, LLC.

Mergoum, M., & Gómez Macpherson, H. (Eds.). (2004). *Triticale improvement and production*. Food and Agriculture Organization of the United Nations.

Mergoum, M., Singh, P. K., Peña, R. J., Lozano-del Río, A. J., Cooper, K. V., Salmon, D. F., & Gómez Macpherson, H. (2009). Triticale: A “new” crop with old challenges. In M. J. Carena (Ed.), *Cereals* (Vol. 3, pp. 267–287). Springer US. https://doi.org/10.1007/978-0-387-72297-9_9

Merkel, E., & Cohen, A. (2015). OER usage by instructional designers and training managers in corporations. *Interdisciplinary Journal of E-Skills and Lifelong Learning*, *11*, 237–256. https://doi.org/10.28945/2307

Meuwissen, T. H. E., Hayes, B. J., & Goddard, M. E. (2001). Prediction of total genetic value using genome-wide dense marker maps. *Genetics*, *157*(4), 1819–1829. https://doi.org/10.1093/genetics/157.4.1819

Mihaylov, R., Atanasov, A., Stoyanov, H., & Paskaleva, S. (2021). Study of the specifics of the spectral reflections of different varieties of cereals harvest 2021, obtained from the visible and near infrared (NIR) frequency range. *2021 International Conference Automatics and Informatics (ICAI)*, 89–92. https://doi.org/10.1109/ICAI52893.2021.9639766

Mueller-Sim, T., Jenkins, M., Abel, J., & Kantor, G. (2017). The Robotanist: A ground-based agricultural robot for high-throughput crop phenotyping. *2017 IEEE International Conference on Robotics and Automation (ICRA)*, 3634–3639. https://doi.org/10.1109/ICRA.2017.7989418

Mukaka, M. (2012). A guide to appropriate use of correlation coefficient in medical research. *Malawi Medical Journal : The Journal of Medical Association of Malawi*, *24*(3), 69–71.

Muniafu, M. M. (2013). Using OER as a tool for agribusiness management training for hard to reach rural farmer populations. *Journal of Asynchronous Learning Networks*, *17*(2). https://doi.org/10.24059/olj.v17i2.358

NAPB. (n.d.). *What is Plant Breeding?* National Association of Plant Breeders. https://www.plantbreeding.org/about-us/what-is-plant-breeding/

Noack, P. O. (2016). Estimating triticale dry matter yield in parcel plot trials from aerial and ground based spectral measurements. *IFAC-PapersOnLine*, *49*(16), 404–408. https://doi.org/10.1016/j.ifacol.2016.10.074

OECD. (2007). *Giving knowledge for free: The emergence of open educational resources*. OECD Publishing. https://doi.org/10.1787/9789264032125-en

Ostos-Garrido, F. J., de Castro, A. I., Torres-Sánchez, J., Pistón, F., & Peña, J. M. (2019). High-throughput phenotyping of bioethanol potential in cereals using UAV-based multi-spectral imagery. *Frontiers in Plant Science, 10*. https://www.frontiersin.org/articles/10.3389/fpls.2019.00948

Peña, J. m., Ostos-Garrido, F. j., Torres-Sánchez, J., Pistón, F., & de Castro, A. i. (2019). A UAV-based system for monitoring crop growth in wheat, barley and triticale phenotyping field trials. In *Precision agriculture ?19* (pp. 397–403). Wageningen Academic Publishers. https://doi.org/10.3920/978-90-8686-888-9_49

Petrosino, J. S., Dille, J. A., Holman, J. D., & Roozeboom, K. L. (2015). Kochia suppression with cover crops in Southwestern Kansas. *Crop, Forage & Turfgrass Management, 1*(1), 1–8. https://doi.org/10.2134/cftm2014.0078

Plaza, J., Criado, M., Sánchez, N., Pérez-Sánchez, R., Palacios, C., & Charfolé, F. (2021). UAV multispectral imaging potential to monitor and predict agronomic characteristics of different forage associations. *Agronomy, 11*(9), Article 9. https://doi.org/10.3390/agronomy11091697

Pounds, A., & Bostock, J. (2019). Open educational resources (OER) in higher education courses in aquaculture and fisheries: Opportunities, barriers, and future perspectives. *Aquaculture International*, *27*(3), 695–710. https://doi.org/10.1007/s10499-019-00355-9

Prabhakara, K., Hively, W. D., & McCarty, G. W. (2015). Evaluating the relationship between biomass, percent groundcover and remote sensing indices across six winter cover crop fields in Maryland, United States. *International Journal of*

Applied Earth Observation and Geoinformation, *39*, 88–102. https://doi.org/10.1016/j.jag.2015.03.002

Pugh, N. A., Horne, D. W., Murray, S. C., Carvalho Jr, G., Malambo, L., Jung, J., Chang, A., Maeda, M., Popescu, S., Chu, T., Starek, M. J., Brewer, M. J., Richardson, G., & Rooney, W. L. (2018). Temporal estimates of crop growth in sorghum and maize breeding enabled by unmanned aerial systems. *The Plant Phenome Journal*, *1*(1), 1–10. https://doi.org/10.2135/tppj2017.08.0006

Roth, R. T., Chen, K., Scott, J. R., Jung, J., Yang, Y., Camberato, J. J., & Armstrong, S. D. (2023). Prediction of cereal rye cover crop biomass and nutrient accumulation using multi-temporal unmanned aerial vehicle based visible-spectrum vegetation indices. *Remote Sensing*, *15*(3), Article 3. https://doi.org/10.3390/rs15030580

Rouse, J. W., Haas, R. H., Schell, J. A., & Deering, D. W. (1974). *Monitoring vegetation systems in the Great Plains with ERTS.*

Sax, K. (1923). The association of size differences with seed-coat pattern and pigmentation in *Phaseolus Vulgaris. Genetics*, *8*(6), 552–560. https://doi.org/10.1093/genetics/8.6.552

Tucker, C. J. (1979). Red and photographic infrared linear combinations for monitoring vegetation. *Remote Sensing of Environment*, *8*(2), 127–150. https://doi.org/10.1016/0034-4257(79)90013-0

UNESCO. (2023). *UNESCO's Mandate in OER*. Open Educational Resources. https://www.unesco.org/en/open-educational-resources/mandate

United Nations, DESA, Population Division. Licensed under Creative Commons license CC BY 3.0 IGO. United Nations, DESA Population Division. *World Population Prospects 2022*. http://population.un.org/wpp/

USDA. (2019). *Crop Production Historical Track Records.* (ISSN: 2157-8990). National Agricultural Statistics Service. https://www.nass.usda.gov/Publications/Todays_Reports/reports/croptr19.pdf

USDA. (n.d). *Extension.* National Institute of Food and Agriculture. http://www.nifa.usda.gov/about-nifa/how-we-work/extension

Virlet, N., Sabermanesh, K., Sadeghi-Tehran, P., & Hawkesford, M. J. (2017). Field Scanalyzer: An automated robotic field phenotyping platform for detailed crop monitoring. *Functional Plant Biology*, *44*(1), 143. https://doi.org/10.1071/FP16163

Walsh, O. S., Shafian, S., Marshall, J. M., Jackson, C., McClintick-Chess, J. R., Blanscet, S. M., Swoboda, K., Thompson, C., Belmont, K. M., & Walsh, W. L. (2018). Assessment of UAV based vegetation indices for nitrogen concentration estimation in spring wheat. *Advances in Remote Sensing*, *7*(2), Article 2. https://doi.org/10.4236/ars.2018.72006

Wang, C., Feng, M., Yang, W.-D., Ding, G.-W., Hui, S., Liang, Z.-Y., Xie, Y.-K., & Qiao, X.-X. (2016). Impact of spectral saturation on leaf area index and above ground biomass estimation of winter wheat. *Spectroscopy Letters*, *49*(4), 241–248. https://doi.org/10.1080/00387010.2015.1133652

Watson, D. J. (1947). Comparative physiological status on the growth of field crops: I. The effect of infection with beet yellows and beet mosaic viruses on the growth

and yield of the sugar-beet root crop. *Annals of Botony, 11*(1), 41–76. https://doi.org/10.1093/oxfordjournals.aob.a083148

Wilson, S. (1873). II. Wheat and rye hybrids. *Transactions of the Botanical Society of Edinburgh, 12*(1–4), 286–288. https://doi.org/10.1080/03746607309469536

Winitzky-Stephens, J. R., & Pickavance, J. (2017). Open educational resources and student course outcomes: A multilevel analysis. *The International Review of Research in Open and Distributed Learning, 18*(4). https://doi.org/10.19173/irrodl.v18i4.3118

Woebbecke, D. M., Meyer, G. E., Von Bargen, K., & Mortensen, D. A. (1995). Color indices for weed identification under various soil, residue, and lighting conditions. *American Society of Agricultural and Biological Engineers, 38*(1), 259–269. https://doi.org/10.13031/2013.27838

Yang, M., Hassan, M. A., Xu, K., Zheng, C., Rasheed, A., Zhang, Y., Jin, X., Xia, X., Xiao, Y., & He, Z. (2020). Assessment of water and nitrogen use efficiencies through UAV-based multispectral phenotyping in winter wheat. *Frontiers in Plant Science, 11*, 927. https://doi.org/10.3389/fpls.2020.00927

Yang, W., Feng, H., Zhang, X., Zhang, J., Doonan, J. H., Batchelor, W. D., Xiong, L., & Yan, J. (2020). Crop phenomics and high-throughput phenotyping: Past decades, current challenges, and future perspectives. *Molecular Plant, 13*(2), 187–214. https://doi.org/10.1016/j.molp.2020.01.008

Yuan, M., Burjel, J. C., Isermann, J., Goeser, N. J., & Pittelkow, C. M. (2019). Unmanned aerial vehicle–based assessment of cover crop biomass and nitrogen

uptake variability. *Journal of Soil and Water Conservation*, *74*(4), 350–359. https://doi.org/10.2489/jswc.74.4.350

APPENDIX A

Table A1

Mead Genotypes Sampled on Date One 2022

Name
NT13443
NE03T416-1*
NT14433*
NT17441*
NT17442
NT19441
NT19443*
NT20401
NT20409
NT20417*
NT20429
NT20432*
NT21409
NT21414
NT21436
NT21440
NT21443
NT441*
OVERLAND

Note. An asterisk (*) denotes correct genotypes that were sampled on all other dates and locations in 2022.

Table A2

Lincoln 05/18/22 Manual Sampling Data

Genotype	Plot ID	Fresh weight (kg/hec)	Dry Weight (kg/hec)	Leaf Area Index	Height (cm)
NE03T416-3	1004	26746.38	3710.31	5.94	78.00
NT14433	1005	47856.63	6956.34	5.93	90.00
NT441	1006	52745.78	7359.67	6.73	88.00
NT17441	1009	34915.29	5453.29	6.33	93.33
NT19443	1011	62411.25	7910.83	9.31	97.33
NT12404-1	1012	38305.27	5062.93	6.65	98.00
NT20417	1015	46960.50	5975.92	6.33	102.00
NT14407	1022	40041.76	5645.22	8.64	92.67
NE03T416-1	1023	51024.85	6344.23	9.26	87.00
NT20432	1029	40531.98	4699.81	7.81	87.33
NT12404-1	1032	38357.15	5401.41	8.44	86.67
NE03T416-1	1035	53617.27	6973.20	9.27	96.33
NT441	1038	38892.75	6236.59	9.52	83.33
NE03T416-3	1040	43861.02	5706.17	8.31	94.00
NT20417	1046	39915.97	5724.33	7.66	99.00
NT19443	1051	49559.40	6266.41	10.23	100.33
NT14407	1055	51432.06	7169.03	9.76	89.00
NT14433	1056	43722.25	6799.42	8.63	108.00
NT20432	1059	64698.91	7848.58	8.20	90.00
NT17441	1060	70777.28	9448.90	8.26	98.00
NE03T416-3	1062	24616.94	2842.71	8.69	88.67
NT20432	1063	55247.42	6550.43	7.08	85.33
NT14407	1065	34366.72	4029.34	7.05	95.00
NT12404-1	1067	45086.54	6685.30	8.20	96.00
NE03T416-1	1071	25856.74	3706.42	8.55	103.00
NT14433	1074	57336.65	8401.04	8.47	104.67
NT20417	1075	61162.38	8450.32	8.06	107.67
NT17441	1079	60249.39	8919.78	8.46	88.00
NT19443	1081	66418.54	8812.15	9.93	94.67
NT441	1082	31673.14	3680.48	7.84	88.33

Table A3

Lincoln 06/02/2022 Manual Sampling Data

Genotype	Plot ID	Fresh Weight (kg/hec)	Dry Weight (kg/hec)	Leaf Area Index	Height (cm)
NE03T416-3	1004	29111.85	7848.58	5.20	108.33
NT14433	1005	21413.71	6524.49	5.07	139.33
NT441	1006	30862.61	7275.37	5.77	129.67
NT17441	1009	47453.30	12731.25	4.31	127.67
NT19443	1011	26765.84	6982.28	6.47	120.00
NT12404-1	1012	39143.04	11097.21	6.05	122.67
NT20417	1015	37662.03	10916.94	5.09	124.67
NT14407	1022	29043.12	8459.40	6.01	122.00
NE03T416-1	1023	47467.57	13414.69	6.00	112.67
NT20432	1029	38516.66	9673.26	6.21	111.67
NT12404-1	1032	40439.90	10435.81	4.96	110.00
NE03T416-1	1035	32733.97	8831.60	6.55	126.33
NT441	1038	31905.28	7881.00	4.77	114.67
NE03T416-3	1040	29168.91	8423.09	5.89	112.67
NT20417	1046	46353.57	12972.46	5.51	122.33
NT19443	1051	36079.87	8419.20	6.39	133.67
NT14407	1055	23121.67	6053.73	6.17	119.67
NT14433	1056	32639.30	9017.05	5.77	149.33
NT20432	1059	38494.61	9681.04	6.13	128.33
NT17441	1060	39744.78	10712.04	5.80	122.67
NE03T416-3	1062	28795.42	7555.49	6.17	114.33
NT20432	1063	17580.20	4168.10	5.52	115.00
NT14407	1065	24178.61	6371.46	5.44	121.33
NT12404-1	1067	29889.97	7630.71	5.64	116.67
NE03T416-1	1071	48817.60	12683.26	5.58	138.67
NT14433	1074	39996.37	10459.15	5.15	130.00
NT20417	1075	26895.52	6890.20	5.66	149.33
NT17441	1079	42950.62	10516.22	5.60	111.67
NT19443	1081	38862.92	10306.12	6.28	121.67
NT441	1082	40519.01	9360.72	5.93	134.00

Table A4

Lincoln 06/27/22 Manual Sampling Data

Genotype	Plot ID	Fresh Weight (kg/hec)	Dry Weight (kg/hec)	Leaf Area Index	Height (cm)
NE03T416-3	1004	23932.20	12884.28	2.69	102.00
NT14433	1005	19998.84	11117.96	3.33	127.00
NT441	1006	30994.89	12759.78	2.70	127.67
NT17441	1009	36350.91	19052.13	3.73	124.67
NT19443	1011	27253.45	13750.58	3.22	114.00
NT12404-1	1012	26000.69	14309.52	3.73	111.67
NT20417	1015	24026.87	14068.31	2.83	113.00
NT14407	1022	23742.86	13619.59	3.00	113.33
NE03T416-1	1023	32892.19	18998.96	3.37	108.00
NT20432	1029	36589.53	17912.19	3.63	112.33
NT12404-1	1032	23580.76	15939.67	3.63	107.33
NE03T416-1	1035	29263.58	17386.96	3.66	127.33
NT441	1038	12407.03	5956.47	2.83	114.33
NE03T416-3	1040	22403.21	14245.98	3.48	106.33
NT20417	1046	14924.23	9644.73	4.00	116.00
NT19443	1051	31176.45	16122.53	3.87	131.00
NT14407	1055	18883.54	12200.83	3.23	111.67
NT14433	1056	19104.00	11477.19	3.20	130.00
NT20432	1059	37492.14	20561.67	3.76	123.33
NT17441	1060	45432.80	23414.76	4.46	117.67
NE03T416-3	1062	23322.68	13152.73	3.08	108.00
NT20432	1063	16396.17	8799.18	3.46	111.33
NT14407	1065	23955.55	12698.83	3.66	118.33
NT12404-1	1067	22644.42	17598.35	3.14	112.33
NE03T416-1	1071	29944.43	16802.08	3.60	132.33
NT14433	1074	2352.50	12745.51	3.32	118.33
NT20417	1075	24819.25	13134.57	3.73	129.67
NT17441	1079	27144.52	12410.92	3.56	105.67
NT19443	1081	26863.10	13418.58	3.90	114.67
NT441	1082	36109.69	17910.90	3.62	136.00

Table A5

Mead 05/18/22 Manual Sampling Data

Genotype	Plot ID	Fresh Weight (kg/hec)	Dry Weight (kg/hec)	Leaf Area Index	Height (cm)
NT21409	1004	15816.47	3103.38	1.23	69.67
NT13443	1005	6856.48	1145.12	1.39	61.00
NT441	1006	24508.01	3839.99	1.25	66.67
NT17441	1009	19646.09	3261.60	2.56	59.33
NT20417	1011	26218.56	5003.28	2.14	62.00
NT19443	1012	15241.96	2569.07	2.96	67.00
NT21443	1015	14284.88	2780.46	2.04	69.67
NE03T416-1	1022	32315.09	5571.30	2.44	64.00
NT21414	1023	24915.61	4267.96	1.57	70.33
NT20401	1029	18363.50	3303.10	2.61	71.33
NT20409	1032	8176.68	1342.25	3.46	46.00
NT21409	1035	11848.09	2163.16	1.91	74.33
NT14433	1038	11509.61	1867.47	3.57	76.33
OVERLAND	1040	8725.26	1704.07	2.51	74.33
NE03T416-1	1046	19273.89	3270.67	2.31	61.33
NT21440	1051	19113.08	3389.98	2.68	79.00
NT20432	1055	14823.08	2377.14	2.26	76.00
NT19443	1056	24138.40	4341.88	2.25	68.00
NT20429	1059	38725.45	6757.92	3.20	63.67
NT21436	1060	29316.75	5306.74	3.23	73.00
NT441	1062	43612.01	6820.17	5.02	87.00
NT19441	1063	20967.59	3671.40	5.03	86.00
NT20417	1065	20136.30	3493.73	3.52	81.00
NT21409	1067	38135.38	6953.75	4.27	80.67
NT20401	1071	34910.10	7312.98	4.26	94.00
OVERLAND	1074	24631.21	4370.41	4.60	86.33
NT17442	1075	36375.55	5659.48	4.23	72.67
NT20409	1079	33932.27	6523.19	4.70	77.67
NT21440	1081	34906.21	5511.64	6.26	91.00
NE03T416-1	1082	42651.04	7126.23	6.16	87.33

Table A6

Mead 06/02/22 Manual Sampling Data

Genotype	Plot ID	Fresh Weight (kg/hec)	Dry Weight (kg/hec)	Leaf Area Index	Height (cm)
NT441	1006	9716.05	2430.31	1.68	100.00
NT17441	1009	27284.58	6097.82	2.63	109.33
NT20417	1011	11047.93	2986.66	2.58	105.00
NT19443	1012	21422.78	5379.36	3.16	105.00
NT14407	1016	25046.20	7004.33	2.13	103.00
NT12404-1	1017	22838.95	6281.98	3.47	104.33
NE03T416-3	1018	26940.91	7322.06	3.27	100.33
NT14433	1019	16189.97	4219.97	3.58	124.00
NE03T416-1	1022	30511.16	8576.12	2.94	95.33
NT20432	1025	24524.87	4746.50	3.73	113.67
NT441	1031	20089.62	4483.24	5.54	114.00
NT12404-1	1033	41011.81	11819.56	2.31	106.00
NT20417	1036	41871.63	13549.56	2.49	104.67
NT14433	1038	17654.12	4852.84	3.36	119.33
NT17441	1039	33368.14	7411.54	2.41	110.00
NE03T416-1	1046	30342.57	8530.73	2.13	99.00
NT14407	1049	26180.95	6297.54	1.88	100.67
NE03T416-3	1052	35332.88	7449.15	3.01	99.33
NT20432	1055	8312.85	425.37	1.95	101.33
NT19443	1056	27462.25	5738.59	2.81	100.00
NT441	1062	30520.24	6860.37	4.27	118.67
NT20417	1065	45017.81	11761.20	3.21	117.00
NE03T416-3	1066	63294.41	15934.48	3.61	104.67
NT20432	1072	45659.75	10001.36	4.21	112.33
NT19443	1073	51587.68	12045.21	4.50	116.00
NT14407	1080	32746.94	8605.94	4.44	117.67
NE03T416-1	1082	28012.12	6838.33	5.34	114.67
NT14433	1085	40821.18	10670.54	3.48	146.00
NT17441	1088	40796.53	10402.09	3.95	133.67
NT12404-1	1089	34456.20	8699.32	3.50	113.00

Table A7

Mead 06/27/22 Manual Sampling Data

Genotype	Plot ID	Fresh Weight (kg/hec)	Dry Weight (kg/hec)	Leaf Area Index	Height (cm)
NT441	1006	37860.45	15764.60	2.10	113.33
NT17441	1009	43851.93	18743.48	2.21	121.00
NT20417	1011	22497.88	11363.06	2.43	106.67
NT19443	1012	27904.48	12955.60	2.26	100.00
NT14407	1016	14316.01	7001.73	1.86	100.00
NT12404-1	1017	38291.01	22146.43	2.98	100.00
NE03T416-3	1018	31922.14	16995.31	2.41	104.00
NT14433	1019	31609.60	16269.07	2.56	115.33
NE03T416-1	1022	30681.05	15975.98	2.70	93.33
NT20432	1025	43558.84	20626.51	2.58	103.33
NT441	1031	42736.63	18707.17	4.20	120.33
NT12404-1	1033	18122.28	10035.08	2.37	99.67
NT20417	1036	28843.40	14594.83	1.55	97.00
NT14433	1038	41061.09	22522.52	2.72	125.00
NT17441	1039	63614.74	27287.17	3.01	119.33
NE03T416-1	1046	44622.26	21658.81	2.46	96.67
NT14407	1049	40525.49	20793.81	2.01	102.67
NE03T416-3	1052	49608.68	24122.84	2.27	95.33
NT20432	1055	27738.48	12504.30	1.90	94.33
NT19443	1056	36636.22	18424.45	2.38	107.33
NT441	1062	53025.90	24688.27	3.33	117.33
NT20417	1065	45930.79	23570.38	2.17	109.33
NE03T416-3	1066	42341.09	20303.60	2.54	102.00
NT20432	1072	39884.84	20896.26	3.35	108.00
NT19443	1073	41316.57	20538.33	2.97	110.67
NT14407	1080	28722.79	15643.99	3.38	114.33
NE03T416-1	1082	35243.39	19503.44	3.95	112.00
NT14433	1085	35070.91	19714.82	4.05	130.67
NT17441	1088	42914.30	23157.98	3.87	123.33
NT12404-1	1089	30878.17	20382.71	3.72	113.33

Table A8

Lincoln 05/10/23 Manual Sampling Data

Genotype	Plot ID	Fresh Weight (kg/hec)	Dry Weight (kg/hec)	Leaf Area Index	Height (cm)
NT19443	1001	958.38	271.04	0.08	19.33
NT14433	1002	1669.06	364.42	0.22	20.00
NT441	1009	1608.10	343.67	0.32	21.00
NT14407	1018	2117.77	470.76	0.32	22.67
NT12404-1	1021	1425.25	291.79	0.19	21.67
NE03T416-3	1024	2094.42	481.13	0.36	23.67
NT19441	1026	2191.69	470.76	0.28	22.67
NE03T416-1	1027	1427.84	339.78	0.15	21.00
NT21436	1030	3082.63	654.91	0.35	21.67
NT20427	1033	2844.01	634.16	0.24	24.00
NT21436	1049	1744.27	379.98	0.27	26.00
NT441	1052	2767.49	560.24	0.08	23.00
NT14407	1054	1416.17	330.70	0.31	24.67
NT20427	1057	2902.37	623.79	0.26	26.00
NT14433	1065	2473.11	507.07	0.25	19.00
NE03T416-1	1066	5060.34	1130.86	0.45	22.67
NT19441	1074	2794.73	556.35	0.36	25.00
NE03T416-3	1075	2124.25	539.49	0.21	25.00
NT19443	1077	3185.08	661.40	0.37	26.67
NT12404-1	1078	2618.35	577.10	0.17	28.00
NT20427	1086	2681.90	591.37	0.22	19.67
NT19441	1094	2074.97	452.60	0.45	22.33
NT14433	1095	1593.84	348.85	0.12	21.00
NE03T416-1	1097	1059.53	252.89	0.29	22.00
NE03T416-3	1102	3335.52	680.85	0.28	22.67
NT21436	1104	2997.04	647.13	0.24	21.67
NT441	1105	1571.79	357.93	0.29	21.33
NT14407	1110	2763.60	590.07	0.11	23.67
NT12404-1	1111	880.57	237.32	0.14	20.67
NT19443	1118	2074.97	442.23	0.05	23.00

Table A9

Lincoln 05/22/23 Manual Sampling Data

Genotype	Plot ID	Fresh Weight (kg/hec)	Dry Weight (kg/hec)	Leaf Area Index	Height (cm)
NT19443	1001	6569.88	1359.11	0.77	65.00
NT14433	1002	11468.11	2496.45	0.76	54.67
NT441	1009	9024.83	2015.32	0.42	50.67
NT14407	1018	5820.30	1259.25	0.18	65.33
NT12404-1	1021	6639.91	1626.26	0.25	54.33
NE03T416-3	1024	8468.48	1969.93	0.74	57.00
NT19441	1026	5572.60	1256.65	0.65	62.00
NE03T416-1	1027	4142.16	941.52	0.42	58.00
NT21436	1030	10038.97	1959.55	0.51	58.00
NT20427	1033	6965.42	1735.19	0.64	58.00
NT21436	1049	13199.41	2736.37	0.39	63.33
NT441	1052	5579.08	1159.39	0.26	59.67
NT14407	1054	6713.83	1387.64	0.46	65.33
NT20427	1057	17696.91	4055.27	0.57	70.00
NT14433	1065	22066.03	4807.45	0.31	68.67
NE03T416-1	1066	14463.85	3312.17	1.04	67.33
NT19441	1074	11543.33	2489.97	0.56	61.33
NE03T416-3	1075	12763.67	2889.40	0.95	61.33
NT19443	1077	14376.96	3177.30	0.65	63.33
NT12404-1	1078	10275.00	2515.90	0.21	60.00
NT20427	1086	8899.03	2233.19	0.37	56.33
NT19441	1094	10522.70	2369.36	0.57	64.00
NT14433	1095	12261.79	2697.46	0.19	66.00
NE03T416-1	1097	10557.71	2313.59	0.39	57.67
NE03T416-3	1102	10348.92	2212.44	0.45	55.00
NT21436	1104	9651.21	2207.25	0.30	54.00
NT441	1105	13318.72	2923.12	0.60	55.33
NT14407	1110	7140.50	2170.94	0.23	65.33
NT12404-1	1111	8660.41	1571.79	0.18	59.33
NT19443	1118	12933.56	3130.61	0.17	59.33

Table A10

Lincoln 06/05/23 Manual Sampling Data

Genotype	Plot ID	Fresh Weight (kg/hec)	Dry Weight (kg/hec)	Leaf Area Index	Height (cm)
NT19443	1001	10736.68	3976.16	0.53	74.00
NT14433	1002	11190.58	4138.27	1.08	80.33
NT441	1009	17486.82	5182.24	0.32	72.00
NT14407	1018	9761.44	3204.53	0.60	76.00
NT12404-1	1021	10076.58	3736.25	0.46	67.00
NE03T416-3	1024	9074.11	3265.49	0.77	66.67
NT19441	1026	12474.47	4143.46	0.77	79.00
NE03T416-1	1027	6612.68	1999.75	0.55	72.67
NT21436	1030	13368.00	4347.07	1.02	79.00
NT20427	1033	8338.79	2963.32	0.67	69.00
NT21436	1049	11555.00	3898.35	0.34	85.67
NT441	1052	10892.30	3138.39	0.40	67.33
NT14407	1054	12694.94	3946.34	0.64	75.00
NT20427	1057	9529.31	3345.89	0.79	75.67
NT14433	1065	12134.69	4350.96	0.58	81.67
NE03T416-1	1066	10337.25	3479.47	0.86	76.33
NT19441	1074	8367.32	2710.43	1.15	80.67
NE03T416-3	1075	7568.46	2231.89	0.78	71.00
NT19443	1077	9761.44	3373.13	0.51	71.67
NT12404-1	1078	8385.48	2872.54	0.52	67.00
NT20427	1086	14628.55	5265.24	0.35	71.00
NT19441	1094	7620.33	2821.96	0.71	73.33
NT14433	1095	9627.87	3362.75	0.22	83.00
NE03T416-1	1097	6472.61	2348.61	0.38	70.00
NE03T416-3	1102	9498.18	3281.05	0.81	64.67
NT21436	1104	11969.99	3624.72	0.31	74.67
NT441	1105	10653.68	2885.51	0.93	75.67
NT14407	1110	13567.72	4813.93	0.23	73.33
NT12404-1	1111	5289.88	1867.47	0.40	68.00
NT19443	1118	8465.88	3275.86	0.26	67.33

Table A11

Mead 05/10/23 Manual Sampling Data

Genotype	Plot ID	Fresh Weight (kg/hec)	Dry Weight (kg/hec)	Leaf Area Index	Height (cm)
NT12404-1	1003	1198.30	254.18	0.24	17.00
NT14407	1006	3321.25	676.96	0.47	21.00
NE03T416-3	1012	1556.23	346.26	0.83	27.00
NT19443	1014	2678.01	538.20	0.63	25.00
NT441	1018	3120.24	597.85	0.45	21.33
NE03T416-1	1022	3679.18	778.11	0.62	24.33
NT20427	1027	2657.26	551.16	0.49	25.00
NT21436	1033	4440.44	966.16	0.76	30.33
NT19441	1035	3607.86	757.36	0.71	33.33
NT14433	1039	4174.58	868.89	0.76	27.33
NT14407	1041	2911.44	591.37	0.55	110.67
NT14433	1046	3041.13	614.71	0.85	26.67
NT441	1050	3155.25	601.74	0.73	23.33
NT19443	1053	1742.98	335.89	0.62	28.67
NT21436	1057	3437.97	695.12	0.58	25.67
NT20427	1064	2679.31	522.63	0.43	27.33
NE03T416-3	1071	3616.93	722.35	0.66	28.00
NT12404-1	1075	3436.67	667.88	0.26	27.00
NE03T416-1	1077	4028.04	791.08	0.69	26.33
NT19441	1079	9486.51	2182.61	2.16	40.33
NT19443	1083	1653.49	334.59	0.59	27.67
NT441	1086	3960.60	837.77	1.13	24.67
NT14433	1092	1338.36	263.26	0.66	26.00
NT19441	1094	6279.38	1369.48	0.68	27.33
NT14407	1101	3229.17	651.02	0.56	31.33
NE03T416-1	1102	1827.27	391.65	0.47	27.67
NT20427	1103	2414.75	509.66	0.57	29.00
NT12404-1	1105	1403.20	296.98	0.23	21.00
NE03T416-3	1107	2746.74	588.77	0.47	22.67
NT21436	1119	3584.51	779.41	0.81	24.33

Table A12

Mead 05/22/23 Manual Sampling Data

Genotype	Plot ID	Fresh Weight (kg/hec)	Dry Weight (kg/hec)	Leaf Area Index	Height (cm)
NT12404-1	1003	7480.27	1784.48	0.39	50.33
NT14407	1006	9601.93	2508.12	0.79	50.33
NE03T416-3	1012	9739.40	2434.20	1.24	52.00
NT19443	1014	10915.65	2439.39	0.96	48.33
NT441	1018	12325.33	2744.15	1.30	50.33
NE03T416-1	1022	12003.71	3144.88	0.59	52.33
NT20427	1027	8876.99	2208.55	0.87	50.67
NT21436	1033	11101.10	2864.76	0.90	54.00
NT19441	1035	11102.39	2596.31	1.34	57.67
NT14433	1039	20315.27	4659.61	1.24	56.67
NT14407	1041	11902.56	3029.46	0.80	55.67
NT14433	1046	19179.22	4108.44	1.15	51.33
NT441	1050	12656.03	3072.25	0.92	57.67
NT19443	1053	8338.79	1982.89	1.13	52.00
NT21436	1057	16082.33	3626.01	0.89	51.00
NT20427	1064	12106.16	2727.29	0.94	50.67
NE03T416-3	1071	12582.11	2736.37	0.77	47.33
NT12404-1	1075	13115.12	2815.48	0.99	48.00
NE03T416-1	1077	13951.59	3052.80	1.31	56.67
NT19441	1079	20306.19	5610.20	2.52	73.67
NT19443	1083	12050.40	2570.37	1.20	61.00
NT441	1086	15863.16	3439.27	2.00	56.67
NT14433	1092	11863.65	2693.57	1.17	56.33
NT19441	1094	11477.19	2698.76	0.98	61.67
NT14407	1101	9717.35	2235.78	0.49	62.00
NE03T416-1	1102	9983.21	2371.95	1.02	57.00
NT20427	1103	10884.52	2567.78	0.76	54.67
NT12404-1	1105	6786.45	1583.46	0.23	52.33
NE03T416-3	1107	11234.67	2563.89	0.82	63.00
NT21436	1119	9837.96	2497.75	1.14	65.33

Table A13

Mead 06/05/23 Manual Sampling Data

Genotype	Plot ID	Fresh Weight (kg/hec)	Dry Weight (kg/hec)	Leaf Area Index	Height (cm)
NT12404-1	1003	6266.41	1811.71	0.00	68.33
NT14407	1006	11609.47	4007.29	0.62	75.33
NE03T416-3	1012	9494.29	2978.88	0.79	79.67
NT19443	1014	7272.78	2317.48	0.92	84.00
NT441	1018	16363.74	5567.41	0.82	91.67
NE03T416-1	1022	10905.27	3754.40	0.54	75.67
NT20427	1027	8962.58	2995.74	0.57	76.33
NT21436	1033	15528.57	5175.76	0.53	84.33
NT19441	1035	11680.79	3876.31	0.54	92.33
NT14433	1039	11414.94	3799.79	0.47	96.33
NT14407	1041	11766.39	4151.24	0.03	74.67
NT14433	1046	11592.61	4063.05	0.08	95.67
NT441	1050	16199.04	4575.31	0.05	89.00
NT19443	1053	10950.66	3475.58	0.04	73.00
NT21436	1057	9784.79	3081.33	0.01	82.33
NT20427	1064	9857.41	3427.59	0.00	78.67
NE03T416-3	1071	10778.18	3819.24	0.00	74.00
NT12404-1	1075	8799.18	2964.62	0.01	78.00
NE03T416-1	1077	10933.80	3847.78	0.24	77.00
NT19441	1079	15724.39	5751.56	0.66	91.00
NT19443	1083	15282.17	4935.84	0.25	76.00
NT441	1086	15502.63	4885.26	0.99	91.33
NT14433	1092	12840.18	4524.73	0.47	87.67
NT19441	1094	15401.48	4821.72	0.61	93.33
NT14407	1101	12867.42	4623.30	0.50	82.67
NE03T416-1	1102	11497.94	3996.91	0.54	80.00
NT20427	1103	8560.55	3003.52	0.40	79.67
NT12404-1	1105	7853.77	2631.32	0.13	80.00
NE03T416-3	1107	13065.84	4712.78	0.08	81.67
NT21436	1119	9498.18	3465.20	0.27	88.67

Table A14

MicaSense Altum Multispectral Sensor Specifications

Spectral Band	Wavelength Center and Bandwidth (nm)
Red	668 ± 14
Green	560 ± 27
Blue	475 ± 32
Red Edge	717 ± 12
Near Infrared	842 ± 57

Note. The wavelength center is the center of the spectral band. Bandwidth is the range of frequencies.

Table A15

DJI Mavic 3M Multispectral Sensor Specifications

Spectral Band	Wavelength Center and Bandwidth (nm)
Red	650 ± 16
Green	560 ± 16
Red Edge	730 ± 16
Near Infrared	860 ± 26

Note. The wavelength center is the center of the spectral band. Bandwidth is the range of frequencies.

Table A16

Pixel Threshold Values for ExG Segmentation

Date	Lincoln	Mead
5/18/22	0.02	0.03
6/2/22	0.02	0.03
6/27/22	0.01	0.002
5/10/23	0.03	0.02
5/22/23	0.004	0.004
6/5/23	0.008	0.01

Note. Every pixel within plot boundaries was compared to the threshold value for its respective location. Values above the threshold were counted as vegetation and values below the threshold were counted as not vegetation. The pixel percent vegetation index is a ratio of these vegetation pixels to total pixels within the plot boundary.

Table A17

Lincoln 05/18/22 Vegetation Index Values

Genotype	Plot ID	NDVI	GNDVI	NDRE	GRVI	GRVIRE	GCI	RCI	Pixel Percent
NE03T416-3	1004	0.912	0.802	0.602	0.420	-0.391	8.558	3.120	0.881
NT14433	1005	0.917	0.807	0.604	0.431	-0.402	8.904	3.154	0.898
NT441	1006	0.916	0.796	0.597	0.456	-0.389	8.668	3.128	0.879
NT17441	1009	0.922	0.815	0.615	0.440	-0.408	9.475	3.317	0.879
NT19443	1011	0.928	0.825	0.641	0.454	-0.397	10.185	3.727	0.895
NT12404-1	1012	0.942	0.845	0.658	0.487	-0.425	11.537	3.970	0.884
NT20417	1015	0.928	0.819	0.623	0.461	-0.406	9.601	3.405	0.892
NT14407	1022	0.928	0.828	0.642	0.439	-0.401	10.163	3.699	0.902
NE03T416-1	1023	0.929	0.826	0.635	0.450	-0.406	10.029	3.591	0.904
NT20432	1029	0.930	0.828	0.637	0.450	-0.411	10.284	3.628	0.889
NT12404-1	1032	0.938	0.845	0.661	0.461	-0.421	11.501	4.022	0.894
NE03T416-1	1035	0.928	0.824	0.635	0.452	-0.400	9.850	3.576	0.900
NT441	1038	0.923	0.810	0.618	0.459	-0.392	9.260	3.374	0.897
NE03T416-3	1040	0.929	0.830	0.644	0.443	-0.405	10.411	3.737	0.895
NT20417	1046	0.928	0.817	0.622	0.471	-0.402	9.448	3.389	0.903
NT19443	1051	0.930	0.832	0.652	0.441	-0.399	10.586	3.894	0.902
NT14407	1055	0.933	0.833	0.648	0.460	-0.407	10.562	3.797	0.900
NT14433	1056	0.933	0.830	0.641	0.471	-0.410	10.330	3.674	0.897
NT20432	1059	0.939	0.832	0.644	0.505	-0.411	10.625	3.756	0.883
NT17441	1060	0.933	0.825	0.633	0.483	-0.409	10.148	3.572	0.888
NE03T416-3	1062	0.925	0.828	0.642	0.427	-0.402	10.199	3.705	0.899
NT20432	1063	0.929	0.831	0.642	0.438	-0.409	10.394	3.711	0.878
NT14407	1065	0.922	0.819	0.630	0.432	-0.395	9.601	3.520	0.895
NT12404-1	1067	0.943	0.846	0.663	0.492	-0.422	11.683	4.073	0.894
NE03T416-1	1071	0.929	0.828	0.641	0.446	-0.403	10.218	3.692	0.900
NT14433	1074	0.930	0.832	0.643	0.440	-0.412	10.597	3.732	0.881
NT20417	1075	0.929	0.823	0.630	0.462	-0.405	9.881	3.523	0.890
NT17441	1079	0.932	0.827	0.637	0.480	-0.408	10.295	3.654	0.887
NT19443	1081	0.929	0.829	0.648	0.446	-0.397	10.334	3.815	0.895
NT441	1082	0.925	0.810	0.619	0.474	-0.393	9.470	3.423	0.893

Note. Normalized index values range from -1 to +1. A number closer to +1 indicates healthy vegetation. The spectral bands used to calculate GRVIRE cause the relationship to be inverse. A GRVIRE value closer to -1 indicates healthy vegetation and a number closer to +1 indicates unhealthy or no vegetation. GCI and RCI are not normalized indices, so they are not bound by the -1 to +1 scale.

Table A18

Lincoln 06/02/22 Vegetation Index Values

Genotype	Plot ID	NDVI	GNDVI	NDRE	GRVI	GRVIRE	GCI	RCI	Pixel Percent
NE03T416-3	1004	0.860	0.768	0.568	0.276	-0.358	6.821	2.675	0.900
NT14433	1005	0.874	0.782	0.577	0.301	-0.377	7.394	2.771	0.893
NT441	1006	0.888	0.795	0.594	0.323	-0.383	8.009	2.984	0.904
NT17441	1009	0.878	0.781	0.576	0.311	-0.375	7.292	2.750	0.898
NT19443	1011	0.889	0.796	0.601	0.321	-0.376	7.961	3.043	0.904
NT12404-1	1012	0.891	0.814	0.623	0.284	-0.390	8.984	3.351	0.900
NT20417	1015	0.884	0.796	0.599	0.304	-0.378	7.978	3.024	0.901
NT14407	1022	0.881	0.796	0.602	0.288	-0.375	7.972	3.059	0.904
NE03T416-1	1023	0.874	0.787	0.591	0.281	-0.368	7.533	2.921	0.903
NT20432	1029	0.883	0.792	0.599	0.305	-0.370	7.785	3.019	0.902
NT12404-1	1032	0.896	0.822	0.636	0.284	-0.392	9.471	3.549	0.900
NE03T416-1	1035	0.885	0.798	0.606	0.302	-0.373	8.039	3.109	0.904
NT441	1038	0.901	0.808	0.612	0.346	-0.388	8.555	3.194	0.904
NE03T416-3	1040	0.884	0.795	0.603	0.301	-0.372	7.954	3.074	0.901
NT20417	1046	0.892	0.803	0.606	0.315	-0.387	8.396	3.128	0.904
NT19443	1051	0.900	0.813	0.625	0.328	-0.383	8.839	3.372	0.903
NT14407	1055	0.897	0.809	0.613	0.321	-0.389	8.604	3.206	0.902
NT14433	1056	0.897	0.810	0.609	0.323	-0.397	8.661	3.151	0.907
NT20432	1059	0.892	0.802	0.611	0.318	-0.377	8.314	3.187	0.904
NT17441	1060	0.892	0.800	0.600	0.326	-0.387	8.212	3.042	0.902
NE03T416-3	1062	0.882	0.797	0.606	0.291	-0.373	8.058	3.113	0.904
NT20432	1063	0.888	0.803	0.611	0.300	-0.380	8.353	3.174	0.902
NT14407	1065	0.894	0.806	0.612	0.318	-0.384	8.473	3.189	0.904
NT12404-1	1067	0.894	0.819	0.631	0.283	-0.392	9.312	3.470	0.894
NE03T416-1	1071	0.882	0.792	0.598	0.301	-0.371	7.801	3.010	0.904
NT14433	1074	0.893	0.804	0.605	0.319	-0.389	8.340	3.092	0.903
NT20417	1075	0.893	0.802	0.610	0.321	-0.380	8.328	3.163	0.904
NT17441	1079	0.896	0.802	0.607	0.338	-0.382	8.295	3.127	0.903
NT19443	1081	0.899	0.812	0.624	0.323	-0.383	8.806	3.358	0.906
NT441	1082	0.905	0.813	0.619	0.352	-0.394	8.982	3.303	0.904

Note. Normalized index values range from -1 to +1. A number closer to +1 indicates healthy vegetation. The spectral bands used to calculate GRVIRE cause the relationship to be inverse. A GRVIRE value closer to -1 indicates healthy vegetation and a number closer to +1 indicates unhealthy or no vegetation. GCI and RCI are not normalized indices, so they are not bound by the -1 to +1 scale.

Table A19

Lincoln 06/27/22 Vegetation Index Values

Genotype	Plot ID	NDVI	GNDVI	NDRE	GRVI	GRVIRE	GCI	RCI	Pixel Percent
NE03T416-3	1004	0.399	0.514	0.224	-0.144	-0.329	2.170	0.586	0.234
NT14433	1005	0.445	0.547	0.242	-0.134	-0.353	2.472	0.647	0.401
NT441	1006	0.569	0.627	0.325	-0.087	-0.381	3.446	0.978	0.643
NT17441	1009	0.470	0.547	0.245	-0.103	-0.352	2.500	0.659	0.660
NT19443	1011	0.484	0.563	0.264	-0.106	-0.354	2.665	0.729	0.617
NT12404-1	1012	0.368	0.517	0.208	-0.185	-0.349	2.212	0.530	0.054
NT20417	1015	0.430	0.546	0.236	-0.151	-0.358	2.470	0.625	0.221
NT14407	1022	0.444	0.537	0.235	-0.121	-0.347	2.390	0.624	0.526
NE03T416-1	1023	0.369	0.489	0.196	-0.145	-0.325	1.960	0.494	0.285
NT20432	1029	0.429	0.531	0.232	-0.132	-0.344	2.346	0.614	0.373
NT12404-1	1032	0.349	0.505	0.195	-0.190	-0.346	2.098	0.489	0.041
NE03T416-1	1035	0.357	0.485	0.191	-0.154	-0.325	1.930	0.478	0.188
NT441	1038	0.520	0.588	0.271	-0.096	-0.378	2.904	0.749	0.760
NE03T416-3	1040	0.367	0.496	0.197	-0.158	-0.333	2.026	0.497	0.173
NT20417	1046	0.383	0.510	0.207	-0.157	-0.341	2.137	0.527	0.211
NT19443	1051	0.471	0.551	0.249	-0.107	-0.353	2.547	0.674	0.629
NT14407	1055	0.405	0.527	0.212	-0.155	-0.356	2.272	0.544	0.290
NT14433	1056	0.427	0.534	0.209	-0.138	-0.367	2.323	0.530	0.515
NT20432	1059	0.409	0.530	0.224	-0.154	-0.349	2.321	0.585	0.216
NT17441	1060	0.468	0.546	0.237	-0.103	-0.357	2.482	0.631	0.708
NE03T416-3	1062	0.384	0.501	0.206	-0.144	-0.331	2.058	0.523	0.243
NT20432	1063	0.413	0.519	0.223	-0.134	-0.337	2.228	0.583	0.341
NT14407	1065	0.411	0.532	0.221	-0.153	-0.354	2.329	0.573	0.257
NT12404-1	1067	0.330	0.498	0.188	-0.201	-0.344	2.030	0.466	0.006
NE03T416-1	1071	0.391	0.500	0.207	-0.134	-0.328	2.059	0.529	0.296
NT14433	1074	0.450	0.541	0.221	-0.119	-0.365	2.397	0.571	0.659
NT20417	1075	0.404	0.520	0.218	-0.146	-0.343	2.235	0.566	0.316
NT17441	1079	0.498	0.566	0.262	-0.093	-0.359	2.693	0.722	0.722
NT19443	1081	0.475	0.555	0.256	-0.106	-0.352	2.593	0.700	0.627
NT441	1082	0.535	0.596	0.287	-0.087	-0.374	3.023	0.816	0.724

Note. Normalized index values range from -1 to +1. A number closer to +1 indicates healthy vegetation. The spectral bands used to calculate GRVIRE cause the relationship to be inverse. A GRVIRE value closer to -1 indicates healthy vegetation and a number closer to +1 indicates unhealthy or no vegetation. GCI and RCI are not normalized indices, so they are not bound by the -1 to +1 scale.

Table A20

Mead 05/18/22 Vegetation Index Values

Genotype	Plot ID	NDVI	GNDVI	NDRE	GRVI	GRVIRE	GCI	RCI	Pixel Percent
NT21409	1004	0.629	0.582	0.345	0.133	-0.313	3.387	1.180	0.603
NT13443	1005	0.516	0.500	0.265	0.058	-0.282	2.320	0.786	0.551
NT441	1006	0.724	0.630	0.384	0.239	-0.339	3.956	1.356	0.849
NT17441	1009	0.720	0.638	0.387	0.202	-0.345	3.953	1.337	0.817
NT20417	1011	0.716	0.633	0.383	0.200	-0.340	3.829	1.314	0.843
NT19443	1012	0.775	0.675	0.428	0.253	-0.356	4.534	1.568	0.858
NT21443	1015	0.677	0.601	0.356	0.172	-0.320	3.328	1.172	0.799
NE03T416-1	1022	0.757	0.656	0.407	0.262	-0.352	4.345	1.478	0.870
NT21414	1023	0.692	0.624	0.387	0.185	-0.329	3.972	1.402	0.758
NT20401	1029	0.802	0.697	0.456	0.280	-0.362	5.007	1.759	0.905
NT20409	1032	0.811	0.698	0.458	0.319	-0.364	5.149	1.796	0.878
NT21409	1035	0.694	0.627	0.390	0.170	-0.327	3.906	1.398	0.743
NT14433	1038	0.742	0.651	0.406	0.219	-0.341	4.079	1.441	0.816
OVERLAND	1040	0.762	0.655	0.404	0.263	-0.350	4.155	1.421	0.892
NE03T416-1	1046	0.752	0.646	0.395	0.245	-0.343	3.928	1.363	0.912
NT21440	1051	0.746	0.646	0.399	0.238	-0.342	4.003	1.394	0.888
NT20432	1055	0.704	0.618	0.371	0.194	-0.329	3.528	1.236	0.828
NT19443	1056	0.773	0.663	0.418	0.260	-0.346	4.202	1.487	0.881
NT20429	1059	0.846	0.740	0.510	0.320	-0.376	6.094	2.167	0.893
NT21436	1060	0.846	0.730	0.492	0.323	-0.376	5.636	1.982	0.914
NT441	1062	0.905	0.768	0.537	0.456	-0.396	6.874	2.371	0.954
NT19441	1063	0.886	0.764	0.541	0.386	-0.383	6.700	2.404	0.924
NT20417	1065	0.824	0.710	0.470	0.342	-0.371	5.498	1.905	0.890
NT21409	1067	0.848	0.741	0.514	0.339	-0.378	6.377	2.250	0.883
NT20401	1071	0.859	0.739	0.504	0.374	-0.382	6.137	2.133	0.926
OVERLAND	1074	0.919	0.802	0.579	0.468	-0.423	8.635	2.847	0.931
NT17442	1075	0.882	0.768	0.537	0.394	-0.400	7.092	2.407	0.888
NT20409	1079	0.888	0.760	0.529	0.420	-0.392	6.671	2.316	0.962
NT21440	1081	0.910	0.788	0.568	0.451	-0.403	7.789	2.705	0.963
NE03T416-1	1082	0.912	0.794	0.573	0.439	-0.408	7.959	2.738	0.973

Note. Normalized index values range from -1 to +1. A number closer to +1 indicates healthy vegetation. The spectral bands used to calculate GRVIRE cause the relationship to be inverse. A GRVIRE value closer to -1 indicates healthy vegetation and a number closer to +1 indicates unhealthy or no vegetation. GCI and RCI are not normalized indices, so they are not bound by the -1 to +1 scale.

Table A21

Mead 06/02/22 Vegetation Index Values

Genotype	Plot ID	NDVI	GNDVI	NDRE	GRVI	GRVIRE	GCI	RCI	Pixel Percent
NT441	1006	0.788	0.707	0.483	0.218	-0.348	5.242	1.960	0.850
NT17441	1009	0.743	0.686	0.465	0.151	-0.333	4.787	1.835	0.628
NT20417	1011	0.736	0.672	0.451	0.160	-0.326	4.487	1.734	0.782
NT19443	1012	0.806	0.724	0.509	0.221	-0.347	5.555	2.138	0.837
NT14407	1016	0.742	0.680	0.459	0.162	-0.331	4.721	1.804	0.661
NT12404-1	1017	0.769	0.711	0.504	0.178	-0.336	5.608	2.197	0.655
NE03T416-3	1018	0.785	0.707	0.492	0.210	-0.337	5.245	2.040	0.830
NT14433	1019	0.805	0.723	0.505	0.233	-0.353	5.657	2.132	0.866
NE03T416-1	1022	0.768	0.688	0.468	0.202	-0.334	4.834	1.854	0.852
NT20432	1025	0.837	0.748	0.540	0.258	-0.352	6.197	2.415	0.896
NT441	1031	0.871	0.776	0.569	0.320	-0.378	7.404	2.740	0.908
NT12404-1	1033	0.739	0.684	0.472	0.137	-0.320	4.670	1.876	0.583
NT20417	1036	0.727	0.665	0.444	0.150	-0.321	4.317	1.681	0.775
NT14433	1038	0.748	0.679	0.451	0.166	-0.334	4.504	1.706	0.812
NT17441	1039	0.784	0.715	0.497	0.184	-0.344	5.332	2.045	0.621
NE03T416-1	1046	0.778	0.693	0.474	0.206	-0.332	4.772	1.860	0.879
NT14407	1049	0.784	0.707	0.488	0.207	-0.342	5.214	1.998	0.822
NE03T416-3	1052	0.761	0.688	0.471	0.184	-0.328	4.729	1.857	0.784
NT20432	1055	0.724	0.666	0.445	0.147	-0.323	4.384	1.700	0.681
NT19443	1056	0.795	0.712	0.488	0.216	-0.348	5.228	1.972	0.781
NT441	1062	0.894	0.790	0.580	0.364	-0.389	7.747	2.812	0.929
NT20417	1065	0.774	0.705	0.486	0.217	-0.348	5.516	2.066	0.773
NE03T416-3	1066	0.786	0.709	0.492	0.223	-0.344	5.417	2.071	0.809
NT20432	1072	0.835	0.754	0.544	0.262	-0.365	6.720	2.528	0.841
NT19443	1073	0.880	0.782	0.575	0.325	-0.378	7.408	2.763	0.930
NT14407	1080	0.872	0.778	0.567	0.308	-0.382	7.330	2.686	0.895
NE03T416-1	1082	0.870	0.776	0.566	0.304	-0.379	7.200	2.664	0.941
NT14433	1085	0.864	0.769	0.551	0.309	-0.383	6.975	2.518	0.922
NT17441	1088	0.866	0.779	0.562	0.295	-0.393	7.478	2.641	0.832
NT12404-1	1089	0.877	0.793	0.590	0.287	-0.383	7.882	2.930	0.836

Note. Normalized index values range from -1 to +1. A number closer to +1 indicates healthy vegetation. The spectral bands used to calculate GRVIRE cause the relationship to be inverse. A GRVIRE value closer to -1 indicates healthy vegetation and a number closer to +1 indicates unhealthy or no vegetation. GCI and RCI are not normalized indices, so they are not bound by the -1 to +1 scale.

Table A22

Mead 06/27/22 Vegetation Index Values

Genotype	Plot ID	NDVI	GNDVI	NDRE	GRVI	GRVIRE	GCI	RCI	Pixel Percent
NT441	1006	0.475	0.529	0.256	-0.069	-0.316	2.279	0.696	0.951
NT17441	1009	0.407	0.461	0.214	-0.064	-0.275	1.734	0.550	0.944
NT20417	1011	0.302	0.422	0.169	-0.138	-0.273	1.480	0.411	0.590
NT19443	1012	0.374	0.463	0.210	-0.107	-0.281	1.752	0.536	0.863
NT14407	1016	0.311	0.421	0.173	-0.126	-0.268	1.471	0.420	0.711
NT12404-1	1017	0.312	0.437	0.173	-0.144	-0.287	1.578	0.421	0.519
NE03T416-3	1018	0.353	0.447	0.186	-0.111	-0.286	1.643	0.461	0.830
NT14433	1019	0.316	0.430	0.166	-0.132	-0.285	1.528	0.402	0.749
NE03T416-1	1022	0.327	0.426	0.172	-0.115	-0.275	1.510	0.419	0.767
NT20432	1025	0.365	0.457	0.199	-0.109	-0.285	1.714	0.503	0.829
NT441	1031	0.532	0.565	0.289	-0.043	-0.331	2.659	0.826	0.949
NT12404-1	1033	0.309	0.428	0.171	-0.136	-0.277	1.512	0.416	0.567
NT20417	1036	0.289	0.408	0.159	-0.135	-0.266	1.393	0.381	0.624
NT14433	1038	0.298	0.410	0.159	-0.127	-0.269	1.399	0.379	0.725
NT17441	1039	0.441	0.475	0.229	-0.041	-0.276	1.837	0.602	0.965
NE03T416-1	1046	0.349	0.432	0.181	-0.097	-0.273	1.543	0.446	0.865
NT14407	1049	0.313	0.430	0.171	-0.134	-0.280	1.524	0.414	0.631
NE03T416-3	1052	0.339	0.432	0.181	-0.108	-0.273	1.543	0.446	0.792
NT20432	1055	0.327	0.420	0.175	-0.106	-0.265	1.477	0.431	0.789
NT19443	1056	0.329	0.427	0.176	-0.114	-0.272	1.509	0.431	0.806
NT441	1062	0.492	0.551	0.260	-0.078	-0.341	2.494	0.708	0.946
NT20417	1065	0.318	0.437	0.172	-0.137	-0.287	1.580	0.421	0.563
NE03T416-3	1066	0.350	0.447	0.182	-0.114	-0.289	1.639	0.450	0.782
NT20432	1072	0.337	0.443	0.182	-0.124	-0.285	1.620	0.450	0.691
NT19443	1073	0.353	0.461	0.189	-0.129	-0.299	1.738	0.470	0.751
NT14407	1080	0.315	0.442	0.170	-0.147	-0.295	1.606	0.411	0.576
NE03T416-1	1082	0.309	0.438	0.161	-0.149	-0.299	1.583	0.387	0.482
NT14433	1085	0.315	0.449	0.161	-0.156	-0.311	1.656	0.388	0.498
NT17441	1088	0.323	0.438	0.164	-0.133	-0.295	1.578	0.397	0.662
NT12404-1	1089	0.260	0.426	0.146	-0.187	-0.299	1.501	0.345	0.055

Note. Normalized index values range from -1 to +1. A number closer to +1 indicates healthy vegetation. The spectral bands used to calculate GRVIRE cause the relationship to be inverse. A GRVIRE value closer to -1 indicates healthy vegetation and a number closer to +1 indicates unhealthy or no vegetation. GCI and RCI are not normalized indices, so they are not bound by the -1 to +1 scale.

Table A23

Lincoln 05/10/23 Vegetation Index Values

Genotype	Plot ID	NDVI	GNDVI	NDRE	GRVI	GRVIRE	GCI	RCI	Pixel Percent
NT19443	1001	0.606	0.758	0.262	-0.271	-0.623	6.648	0.717	0.072
NT14433	1002	0.600	0.757	0.260	-0.278	-0.621	6.501	0.707	0.060
NT441	1009	0.646	0.779	0.310	-0.256	-0.620	7.338	0.905	0.098
NT14407	1018	0.656	0.785	0.318	-0.257	-0.625	7.554	0.937	0.081
NT12404-1	1021	0.588	0.751	0.261	-0.288	-0.612	6.247	0.710	0.030
NE03T416-3	1024	0.643	0.775	0.289	-0.253	-0.628	7.122	0.815	0.096
NT19441	1026	0.639	0.778	0.310	-0.267	-0.620	7.337	0.907	0.087
NE03T416-1	1027	0.598	0.758	0.296	-0.288	-0.596	6.393	0.845	0.030
NT21436	1030	0.641	0.778	0.304	-0.262	-0.623	7.328	0.880	0.101
NT20427	1033	0.634	0.771	0.283	-0.260	-0.625	6.927	0.792	0.064
NT21436	1049	0.658	0.784	0.303	-0.247	-0.634	7.695	0.877	0.121
NT441	1052	0.618	0.760	0.266	-0.257	-0.620	6.574	0.730	0.118
NT14407	1054	0.628	0.767	0.285	-0.258	-0.621	6.940	0.801	0.106
NT20427	1057	0.683	0.794	0.310	-0.227	-0.645	8.143	0.906	0.174
NT14433	1065	0.641	0.775	0.294	-0.250	-0.627	7.386	0.842	0.138
NE03T416-1	1066	0.697	0.801	0.318	-0.217	-0.651	8.524	0.939	0.246
NT19441	1074	0.657	0.782	0.294	-0.245	-0.637	7.605	0.841	0.148
NE03T416-3	1075	0.643	0.775	0.289	-0.252	-0.629	7.212	0.819	0.131
NT19443	1077	0.680	0.796	0.311	-0.235	-0.647	8.258	0.910	0.191
NT12404-1	1078	0.638	0.777	0.293	-0.267	-0.628	7.199	0.831	0.065
NT20427	1086	0.637	0.776	0.295	-0.265	-0.626	7.196	0.841	0.099
NT19441	1094	0.632	0.770	0.280	-0.259	-0.628	7.013	0.782	0.106
NT14433	1095	0.605	0.758	0.274	-0.274	-0.614	6.565	0.760	0.092
NE03T416-1	1097	0.632	0.773	0.288	-0.263	-0.625	7.069	0.814	0.134
NE03T416-3	1102	0.630	0.765	0.264	-0.245	-0.630	6.873	0.724	0.160
NT21436	1104	0.610	0.759	0.273	-0.270	-0.616	6.578	0.754	0.069
NT441	1105	0.623	0.765	0.279	-0.259	-0.620	6.821	0.778	0.126
NT14407	1110	0.611	0.760	0.260	-0.269	-0.625	6.598	0.707	0.102
NT12404-1	1111	0.562	0.733	0.249	-0.287	-0.593	5.616	0.666	0.022
NT19443	1118	0.614	0.764	0.273	-0.271	-0.623	6.809	0.756	0.096

Note. Normalized index values range from -1 to +1. A number closer to +1 indicates healthy vegetation. The spectral bands used to calculate GRVIRE cause the relationship to be inverse. A GRVIRE value closer to -1 indicates healthy vegetation and a number closer to +1 indicates unhealthy or no vegetation. GCI and RCI are not normalized indices, so they are not bound by the -1 to +1 scale.

Table A24

Lincoln 05/22/23 Vegetation Index Values

Genotype	Plot ID	NDVI	GNDVI	NDRE	GRVI	GRVIRE	GCI	RCI	Pixel Percent
NT19443	1001	0.569	0.565	0.310	0.024	-0.315	2.814	0.910	0.394
NT14433	1002	0.556	0.557	0.311	0.010	-0.303	2.690	0.911	0.376
NT441	1009	0.629	0.592	0.341	0.078	-0.320	3.116	1.046	0.529
NT14407	1018	0.608	0.578	0.340	0.055	-0.299	2.844	1.034	0.414
NT12404-1	1021	0.511	0.520	0.290	-0.005	-0.274	2.268	0.824	0.176
NE03T416-3	1024	0.600	0.572	0.327	0.053	-0.305	2.776	0.975	0.478
NT19441	1026	0.596	0.573	0.341	0.047	-0.292	2.838	1.047	0.422
NE03T416-1	1027	0.542	0.526	0.314	0.031	-0.257	2.308	0.919	0.242
NT21436	1030	0.628	0.584	0.331	0.088	-0.319	3.009	0.999	0.503
NT20427	1033	0.579	0.559	0.318	0.038	-0.296	2.636	0.937	0.386
NT21436	1049	0.628	0.581	0.338	0.089	-0.308	2.966	1.031	0.486
NT441	1052	0.607	0.577	0.315	0.067	-0.326	2.944	0.928	0.537
NT14407	1054	0.578	0.556	0.322	0.045	-0.290	2.665	0.958	0.428
NT20427	1057	0.662	0.612	0.357	0.102	-0.331	3.362	1.123	0.614
NT14433	1065	0.614	0.584	0.340	0.065	-0.311	3.065	1.048	0.437
NE03T416-1	1066	0.671	0.620	0.360	0.105	-0.339	3.439	1.133	0.626
NT19441	1074	0.629	0.593	0.339	0.073	-0.323	3.106	1.039	0.521
NE03T416-3	1075	0.615	0.581	0.335	0.067	-0.310	2.932	1.015	0.477
NT19443	1077	0.653	0.609	0.353	0.093	-0.331	3.337	1.104	0.549
NT12404-1	1078	0.589	0.562	0.332	0.049	-0.286	2.669	1.001	0.313
NT20427	1086	0.611	0.579	0.337	0.060	-0.303	2.873	1.026	0.398
NT19441	1094	0.623	0.583	0.332	0.075	-0.315	2.930	1.000	0.542
NT14433	1095	0.582	0.553	0.320	0.057	-0.288	2.629	0.950	0.341
NE03T416-1	1097	0.602	0.565	0.324	0.068	-0.299	2.721	0.964	0.411
NE03T416-3	1102	0.617	0.572	0.312	0.088	-0.322	2.857	0.916	0.524
NT21436	1104	0.606	0.568	0.323	0.070	-0.304	2.770	0.960	0.440
NT441	1105	0.631	0.585	0.332	0.091	-0.321	3.034	1.002	0.532
NT14407	1110	0.584	0.547	0.301	0.066	-0.298	2.543	0.868	0.433
NT12404-1	1111	0.515	0.496	0.274	0.032	-0.260	2.046	0.758	0.165
NT19443	1118	0.563	0.539	0.311	0.050	-0.280	2.543	0.916	0.303

Note. Normalized index values range from -1 to +1. A number closer to +1 indicates healthy vegetation. The spectral bands used to calculate GRVIRE cause the relationship to be inverse. A GRVIRE value closer to -1 indicates healthy vegetation and a number closer to +1 indicates unhealthy or no vegetation. GCI and RCI are not normalized indices, so they are not bound by the -1 to +1 scale.

Table A25

Lincoln 06/05/23 Vegetation Index Values

Genotype	Plot ID	NDVI	GNDVI	NDRE	GRVI	GRVIRE	GCI	RCI	Pixel Percent
NT19443	1001	0.535	0.530	0.325	0.015	-0.251	2.370	0.974	0.243
NT14433	1002	0.516	0.518	0.323	0.005	-0.238	2.256	0.961	0.185
NT441	1009	0.548	0.528	0.335	0.039	-0.238	2.348	1.016	0.291
NT14407	1018	0.524	0.520	0.345	0.011	-0.215	2.228	1.060	0.107
NT12404-1	1021	0.453	0.483	0.309	-0.034	-0.206	1.917	0.899	0.030
NE03T416-3	1024	0.527	0.525	0.345	0.006	-0.223	2.270	1.057	0.136
NT19441	1026	0.527	0.530	0.352	0.003	-0.222	2.342	1.093	0.186
NE03T416-1	1027	0.474	0.478	0.317	0.000	-0.193	1.901	0.934	0.125
NT21436	1030	0.532	0.520	0.329	0.027	-0.233	2.264	0.991	0.242
NT20427	1033	0.492	0.506	0.328	-0.015	-0.216	2.103	0.981	0.085
NT21436	1049	0.499	0.499	0.322	0.005	-0.214	2.066	0.956	0.149
NT441	1052	0.563	0.551	0.341	0.030	-0.264	2.596	1.043	0.383
NT14407	1054	0.508	0.515	0.340	-0.003	-0.215	2.214	1.041	0.153
NT20427	1057	0.547	0.535	0.344	0.025	-0.236	2.387	1.058	0.247
NT14433	1065	0.558	0.548	0.366	0.024	-0.233	2.559	1.166	0.245
NE03T416-1	1066	0.558	0.541	0.356	0.032	-0.231	2.429	1.112	0.172
NT19441	1074	0.561	0.549	0.357	0.024	-0.242	2.540	1.121	0.218
NE03T416-3	1075	0.538	0.531	0.355	0.017	-0.219	2.345	1.110	0.131
NT19443	1077	0.547	0.529	0.342	0.035	-0.232	2.358	1.050	0.283
NT12404-1	1078	0.475	0.479	0.320	-0.003	-0.190	1.885	0.946	0.043
NT20427	1086	0.511	0.510	0.342	0.007	-0.205	2.134	1.046	0.110
NT19441	1094	0.531	0.531	0.347	0.005	-0.227	2.323	1.068	0.126
NT14433	1095	0.508	0.511	0.347	0.000	-0.202	2.163	1.070	0.121
NE03T416-1	1097	0.480	0.482	0.322	0.002	-0.191	1.907	0.955	0.096
NE03T416-3	1102	0.531	0.525	0.335	0.015	-0.234	2.300	1.014	0.214
NT21436	1104	0.521	0.516	0.346	0.011	-0.210	2.192	1.062	0.156
NT441	1105	0.577	0.556	0.371	0.039	-0.237	2.621	1.188	0.339
NT14407	1110	0.493	0.482	0.312	0.020	-0.203	1.930	0.914	0.140
NT12404-1	1111	0.451	0.467	0.308	-0.017	-0.188	1.814	0.897	0.030
NT19443	1118	0.475	0.475	0.318	0.008	-0.189	1.909	0.942	0.165

Note. Normalized index values range from -1 to +1. A number closer to +1 indicates healthy vegetation. The spectral bands used to calculate GRVIRE cause the relationship to be inverse. A GRVIRE value closer to -1 indicates healthy vegetation and a number closer to +1 indicates unhealthy or no vegetation. GCI and RCI are not normalized indices, so they are not bound by the -1 to +1 scale.

Table A26

Mead 05/10/23 Vegetation Index Values

Genotype	Plot ID	NDVI	GNDVI	NDRE	GRVI	GRVIRE	GCI	RCI	Pixel Percent
NT12404-1	1003	0.439	0.649	0.193	-0.290	-0.524	3.850	0.482	0.073
NT14407	1006	0.542	0.692	0.214	-0.232	-0.564	4.723	0.550	0.306
NE03T416-3	1012	0.579	0.715	0.244	-0.221	-0.574	5.276	0.650	0.415
NT19443	1014	0.605	0.729	0.258	-0.211	-0.584	5.676	0.704	0.393
NT441	1018	0.667	0.758	0.288	-0.167	-0.604	6.580	0.818	0.666
NE03T416-1	1022	0.592	0.722	0.250	-0.216	-0.579	5.430	0.672	0.498
NT20427	1027	0.549	0.702	0.249	-0.241	-0.552	4.923	0.668	0.218
NT21436	1033	0.599	0.731	0.259	-0.225	-0.586	5.695	0.704	0.395
NT19441	1035	0.614	0.733	0.260	-0.206	-0.587	5.729	0.710	0.416
NT14433	1039	0.613	0.739	0.281	-0.219	-0.581	5.929	0.788	0.455
NT14407	1041	0.553	0.710	0.245	-0.250	-0.566	5.133	0.654	0.351
NT14433	1046	0.615	0.731	0.254	-0.199	-0.589	5.731	0.687	0.500
NT441	1050	0.665	0.761	0.289	-0.178	-0.608	6.688	0.821	0.756
NT19443	1053	0.526	0.694	0.212	-0.255	-0.568	4.779	0.544	0.278
NT21436	1057	0.583	0.724	0.252	-0.236	-0.581	5.511	0.678	0.290
NT20427	1064	0.505	0.686	0.203	-0.270	-0.564	4.551	0.515	0.164
NE03T416-3	1071	0.563	0.722	0.228	-0.256	-0.594	5.435	0.595	0.298
NT12404-1	1075	0.499	0.687	0.199	-0.281	-0.568	4.578	0.502	0.132
NE03T416-1	1077	0.617	0.741	0.253	-0.218	-0.603	5.957	0.683	0.533
NT19441	1079	0.817	0.844	0.383	-0.074	-0.684	11.293	1.255	0.880
NT19443	1083	0.562	0.722	0.222	-0.259	-0.598	5.435	0.575	0.312
NT441	1086	0.712	0.784	0.274	-0.147	-0.652	7.588	0.762	0.821
NT14433	1092	0.539	0.712	0.220	-0.271	-0.586	5.166	0.567	0.201
NT19441	1094	0.627	0.751	0.254	-0.222	-0.617	6.305	0.689	0.376
NT14407	1101	0.560	0.724	0.246	-0.267	-0.584	5.435	0.658	0.212
NE03T416-1	1102	0.565	0.722	0.232	-0.256	-0.591	5.409	0.610	0.310
NT20427	1103	0.526	0.705	0.224	-0.277	-0.573	4.948	0.582	0.195
NT12404-1	1105	0.414	0.644	0.184	-0.311	-0.523	3.703	0.453	0.036
NE03T416-3	1107	0.582	0.722	0.252	-0.233	-0.577	5.405	0.678	0.333
NT21436	1119	0.619	0.749	0.294	-0.235	-0.587	6.206	0.838	0.329

Note. Normalized index values range from -1 to +1. A number closer to +1 indicates healthy vegetation. The spectral bands used to calculate GRVIRE cause the relationship to be inverse. A GRVIRE value closer to -1 indicates healthy vegetation and a number closer to +1 indicates unhealthy or no vegetation. GCI and RCI are not normalized indices, so they are not bound by the -1 to +1 scale.

Table A27

Mead 05/22/23 Vegetation Index Values

Genotype	Plot ID	NDVI	GNDVI	NDRE	GRVI	GRVIRE	GCI	RCI	Pixel Percent
NT12404-1	1003	0.538	0.579	0.256	-0.052	-0.382	2.854	0.695	0.424
NT14407	1006	0.609	0.628	0.284	-0.019	-0.423	3.555	0.800	0.655
NE03T416-3	1012	0.639	0.639	0.300	0.011	-0.422	3.686	0.866	0.830
NT19443	1014	0.676	0.668	0.311	0.028	-0.454	4.193	0.908	0.844
NT441	1018	0.737	0.717	0.357	0.059	-0.488	5.327	1.123	0.860
NE03T416-1	1022	0.638	0.637	0.302	0.011	-0.417	3.632	0.871	0.833
NT20427	1027	0.640	0.653	0.317	-0.015	-0.427	3.901	0.933	0.798
NT21436	1033	0.613	0.632	0.309	-0.022	-0.405	3.578	0.903	0.752
NT19441	1035	0.665	0.664	0.317	0.012	-0.441	4.071	0.934	0.859
NT14433	1039	0.674	0.681	0.337	-0.002	-0.449	4.417	1.025	0.825
NT14407	1041	0.624	0.632	0.317	-0.003	-0.397	3.560	0.934	0.820
NT14433	1046	0.697	0.688	0.341	0.027	-0.457	4.566	1.041	0.875
NT441	1050	0.742	0.722	0.353	0.056	-0.498	5.397	1.101	0.894
NT19443	1053	0.627	0.636	0.308	-0.003	-0.411	3.644	0.899	0.805
NT21436	1057	0.661	0.673	0.333	-0.012	-0.440	4.264	1.007	0.813
NT20427	1064	0.598	0.617	0.288	-0.022	-0.404	3.346	0.814	0.736
NE03T416-3	1071	0.638	0.637	0.304	0.013	-0.416	3.637	0.879	0.853
NT12404-1	1075	0.594	0.619	0.289	-0.032	-0.405	3.375	0.819	0.593
NE03T416-1	1077	0.672	0.668	0.317	0.019	-0.448	4.154	0.934	0.847
NT19441	1079	0.787	0.756	0.395	0.090	-0.518	6.435	1.319	0.886
NT19443	1083	0.647	0.649	0.291	0.008	-0.444	3.838	0.828	0.854
NT441	1086	0.759	0.723	0.341	0.091	-0.510	5.395	1.040	0.909
NT14433	1092	0.619	0.635	0.273	-0.014	-0.440	3.605	0.757	0.812
NT19441	1094	0.670	0.666	0.290	0.015	-0.469	4.129	0.823	0.878
NT14407	1101	0.619	0.635	0.264	-0.018	-0.448	3.584	0.724	0.841
NE03T416-1	1102	0.621	0.633	0.257	-0.010	-0.451	3.552	0.697	0.862
NT20427	1103	0.617	0.634	0.261	-0.019	-0.449	3.563	0.711	0.822
NT12404-1	1105	0.516	0.573	0.233	-0.076	-0.394	2.758	0.611	0.311
NE03T416-3	1107	0.661	0.665	0.297	0.002	-0.461	4.088	0.850	0.842
NT21436	1119	0.653	0.674	0.317	-0.030	-0.457	4.273	0.936	0.786

Note. Normalized index values range from -1 to +1. A number closer to +1 indicates healthy vegetation. The spectral bands used to calculate GRVIRE cause the relationship to be inverse. A GRVIRE value closer to -1 indicates healthy vegetation and a number closer to +1 indicates unhealthy or no vegetation. GCI and RCI are not normalized indices, so they are not bound by the -1 to +1 scale.

Table A28

Mead 06/05/23 Vegetation Index Values

Genotype	Plot ID	NDVI	GNDVI	NDRE	GRVI	GRVIRE	GCI	RCI	Pixel Percent
NT12404-1	1003	0.489	0.483	0.267	0.014	-0.249	1.918	0.735	0.109
NT14407	1006	0.542	0.517	0.286	0.043	-0.273	2.205	0.806	0.305
NE03T416-3	1012	0.582	0.539	0.302	0.068	-0.284	2.383	0.871	0.303
NT19443	1014	0.651	0.582	0.315	0.117	-0.328	2.838	0.925	0.633
NT441	1018	0.668	0.607	0.341	0.112	-0.338	3.167	1.041	0.710
NE03T416-1	1022	0.587	0.540	0.301	0.074	-0.286	2.377	0.865	0.282
NT20427	1027	0.596	0.563	0.324	0.054	-0.294	2.625	0.964	0.262
NT21436	1033	0.563	0.543	0.311	0.035	-0.280	2.416	0.910	0.150
NT19441	1035	0.597	0.561	0.309	0.059	-0.306	2.599	0.899	0.396
NT14433	1039	0.603	0.572	0.321	0.054	-0.308	2.717	0.952	0.501
NT14407	1041	0.590	0.549	0.309	0.066	-0.290	2.470	0.900	0.336
NT14433	1046	0.653	0.599	0.332	0.094	-0.334	3.027	0.999	0.610
NT441	1050	0.682	0.623	0.347	0.109	-0.352	3.345	1.069	0.752
NT19443	1053	0.613	0.565	0.313	0.080	-0.307	2.636	0.915	0.525
NT21436	1057	0.598	0.575	0.330	0.040	-0.304	2.750	0.988	0.273
NT20427	1064	0.560	0.536	0.295	0.038	-0.288	2.350	0.841	0.216
NE03T416-3	1071	0.572	0.539	0.301	0.054	-0.285	2.374	0.865	0.358
NT12404-1	1075	0.561	0.547	0.311	0.027	-0.286	2.455	0.906	0.194
NE03T416-1	1077	0.594	0.557	0.313	0.060	-0.296	2.551	0.916	0.351
NT19441	1079	0.673	0.622	0.356	0.093	-0.344	3.360	1.111	0.761
NT19443	1083	0.626	0.577	0.319	0.082	-0.318	2.774	0.942	0.533
NT441	1086	0.694	0.626	0.346	0.127	-0.358	3.388	1.064	0.798
NT14433	1092	0.587	0.554	0.305	0.055	-0.300	2.520	0.883	0.365
NT19441	1094	0.619	0.578	0.320	0.069	-0.318	2.781	0.946	0.443
NT14407	1101	0.587	0.550	0.306	0.059	-0.295	2.484	0.886	0.315
NE03T416-1	1102	0.566	0.536	0.295	0.046	-0.287	2.341	0.843	0.194
NT20427	1103	0.598	0.562	0.312	0.059	-0.304	2.591	0.910	0.256
NT12404-1	1105	0.524	0.524	0.301	0.005	-0.265	2.232	0.865	0.072
NE03T416-3	1107	0.608	0.569	0.323	0.064	-0.303	2.673	0.958	0.338
NT21436	1119	0.599	0.580	0.336	0.032	-0.304	2.795	1.018	0.180

Note. Normalized index values range from -1 to +1. A number closer to +1 indicates healthy vegetation. The spectral bands used to calculate GRVIRE cause the relationship to be inverse. A GRVIRE value closer to -1 indicates healthy vegetation and a number closer to +1 indicates unhealthy or no vegetation. GCI and RCI are not normalized indices, so they are not bound by the -1 to +1 scale.

Table A29

VI vs. Dry Biomass Confusion Matrices 05/18/22

			Actual Biomass Classification of Genotypes					
	Vegetation Indices		Lincoln			Mead		
			Low	Mid	High	Low	Mid	High
VI-Based Genotype Classification	GCI	Low	1	2	0	1	1	0
		Mid	0	2	3	0	3	3
		High	0	2	0	1	0	0
	GNDVI	Low	0	2	0	0	1	0
		Mid	1	2	3	1	2	3
		High	0	2	0	1	1	0
	GRVI	Low	1	1	0	1	1	0
		Mid	0	3	2	0	2	3
		High	0	2	1	1	1	0
	GRVIRE	Low	0	2	0	1	1	0
		Mid	0	3	2	0	2	3
		High	1	1	1	1	1	0
	NDRE	Low	0	2	0	1	1	0
		Mid	1	3	2	0	2	3
		High	0	1	1	1	1	0
	NDVI	Low	1	1	0	0	1	0
		Mid	0	3	3	1	2	3
		High	0	2	0	1	1	0
	Pixel Percent	Low	0	1	1	0	1	0
		Mid	1	3	1	2	1	2
		High	0	2	1	0	2	1
	RCI	Low	0	2	0	1	0	0
		Mid	1	3	2	0	4	3
		High	0	1	1	1	0	0

Note. The numbers on the diagonal from top left to bottom right indicate an agreeance between actual biomass classification and VI-Based genotype classification.

Table 30

VI vs. Dry Biomass Confusion Matrices 06/02/22

			Actual Biomass Classification of Genotypes					
	Vegetation Indices		Lincoln			Mead		
			Low	Mid	High	Low	Mid	High
VI-Based Genotype Classification	GCI	Low	1	0	2	0	0	2
		Mid	2	1	1	1	6	0
		High	0	3	0	1	0	0
	GNDVI	Low	1	0	2	0	0	2
		Mid	2	2	1	1	6	0
		High	0	2	0	1	0	0
	GRVI	Low	1	1	1	0	0	1
		Mid	2	1	1	1	5	1
		High	0	2	1	1	1	0
	GRVIRE	Low	0	3	0	1	0	0
		Mid	1	1	2	1	6	0
		High	2	0	1	0	0	2
	NDRE	Low	1	1	2	0	0	2
		Mid	2	1	1	1	6	0
		High	0	2	0	1	0	0
	NDVI	Low	1	0	1	0	0	2
		Mid	2	1	2	1	5	0
		High	0	3	0	1	1	0
	Pixel Percent	Low	0	1	0	0	2	0
		Mid	3	1	2	1	2	2
		High	0	2	1	1	2	0
	RCI	Low	1	1	2	0	0	2
		Mid	2	1	1	1	6	0
		High	0	2	0	1	0	0

Note. The numbers on the diagonal from top left to bottom right indicate an agreeance between actual biomass classification and VI-Based genotype classification.

Table A31

VI vs. Dry Biomass Confusion Matrices 06/27/22

			Actual Biomass Classification of Genotypes					
	Vegetation Indices		Lincoln			Mead		
			Low	Mid	High	Low	Mid	High
VI-Based Genotype Classification	GCI	Low	0	2	1	2	2	0
		Mid	3	1	0	0	4	1
		High	1	1	1	0	1	0
	GNDVI	Low	0	2	1	2	3	0
		Mid	3	1	0	0	3	1
		High	1	1	1	0	1	0
	GRVI	Low	1	2	0	2	2	0
		Mid	2	1	1	0	4	0
		High	1	1	1	0	1	1
	GRVIRE	Low	2	0	1	0	1	0
		Mid	2	3	0	1	5	1
		High	0	1	1	1	1	0
	NDRE	Low	0	2	1	2	3	0
		Mid	3	1	0	0	3	0
		High	1	1	1	0	1	1
	NDVI	Low	0	2	1	2	2	0
		Mid	3	1	0	0	4	0
		High	1	1	1	0	1	1
	Pixel Percent	Low	1	2	1	1	1	0
		Mid	1	1	0	1	3	0
		High	2	1	1	0	3	1
	RCI	Low	0	2	1	2	3	0
		Mid	3	1	0	0	3	0
		High	1	1	1	0	1	1

Note. The numbers on the diagonal from top left to bottom right indicate an agreeance between actual biomass classification and VI-Based genotype classification.

Table A32

VI vs. Dry Biomass Confusion Matrices 05/10/23

	Vegetation Indices		Actual Biomass Classification of Genotypes: Lincoln Low	Lincoln Mid	Lincoln High	Mead Low	Mead Mid	Mead High
VI-Based Genotype Classification	GCI	Low	1	0	0	1	1	0
		Mid	1	6	1	1	5	0
		High	0	0	1	0	1	1
	GNDVI	Low	2	0	0	1	1	0
		Mid	0	5	0	1	5	0
		High	0	1	2	0	1	1
	GRVI	Low	2	0	0	1	1	0
		Mid	0	5	1	1	5	0
		High	0	1	1	0	1	1
	GRVIRE	Low	0	1	1	0	1	1
		Mid	1	5	1	1	4	0
		High	1	0	0	1	2	0
	NDRE	Low	2	0	0	1	1	0
		Mid	0	5	0	1	4	0
		High	0	1	2	0	2	1
	NDVI	Low	2	0	0	1	1	0
		Mid	0	6	1	1	5	0
		High	0	0	1	0	1	1
	Pixel Percent	Low	1	0	0	1	1	0
		Mid	1	5	1	1	5	0
		High	0	1	1	0	1	1
	RCI	Low	2	0	0	1	1	0
		Mid	0	5	0	1	4	0
		High	0	1	2	0	2	1

Note. The numbers on the diagonal from top left to bottom right indicate an agreeance between actual biomass classification and VI-Based genotype classification.

Table A33

VI vs. Dry Biomass Confusion Matrices 05/22/23

	Vegetation Indices	Actual Biomass Classification of Genotypes	Lincoln			Mead		
			Low	Mid	High	Low	Mid	High
VI-Based Genotype Classification	GCI	Low	2	0	0	1	2	0
		Mid	0	4	2	1	3	1
		High	0	2	0	0	1	1
	GNDVI	Low	1	0	0	1	2	0
		Mid	1	4	1	1	3	1
		High	0	2	1	0	1	1
	GRVI	Low	1	0	1	1	3	0
		Mid	1	4	1	1	2	1
		High	0	2	0	0	1	1
	GRVIRE	Low	0	1	0	0	1	1
		Mid	1	5	2	1	4	1
		High	1	0	0	1	1	0
	NDRE	Low	1	0	0	1	2	0
		Mid	1	5	1	1	3	1
		High	0	1	1	0	1	1
	NDVI	Low	1	0	0	1	2	0
		Mid	1	4	1	1	3	1
		High	0	2	1	0	1	1
	Pixel Percent	Low	1	0	0	1	0	0
		Mid	1	3	2	1	5	1
		High	0	3	0	0	1	1
	RCI	Low	1	0	0	1	2	0
		Mid	1	5	1	1	3	1
		High	0	1	1	0	1	1

Note. The numbers on the diagonal from top left to bottom right indicate an agreeance between actual biomass classification and VI-Based genotype classification.

Table A34

VI vs. Dry Biomass Confusion Matrices 06/05/23

	Vegetation Indices		Actual Biomass Classification of Genotypes: Lincoln Low	Lincoln Mid	Lincoln High	Mead Low	Mead Mid	Mead High
VI-Based Genotype Classification	GCI	Low	2	0	1	1	3	0
		Mid	1	1	2	1	3	0
		High	0	2	1	0	0	2
	GNDVI	Low	2	0	0	1	2	0
		Mid	0	1	4	1	4	0
		High	1	2	0	0	0	2
	GRVI	Low	1	0	0	1	1	0
		Mid	2	1	4	1	4	1
		High	0	2	0	0	1	1
	GRVIRE	Low	0	2	0	0	2	2
		Mid	1	1	3	1	1	0
		High	2	0	1	1	3	0
	NDRE	Low	1	1	0	1	2	0
		Mid	1	0	3	1	3	0
		High	1	2	1	0	1	2
	NDVI	Low	2	0	0	1	1	0
		Mid	1	1	4	1	4	0
		High	0	2	0	0	1	2
	Pixel Percent	Low	2	0	1	2	2	0
		Mid	1	1	3	0	2	0
		High	0	2	0	0	2	2
	RCI	Low	1	1	0	1	2	0
		Mid	1	0	3	1	3	0
		High	1	2	1	0	1	2

Note. The numbers on the diagonal from top left to bottom right indicate an agreeance between actual biomass classification and VI-Based genotype classification.

Table A30

Removed Genotypes

Name
NT13443
NT14433
NT17441
NT17442
NT19441
NT20429
NT20432
NT21414
NT21436
NT21443

Note. Incorrect sampling on 05/18/22 at the Mead location resulted in the above genotypes being sampled only once. These were removed from the data set prior to statistical analysis.

APPENDIX B

Table B1

High Throughput Phenotyping in Plant Breeding Outline

1. Farming Success in a Changing World
    a. Plant Breeding History
    b. Plant Breeding Process
2. Can New Technology Help Plant Breeding Decision Making?
    a. High Throughput Phenotyping Technology
    b. Plant Structure and Light Interactions
3. High Throughput Phenotyping Sensors
4. UAV Flight
5. Ground-Truthing
6. Data Analysis
    a. Data Processing
    b. Making Decision
7. Limitations to High Throughput Phenotyping
8. Use of High Throughput Phenotyping Today

Table B2

High Throughput Phenotyping in Plant Breeding Objectives

1. Explain plant breeding and the goals of the plant breeding process.
2. Compare and contrast different *High Throughput Phenotyping (*HTP) methods and their potential to improve the plant breeding process.
3. Outline the steps necessary to collect data using Unmanned Aerial Vehicle (UAV)-based HTP methods: pre-flight mission planning, pre-flight set up, and flight.
4. Summarize the general process of storing, processing, and extracting information from raw UAV data and how it can be used to make reliable plant breeding decisions.
5. Identify the limitations to HTP and the status of HTP in current breeding programs.

Table B3

Pre- and Post-Survey Questionnaire

Demographic Question

1. What best describes your current position?
    a. Undergraduate student
    b. Graduate student
    c. Agriculture industry professional
    d. Producer
    e. Other

Self-Assessed Knowledge Questions

1. Rate your comfortability with implementing UAV technology in plant breeding or agronomic management (1=not comfortable, 2=somewhat comfortable, 3=comfortable, 4=very comfortable 5= extremely comfortable)

    1 2 3 4 5

2. Rate your knowledge about the following topics (1=nothing, 2=a small amount, 3=average amount, 4=a large amount 5=expert on the topic)
    a. Processing large amounts of data collected by UAV

    1 2 3 4 5
    b. Steps needed to fly a UAV

    1 2 3 4 5
    c. Plant breeding

    1 2 3 4 5
    d. UAV sensors

    1 2 3 4 5
    e. Timeline of plant breeding

    1 2 3 4 5
3. How confident are you in selecting the type of sensor to use for data collection with the UAV? Rate 1-5

    1 2 3 4 5

Content Questions

1. Select the correct order in which the plant breeder makes the seven decisions below.

    _2_ Source/introgression of germplasm from external pools
    _8_ Release Cultivar
    _1_ Determine the target product
    _6_ Select plant phenotypes based on desired traits

_4_ Make crosses to create genetic variation from recombination
_5_ Evaluate plant phenotypes for desired traits
_3_ Source/introgression of germplasm from internal pools
_7_ Advance or recycle phenotypes based on selection

2. A cultivar is a plant that has a genotype that....
    a. ... a plant breeder would use as a parent but not a genotype that a farmer would grow.
    b. *... a plant breeder would use as a parent, and it could be a genotype that a farmer would grow.
    c. ... a farmer would grow but not a genotype that a plant breeder would use as parent.
    d. … is not of interest to either a farmer to grow for production or a breeder to use as a parent.

3. Which of these statements must be true about the parents selected by the breeder?
    a. *****The parents must have gene versions that can recombine to produce a new genotype that meets the breeder's goals for a new cultivar
    b. The parents must already have the gene combination that meets the breeder's goals cultivar.
    c. One parent must have the phenotype combination that is better than the cultivars already available to farmers.
    d. Neither parent would be a genotype that farmers would grow in their field for production.

4. Which statement is true about the role that environment can play on the variation in traits that a plant breeder measures when they evaluate genotypes in their breeding program?
    a. The breeder can only work with traits that are not influenced by environmental variation.
    b. All traits a breeder will work with are influenced by environmental variation to the same degree, so the breeder uses a standard method for evaluation of all traits during the breeding process.
    c. The role of environmental variation is greater for some traits than for others, but the plant breeder cannot modify their evaluation for different traits.
    d. *The role of environmental variation is greater for some traits than for others so the plant breeder will modify their evaluation for different traits.

5. Which of these roles do plant breeders have in crop production?
    a. They domesticate wild plants by selecting plants that grow more of the harvested part of the plant or are easier to grow and harvest.
    b. They increase the seeds available of plants local farmers have domesticated so that more farmers have access to this seed.

c. *They create new genetic combinations by crossing between parents that are already domesticated and grown by farmers so that the new combinations are more productive than the parents.
d. They make numerous genetic changes that create new species that can no longer produce sexual offspring if crossed with the older domesticated land races.

6. High throughput phenotyping using remote sensing can improve which part of the plant breeding process?
    a. Selection of the new cultivars that will be released for seed increase.
    b. Selection of genotypes that the plant breeder will advance for further evaluation at more environments.
    c. *Evaluation of genotypes that have been through the first few generations of advance and are now grown in replicated field tests.
    d. Evaluation of genotypes at the stage where a row of 100 plant representants that genotype.

7. Which of these is an advantage of using remote methods for data collection in breeder's plots?
    a. *It will take less time in the field which could allow for more collection of important data in each day.
    b. The number of locations that the breeder uses to obtain the data they need for their selection decisions is reduced because of the nature of remote data.
    c. Randomization of entries and uniform plot size would not be a planning concern for plant breeders who use remote data collection.
    d. UAV readily identify the worst plant in a field so a breeder can discard these genotypes.

8. Based on your current understanding what steps of the plant breeding process can be improved using UAV technology?
    a. The seeding rate in each plot can be reduced so that the breeder needs less seed for replicated yield trials.
    b. *Plots that have experienced environmental effects can be identified before harvest.
    c. Replication of genotypes at a specific environment will not be necessary reducing the amount of seed needed for analysis of genotypes.
    d. The need to harvest seed from plots is eliminated.
9. Which of these phenotypes would be the most likely to be better measured by remote sensing compared with current field methods to provide more reliable data to support the plant breeder's decision making?
    a. Harvestable grain yield
    b. Seeding rate during planting
    c. *Vegetative growth area that covers the plot
    d. Date where 50% of the plants in the plot have headed.

10. Select all the environmental factors which could influence the data measurement process with remote sensing but would not influence data collection by current field methods?
    a. *Wind speed and direction
    b. Temperature
    c. Humidity
    d. *Cloud cover
    e. *Precipitation

11. The remote sensing experts have developed sensor techniques that can measure the time it takes for signals to travel from the sensor to the ground and back to the sensor. Which trait would this technology allow the plant breeder to measure?
    a. Leaves per plant
    b. Vegetative coverage of the plot.
    c. *Plant height
    d. Date of flowering.

12. The remote sensing experts have developed sensor techniques that can measure the number of green pixels in a plot area. Which trait would this technology allow the plant breeder to measure?
    a. Leaves per plant
    b. *Vegetative coverage of the plot.
    c. Plant height
    d. Date of flowering

13. Which procedures will confirm the accuracy of UAV collected data? (Multiple Answers)
    a. *Ground truthing is done on some plots in some parts of the field
    b. Ground truthing is done on all plots in the field
    c. *Sensors are calibrated to a standard
    d. Raw data is processed to remove inconsistencies
    e. Data is always collected from two flights completed at the same time.

14. Which is the best description of the status of the use of remote sensing by plant breeders for data collection that guides their selection decisions?
    a. Remote data collection is ready to replace all field data collection currently used by plant breeders.
    b. *There are several types of data plant breeders collect in the field that can now be completed with remote methods and more are being explored at this time.
    c. Remote data is always going to be supplemental observations and will not replace any of the data collection that plant breeders currently must do for selection decisions.

15. As a plant breeder you are tasked with choosing one plant to move forward in the breeding process. You have only been provided vegetative indices to make this decision. Which of the following genotypes would you choose to move forward in the program?
    a. Variety N2938
    b. Variety N7236
    c. Variety N8478
    d. *Variety N5536
    e. Variety N0293

Plot ID	Variety	NDVI
094	N2938	0.468008
278	N7236	0.562577
290	N8478	0.564904
837	N5536	0.666813
987	N0293	0.563353

16. You used a UAV to collect high throughput phenotyping data on a crop and then graphed the vegetation reflectance of each wavelength. Which line on the graph below depicts a spectral reflectance profile for the healthiest crop?
    a. Dotted line
    b. Dashed line
    c. *Solid line

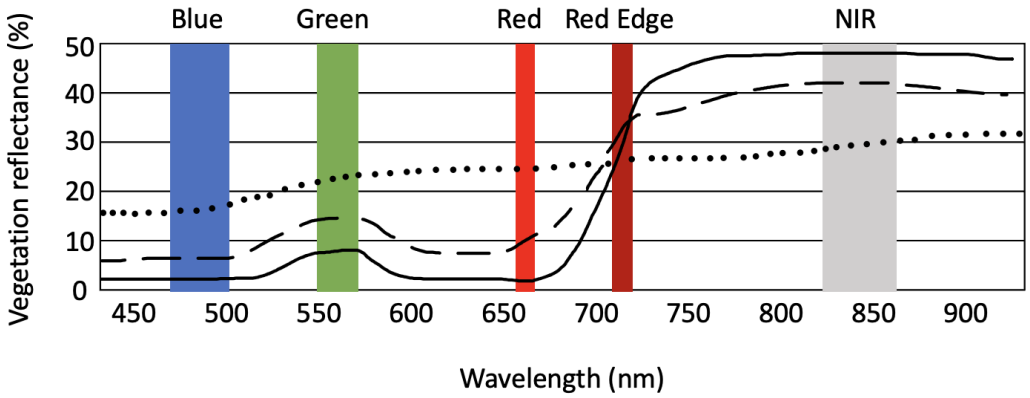

17. Which situation would result in the biggest benefit for a breeder from remote data collection? Assume that data was collected by drone flight that was a reliable measure of plant growth.
    a. *A testing location has a hailstorm just before harvest which prevents grain yield data collection at that location.
    b. A foliar disease causes severe chlorosis on some entries in the plots at one of the locations and this impacts grain yield in those plots.

c. An error in N fertilizer application causes a non-random difference in N availability for plots at a location. This difference was detected by remote data analysis.

18. Height is an important trait to measure because the plant breeder will cull plants that are too tall. In some families, there is height variation from plant to plant because genes controlling height are still segregating. Select the true statement.
    a. The meter stick measurement of height will be more accurate than height from remote imaging because the field crew will have a reliable routine for how they collect height as they walk the plots.
    b. Collecting height data from a meter stick will be more accurate than collecting with a plot image from remote data collection because all plants in the plot contribute to the measured value.
    c. *Collecting height data from remote images will be a more representative measure of the plants in the plot than collecting with a meter stick because all plants in the plot contribute to the measured value.

Note. An asterisk (*) denotes correct answers.

Table B4

Data Subsets

Category	Number of Questions in Subset
Overall Self-Report Knowledge	7
Overall Objectively Assessed Knowledge	17
UAV Self-Report Knowledge	3
Plant Breeding Self-Report Knowledge	2
Cross-Listed Self-Report Knowledge	2
Plant Breeding Objectively Assessed Knowledge	4
Cross-Listed Objectively Assessed Knowledge	13

Note. Some questions fall under more than one category.

Graph B1

Box and Dot Plot of Overall Self-Reported Knowledge

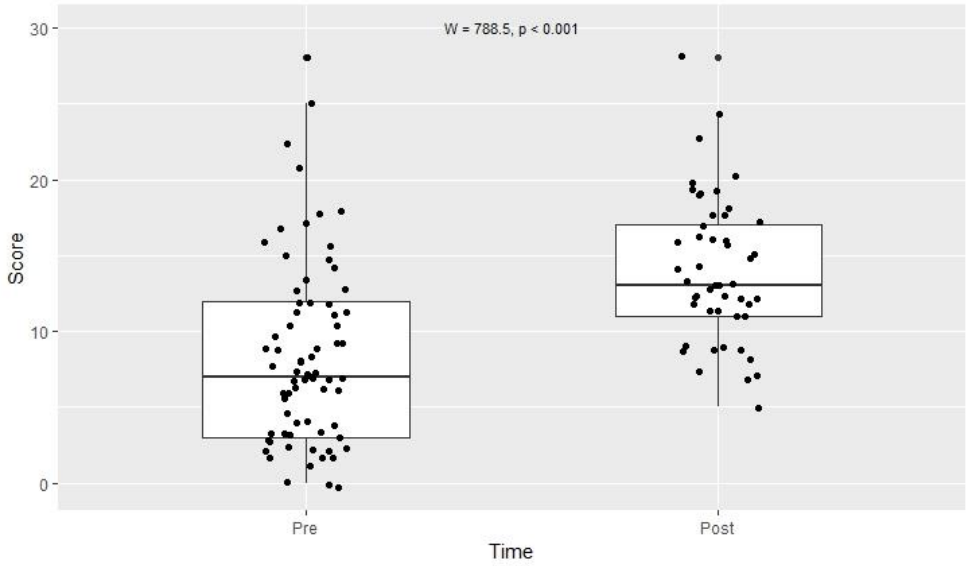

Note. Results for pre-survey scores and post-survey scores. Data includes 69 pre-surveys and 49 post-surveys. A p-value <0.05 indicates a significant difference in pre- and post-survey scores. The W statistic indicates the number of times a pre-survey score is lower than a post-survey score.

Graph B2

Box and Dot Plot of Overall Objectively Assessed Knowledge

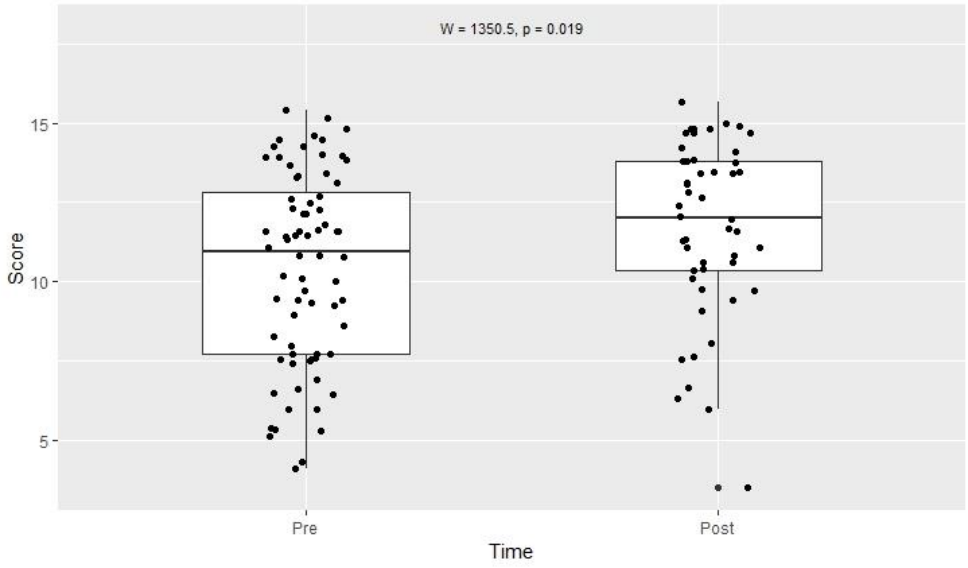

Note. Results for pre-survey scores and post-survey scores. Data includes 69 pre-surveys and 49 post-surveys. A p-value <0.05 indicates a significant difference in pre- and post-survey scores. The W statistic indicates the number of times a pre-survey score is lower than a post-survey score.

Graph B3

Box and Dot Plot of Plant Breeding Self-Reported Knowledge

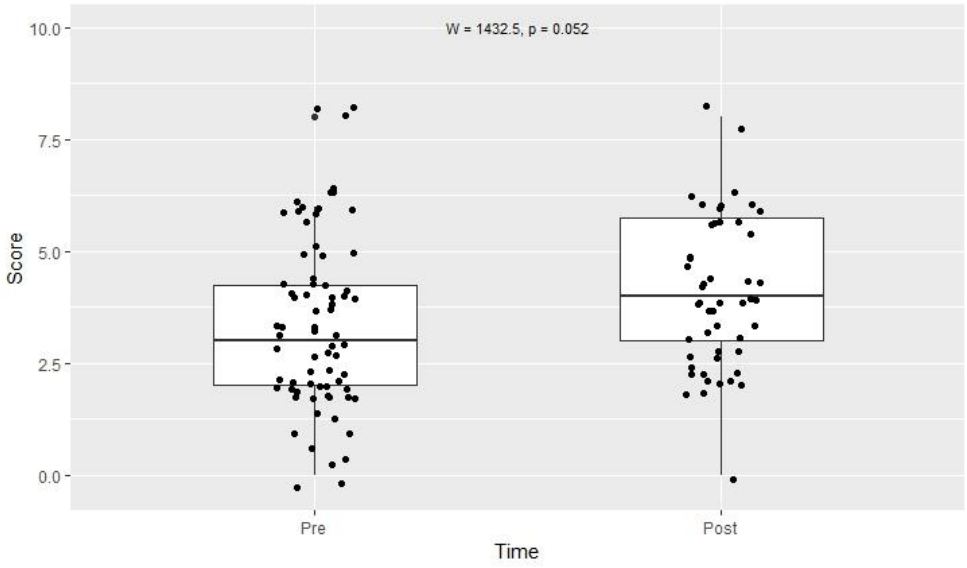

Note. Results for pre-survey scores and post-survey scores. Data includes 69 pre-surveys and 49 post-surveys. A p-value <0.05 indicates a significant difference in pre- and post-survey scores. The W statistic indicates the number of times a pre-survey score is lower than a post-survey score.

Graph B4

Box and Dot Plot of UAV Self-Reported Knowledge

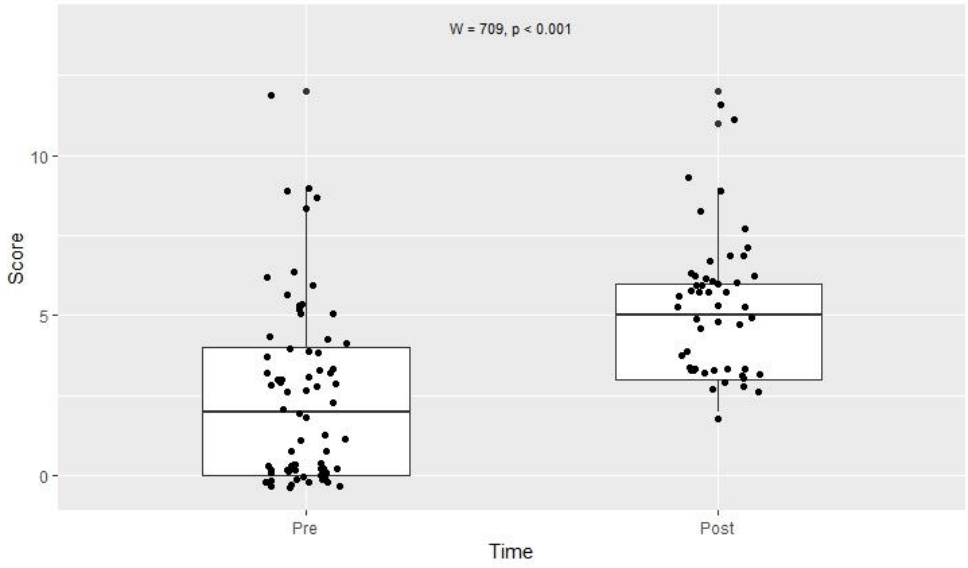

Note. Results for pre-survey scores and post-survey scores. Data includes 69 pre-surveys and 49 post-surveys. A p-value <0.05 indicates a significant difference in pre- and post-survey scores. The W statistic indicates the number of times a pre-survey score is lower than a post-survey score.

Graph B5

Box and Dot Plot of Cross Listed Self-Reported Knowledge

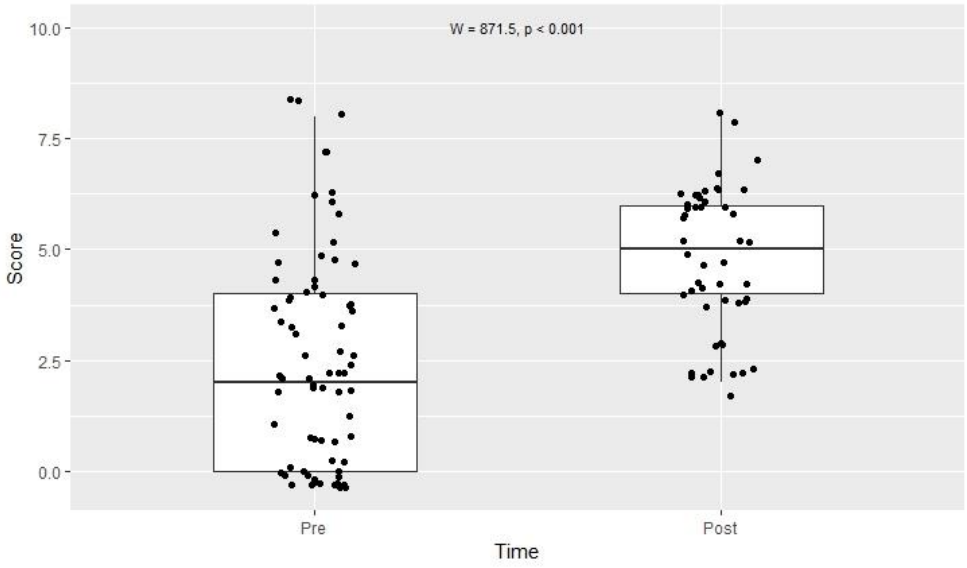

Note. Results for pre-survey scores and post-survey scores. Data includes 69 pre-surveys and 49 post-surveys. A p-value <0.05 indicates a significant difference in pre- and post-survey scores. The W statistic indicates the number of times a pre-survey score is lower than a post-survey score.

Graph B6

Box and Dot Plot of Plant Breeding Objectively Assessed Knowledge

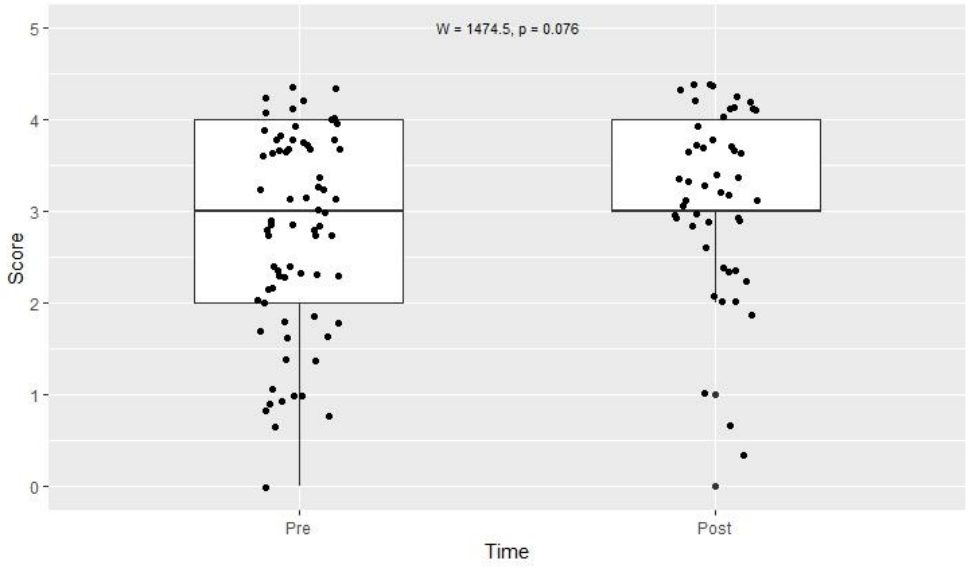

Note. Results for pre-survey scores and post-survey scores. Data includes 69 pre-surveys and 49 post-surveys. A p-value <0.05 indicates a significant difference in pre- and post-survey scores. The W statistic indicates the number of times a pre-survey score is lower than a post-survey score.

Graph B7

Box and Dot Plot of Cross Listed Objectively Assessed Knowledge

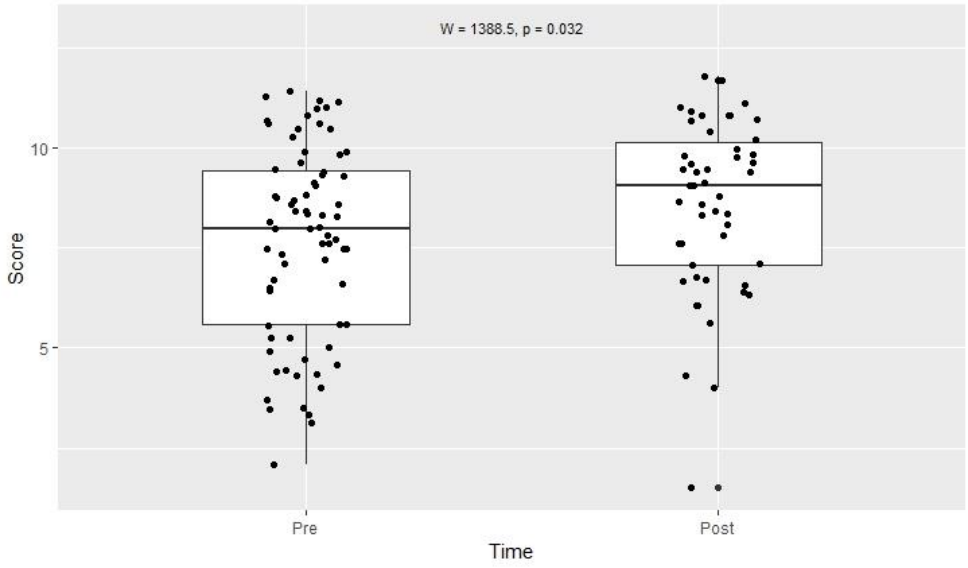

Note. Results for pre-survey scores and post-survey scores. Data includes 69 pre-surveys and 49 post-surveys. A p-value <0.05 indicates a significant difference in pre- and post-survey scores. The W statistic indicates the number of times a pre-survey score is lower than a post-survey score.